

NAS  
R NAE  
C IOM

7N #64208

7.121

LIBRARY COPY

MAY 15 1991

LANGLEY RESEARCH CENTER  
LIBRARY NASA  
HAMPTON, VIRGINIA

(NASA-CR-189919) RESEARCH OPPORTUNITIES FOR  
MATERIALS WITH ULTRAFINE MICROSTRUCTURES  
Report, 1986-1989 (National Materials  
Advisory Board) 121 p

N92-70571

29/24 Unclas  
0064208

NATIONAL RESEARCH COUNCIL  
COMMISSION ON ENGINEERING AND TECHNICAL SYSTEMS

**NATIONAL MATERIALS ADVISORY BOARD**

The purpose of the National Materials Advisory Board  
is the advancement of materials science and engineering in the national interest.

**CHAIRMAN**

Dr. James C. Williams  
General Manager  
Materials Technology Laboratories  
Mail Drop #85  
General Electric Company  
1 Neumann Way  
Cincinnati, OH 45215-6301

**PAST CHAIRMAN**

Dr. Bernard H. Kear  
Chairman, Department of  
Mechanics and Materials Science  
Director, Center for Materials  
Synthesis  
College of Engineering  
Rutgers University  
P.O. Box 909  
Piscataway, NJ 08854

**MEMBERS**

Dr. Norbert S. Baer  
Hagop Kevorkian Professor of  
Conservation  
New York University  
Conservation Center of the Institute  
of Fine Arts  
14 East 78th Street  
New York, NY 10021

Mr. Robert R. Beebe  
Senior Vice President  
Homestake Mining Company  
650 California Street  
San Francisco, CA 94108

Dr. Frank W. Crossman  
Assistant Director  
Information Services  
Lockheed Missiles & Space Co.,  
Inc.  
Org./19-60, Bldg. 102  
P.O. Box 3504  
Sunnyvale, CA 94088-3504

Dr. James Economy  
Professor & Head of Materials  
Science  
University of Illinois  
Department of Materials Science &  
Engineering  
1304 Green Street  
Urbana, IL 61801

Dr. James A. Ford  
Consultant  
703 Judith Drive  
Johnson City, TN 37604

Dr. Robert E. Green, Jr.  
Director of Center for NDE  
Professor, Materials Science  
Department  
Johns Hopkins University  
Baltimore, MD 21218

Dr. John K. Hulm  
Chief Scientist Emeritus  
Westinghouse Research  
Laboratories  
1310 Beulah Road  
Pittsburgh, PA 15235

Dr. Frank E. Jamerson  
Manager  
Division and Staff Contacts  
General Motors Research  
Laboratories  
30500 Mound Road  
Warren, MI 48090-9055

Dr. Melvin F. Kanninen  
Institute Scientist  
Southwest Research Institute  
P.O. Drawer 28510  
San Antonio, TX 78284

Dr. Ronald M. Latanision  
Professor of Materials Science &  
Engineering, and Director,  
Materials Processing Center  
Room 8-202  
Massachusetts Institute of  
Technology  
Cambridge, MA 02139

Dr. Robert A. Laudise  
Director, Physical and Inorganic  
Chemistry Research Laboratory  
Room 1A-264  
AT&T Bell Laboratories  
Murray Hill, NJ 07974

Dr. William D. Nix  
Professor, Department of Materials  
Science and Engineering  
Stanford University  
Stanford, CA 94305

Dr. Donald R. Paul  
Melvin H. Gertz Regents Chair  
in Chemical Engineering  
Director, Center for Polymer  
Research  
Department of Chemical  
Engineering  
University of Texas  
Austin, TX 78712

Dr. Joseph L. Pentecost  
Professor  
School of Materials Engineering  
Georgia Institute of Technology  
Atlanta, GA 30332

Dr. John P. Riggs  
Vice President, R&D Research  
Division  
Managing Director, Mitchell  
Technical Center  
Hoechst Celanese Corporation  
86 Morris Avenue  
Summit, NJ 07901

Dr. Maxine L. Savitz  
Director  
Garrett Ceramic Components  
Division  
Allied-Signal Aerospace Co.  
19800 South Van Ness Avenue  
Torrence, CA 90509

Dr. Dale F. Stein  
President  
Michigan Technological University  
Houghton, MI 49931

Dr. Earl R. Thompson  
Assistant Director of Research for  
Materials Technology  
United Technologies Research  
Center  
Silver Lane  
East Hartford, CT 06108

Mr. James R. Weir, Jr.  
Associate Director  
Metals & Ceramics Division  
Oak Ridge National Laboratory  
P.O. Box X  
Oak Ridge, TN 37830

Dr. Robert M. White  
Vice President, Research &  
Engineering  
Control Data Corporation  
8100 34th Avenue South  
Minneapolis, MN 55440

**NMAB STAFF**

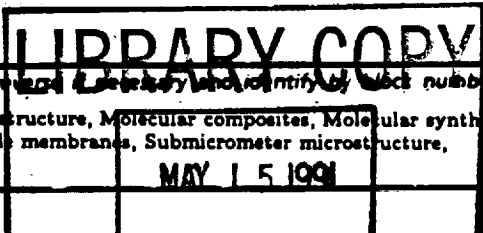
K.M. Zwilsky, Director  
S.M. Barkin, Assoc. Director  
Mary Brittain, Adm. Officer  
2101 Constitution Ave., NW  
Washington, DC 20418

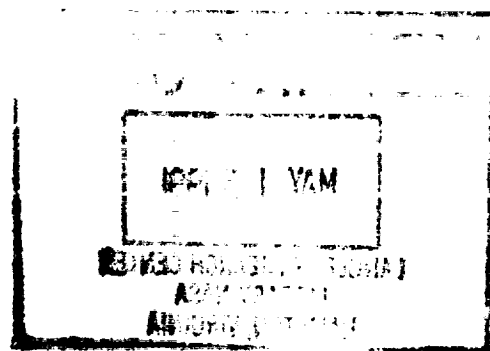
UNCLASSIFIED

SECURITY CLASSIFICATION OF THIS PAGE

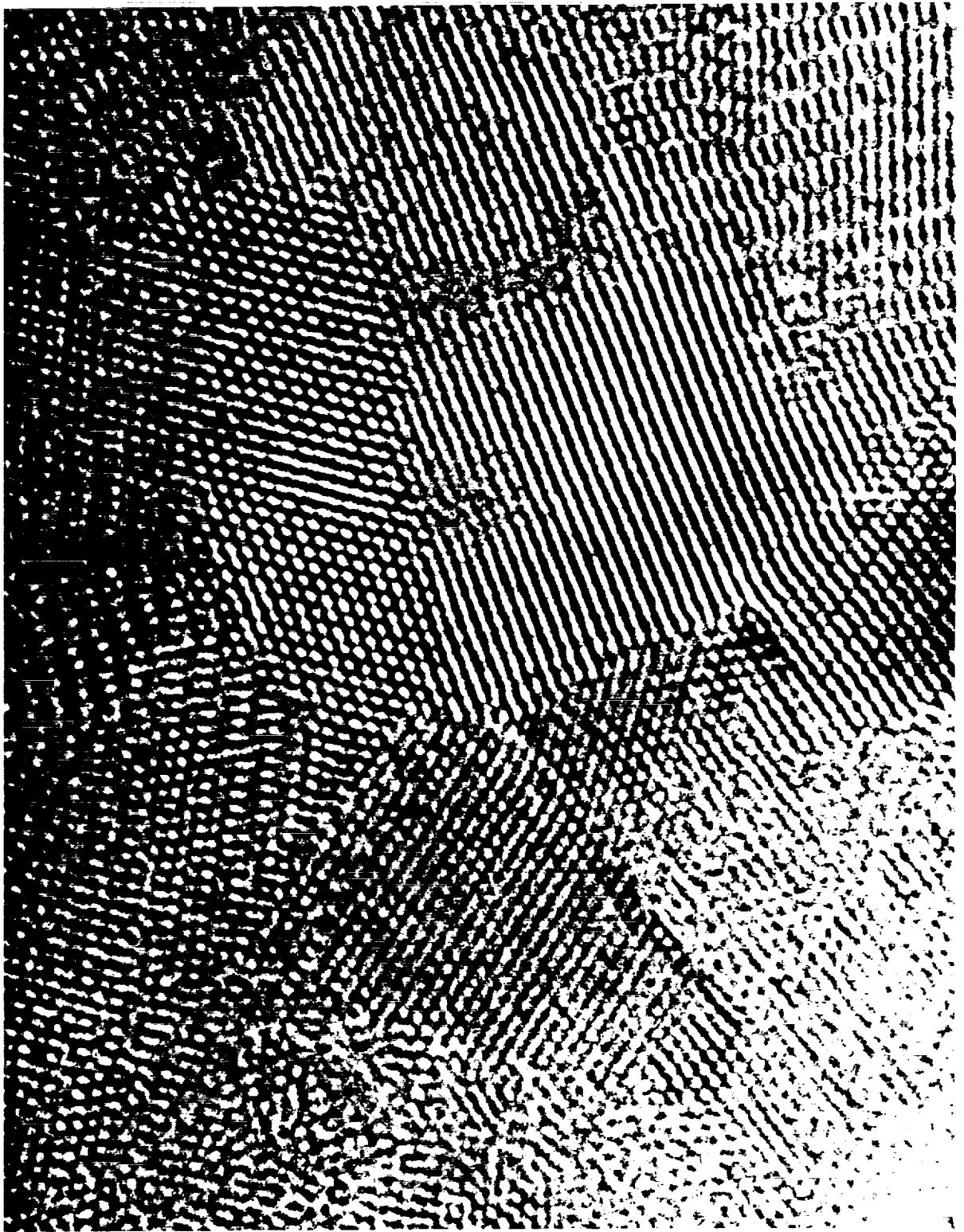
## REPORT DOCUMENTATION PAGE

1a REPORT SECURITY CLASSIFICATION Unclassified			1b RESTRICTIVE MARKINGS NONE		
2a SECURITY CLASSIFICATION AUTHORITY N/A			3. DISTRIBUTION/AVAILABILITY OF REPORT Approved for Public Release Distribution Unlimited		
2b DECLASSIFICATION/DOWNGRADING SCHEDULE N/A					
4 PERFORMING ORGANIZATION REPORT NUMBER(S)  NMAB-454			5 MONITORING ORGANIZATION REPORT NUMBER(S)		
6a NAME OF PERFORMING ORGANIZATION National Materials Advisory Board		6b OFFICE SYMBOL (If applicable)  NMAB	7a NAME OF MONITORING ORGANIZATION Department of Defense/National Aeronautics & Space Administration		
6c ADDRESS (City, State, and ZIP Code) 2101 Constitution Avenue, NW Washington, DC 20418			7b ADDRESS (City, State, and ZIP Code)  Washington, DC 20301		
8a NAME OF FUNDING/SPONSORING ORGANIZATION See 7a		8b OFFICE SYMBOL (If applicable)  DOD/NASA	9. PROCUREMENT INSTRUMENT IDENTIFICATION NUMBER  MAD903-89-K-0078		
8c ADDRESS (City, State, and ZIP Code)  Washington, DC 20301			10 SOURCE OF FUNDING NUMBERS		
			PROGRAM ELEMENT NO.	PROJECT NO.	TASK NO.
11. TITLE (Include Security Classification)  Research Opportunities for Materials with Ultrafine Microstructures					
12. PERSONAL AUTHOR(S) NAMB Committee on Materials with Submicron-sized Microstructures					
13a TYPE OF REPORT One of a series under subj. cont.		13b TIME COVERED FROM 1986 TO 1989		14. DATE OF REPORT (Year, Month, Day) December 31, 1989	
15. PAGE COUNT 122					
16 SUPPLEMENTARY NOTATION  NONE					
17 COSATI CODES			18 SUBJECT TERMS (Continue on reverse if necessary and identify by block number)		
FIELD	GROUP	SUB-GROUP	Catalysts, Characterization, Microstructure, Molecular composites, Molecular synthesis, Nanoscale structure, Semipermeable membranes, Submicrometer microstructure, Ultrafine structure		
19. ABSTRACT (Continue on reverse if necessary and identify by block number)					
<p>A state-of-the-art survey of research findings on materials with nanoscale structure (materials with a characteristic structure less than 100 nm in size) revealed that there is a large number of methods for producing such structures, that they possess a number of unique properties when compared to coarser-scaled structures, and that they have several possible applications with significant technological importance. Based on findings to date and prospects for commercialization, a number of recommendations for specific research and development activities are made. The principal conclusion is that a new and exciting field of research and possible application has been opened, but much work remains in characterizing the unique microstructures, with their correspondingly exceptional properties. To utilize these materials, processes to yield much larger quantities must be developed; examples of possible processes are described.</p>					
20 DISTRIBUTION/AVAILABILITY OF ABSTRACT <input checked="" type="checkbox"/> UNCLASSIFIED/UNLIMITED <input type="checkbox"/> SAME AS RPT. <input checked="" type="checkbox"/> DTIC USERS			21. ABSTRACT SECURITY CLASSIFICATION Unclassified		
22a NAME OF RESPONSIBLE INDIVIDUAL Jerome Persh			22b TELEPHONE (Include Area Code) (202) 695-0005		22c. OFFICE SYMBOL OUSDR&E/R&AT/MST





# **RESEARCH OPPORTUNITIES FOR MATERIALS WITH ULTRAFINE MICROSTRUCTURES**



**RESEARCH OPPORTUNITIES FOR MATERIALS  
WITH ULTRAFINE MICROSTRUCTURES**

**Report of the  
Committee on Materials with Submicron-Sized Microstructures**

**NATIONAL MATERIALS ADVISORY BOARD  
Commission on Engineering and Technical Systems  
National Research Council**

**NMAB-454  
National Academy Press  
1989**

NOTICE: The project that is the subject of this report was approved by the Governing Board of the National Research Council, whose members are drawn from the councils of the National Academy of Sciences, the National Academy of Engineering, and the Institute of Medicine. The members of the committee responsible for the report were chosen for their special competences and with regard for appropriate balance.

This report has been reviewed by a group other than the authors according to procedures approved by a Report Review Committee consisting of members of the National Academy of Sciences, the National Academy of Engineering, and the Institute of Medicine.

The National Academy of Sciences is a private, nonprofit, self-perpetuating society of distinguished scholars engaged in scientific and engineering research, dedicated to the furtherance of science and technology and to their use for the general welfare. Upon the authority of the charter granted to it by the Congress in 1863, the Academy has a mandate that requires it to advise the federal government on scientific and technical matters. Dr. Frank Press is president of the National Academy of Sciences.

The National Academy of Engineering was established in 1964, under the charter of the National Academy of Sciences, as a parallel organization of outstanding engineers. It is autonomous in its administration and in the selection of its members, sharing with the National Academy of Sciences the responsibility for advising the federal government. The National Academy of Engineering also sponsors engineering programs aimed at meeting national needs, encourages education and research, and recognizes the superior achievements of engineers. Dr. Robert M. White is president of the National Academy of Engineering.

The Institute of Medicine was established in 1970 by the National Academy of Sciences to secure the services of eminent members of appropriate professions in the examination of policy matters pertaining to the health of the public. The Institute acts under the responsibility given to the National Academy of Sciences by its congressional charter to be an advisor to the federal government and, upon its own initiative, to identify issues of medical care, research, and education. Dr. Samuel O. Thier is president of the Institute of Medicine.

The National Research Council was organized by the National Academy of Sciences in 1916 to associate the broad community of science and technology with the Academy's purposes of furthering knowledge and advising the federal government. Functioning in accordance with general policies determined by the Academy, the Council has become the principal operating agency of both the National Academy of Sciences and the National Academy of Engineering in providing services to the government, the public, and the scientific and engineering communities. The Council is administered jointly by both Academies and the Institute of Medicine. Dr. Frank Press and Dr. Robert M. White are chairman and vice chairman, respectively, of the National Research Council.

-----

This study by the National Materials Advisory Board was conducted under Contract No. MDA-903-89-K-0078 with the Department of Defense and the National Aeronautics and Space Administration.

Library of Congress Catalog Card Number 89-63756

International Standard Book Number 0-309-04183-X.

This report is available from the Defense Technical Information Center, Cameron Station, Alexandria, VA 22304-6145.

SO72

Printed in the United States of America.

First Printing, December 1989

Second Printing, November 1990



## ABSTRACT

A state-of-the-art survey of research findings on materials with nanoscale structure (materials with a characteristic structure less than 100 nm in size) revealed that there is a large number of methods for producing such structures, that they possess a number of unique properties when compared to coarser-scaled structures, and that they have several possible applications with significant technological importance. Based on findings to date and prospects for commercialization, a number of recommendations for specific research and development activities are made. The principal conclusion is that a new and exciting field of research and possible application has been opened, but much work remains in characterizing the unique microstructures, with their correspondingly exceptional properties. To utilize these materials, processes to yield much larger quantities must be developed; examples of possible processes are described.

*Cover: Schematic representation of a nanophase material.*

*Frontispiece: High-resolution electron micrograph of nanophase palladium.*



### ACKNOWLEDGMENTS

The assistance of Dr. Martin B. Sherwin of W. R. Grace and Company, for providing input on chemical vapor synthesis, and Professor R. E. Newnham, who described interesting work in progress at Pennsylvania State University, is noted with appreciation.

v



**Committee on  
Materials With Submicron-Sized Microstructures**

**Chairman**

BERNARD H. KEAR, Rutgers University, Piscataway, New Jersey

**Members**

L. ERIC CROSS, Pennsylvania State University, University Park

JOHN E. KEEM, Ovonic Synthetic Materials Company, Troy, Michigan

RICHARD W. SIEGEL, Argonne National Laboratory, Argonne, Illinois

FRANS A. SPAEPEN, Harvard University, Cambridge, Massachusetts

KATHLEEN C. TAYLOR, General Motors Research Laboratories, Warren, Michigan

EDWIN L. THOMAS, Massachusetts Institute of Technology, Cambridge

KING-NING TU, IBM Corporation, Yorktown Heights, New York

**Liaison**

ANDREW CROWSON, Army Research Office, Research Triangle Park, North Carolina

JOSEPH P. DARBY, Department of Energy, Germantown, Maryland

PHILLIP PARRISH, BDM International, Arlington, Virginia

JEROME PERSH, Department of Defense (DUSDR&E), Washington, D.C.

DONALD E. POLK, Office of Naval Research, Arlington, Virginia

ROBERT J. REYNIK, National Science Foundation, Washington, D.C.

A. ROSENSTEIN, Office of Scientific Research, Bolling Air Force Base,  
Washington, D.C.

J. TARNACKI, Air Force Wright Aeronautical Laboratory, Wright-Patterson Air  
Force Base, Ohio

DONALD R. ULRICH, Air Force Office of Scientific Research, Washington, D.C.

NMAB Staff

Joseph R. Lane, Program Officer

Judith Amri, Senior Secretary

Cathryn Summers, Senior Secretary

## CONTENTS

EXECUTIVE SUMMARY	1
1 INTRODUCTION	7
References	9
2 SYNTHESIS AND PROCESSING: GENERAL METHODS	11
Molecular Synthesis	11
Reductive Pyrolysis	13
Gel Synthesis	14
Supercritical Fluid Processing	20
Laser Pyrolysis	21
Colloidal Synthesis	22
Reactive Sputtering	25
Cryochemical Synthesis	27
Chemical Vapor Synthesis	28
Ion-Beam Processing	29
Mechanical Processing	30
Gas-Condensation Synthesis	31
Rapid Solidification Processing	34
References	35
3 SYNTHESIS AND PROCESSING: MORPHOLOGICALLY SPECIFIC METHODS	39
Filamentary Structures	39
Multilayer Structures	42
Dispersed-Phase Structures	44
Macromolecular Composite Structures	46
Heterogeneous Nanocomposites	49

	High-Surface-Area Materials	51
	Membranes	54
	References	56
4	CHARACTERIZATION METHODS	59
	X-Ray and Neutron Scattering	60
	Transmission Electron Microscopy	62
	Spectroscopies	64
	Calorimetry	66
	Other Promising Methods	66
	References	67
5	PROPERTIES	71
	Nanophase Compacts	71
	Mechanical Properties	77
	Catalytic Properties	79
	Stability	82
	References	86
6	SELECTED APPLICATION AREAS	89
	Electroceramics	89
	Ultrastructured Ceramics	91
	Permanent Magnets	93
	Polymer-Silica Microcomposites	95
	Catalysts	96
	Cermets	96
	Multilayer Coatings	97
	References	97
7	SUMMARY AND RECOMMENDATIONS	99
	BIBLIOGRAPHY	105
	Appendix A DEFINITION OF ACRONYMS	107
	Appendix B BIOGRAPHICAL SKETCHES OF COMMITTEE MEMBERS	109



## TABLES AND FIGURES

FIGURE 1	Schematic of the bacteriorhodopsin macromolecule	12
FIGURE 2	Control of sol-gel processing with organic acid DCCAs	16
FIGURE 3	Densification microstructures for $\text{SiO}_2$ gels	16
FIGURE 4	Superior properties of sol-gel samples	17
FIGURE 5	Schematic of composite structures	18
FIGURE 6	Supercritical fluids have high solubility for other materials	21
FIGURE 7	Schematic form of the nonequilibrium colloidal phase diagram.	24
FIGURE 8	(a) Fractal clusters of 15 nm gold particles that result in the formation of low density compacts; (b) the dense packing of the same gold particles after they are first coated with lubricating surfactants	26
FIGURE 9	Schematic drawing of a gas-condensation chamber for the synthesis of nanophase materials	33
FIGURE 10	Baker mechanism for filamentous carbon growth	40
FIGURE 11	Cluster sources	43
FIGURE 12	Schematic phase diagram for polymer blends	47

- FIGURE 13 Computer generated image of triply periodic surface of constant mean curvature. 49
- FIGURE 14 The four types of ordered microdomain morphology of diblock copolymers 49
- FIGURE 15 Sol-gel design of zero expansion nanocomposites 50
- Figure 16 High-resolution transmission electron micrograph of nanophase  $\text{TiO}_2$  (rutile) after sintering for one-half hour at  $500^\circ\text{C}$  62
- Figure 17 Grain-size distribution for an as-compacted  $\text{TiO}_2$  (rutile) sample determined using TEM 63
- FIGURE 18 Reciprocal magnetic susceptibility versus temperature for three Er samples from the same starting material, but with different grain sizes 72
- FIGURE 19 Vickers microhardness of  $\text{TiO}_2$  (rutile) measured at room temperature as a function of 1/2-hour sintering at successively increased temperatures 73
- FIGURE 20 He-backscattering spectra for a nanocrystalline sample with an 80-nm thick Bi film deposited onto its surface after sputter cleaning 76
- FIGURE 21 Young's modulus of in situ formed Cu-Nb filamentary as a function of wire diameter, thermal history, and composition 77
- FIGURE 22 The impact of ultrastructure processing on ceramic performance 83
- FIGURE 23 Comparison of conventional and sol-gel mullite 84
- FIGURE 24 Infrared transparent mullite from sol-gel 84
- FIGURE 25 Average grain size (diameter) of nanophase  $\text{TiO}_2$  (rutile) determined by TEM as a function of sintering temperature 85
- FIGURE 26 Schematic diagram of the coarsening mechanism in a lamellar structure 91
- FIGURE 27 Schematic diagram of the coarsening of perfect layers by diffusion-induced doubling 92

FIGURE 28	Infrared transparent mullite from sol-gel	93
FIGURE 29	Bright-field image and selected area diffraction of enhanced remanence material	94
FIGURE 30	PBZT-sol-gel glass interpenetrating networks	95
TABLE 1	Properties of Nano Materials Compared With Their Crystalline Counterparts	8
TABLE 2	Glass Transition and Curing Temperature for PMMA	19
TABLE 3	Magnetron Reactively Sputtered Coating Materials and Measured Properties	27
TABLE 4	Dispersed-Phase Ceramic Composites Prepared by CVD	45



## EXECUTIVE SUMMARY

Materials synthesis--the preparation of materials from atomic or molecular precursors--and materials processing--the manipulation of microstructures to effect desired properties--are both critical to the development of advanced materials with engineered properties. Ceramics, polymers, and semiconductors are just some of the materials for which significant new achievements in synthesis and processing are taking place. Current research is focused on the design, synthesis, and processing of ultrafine material microstructures that extend into the nanoscale (less than 100 nanometer) regime. This research has been inspired by the realization that significant beneficial changes in the properties of materials can be achieved by progressively reducing the scale of their microstructure, while maintaining chemical and microstructural uniformity. Another incentive has been the discovery of novel and improved materials properties when their microstructure approaches nanoscale dimensions.

These findings have generated much interest in materials synthesis and processing research in the United States and abroad. This report presents a state-of-the-art assessment of the activity in this rapidly growing field of research and identifies new areas of research opportunity and some potential application areas for the future. The focus is on materials with submicron-sized microstructure (i.e., less than 100 nanometers), regardless of the specific type of material being considered. The scope includes what is known about metal, ceramic, and polymeric materials and their composites, but the report deliberately avoids significant discussion of semiconductor and superconductor materials, electronic, magnetic, and optical properties of multilayers, and rapidly solidified materials. These have been adequately treated in other publications.

The structure-related properties of materials with phase structures on a nanometer scale (nanophase materials) are expected to be different from normally available single-crystal, polycrystal, or amorphous materials because their aggregate atomic structure may be unique. Initial investigations

indicate some support for this view. Properties measured on nanocrystalline metals have been tabulated and compared with values for their coarse-grained counterparts and similar glassy materials. The change in a number of properties appears to be significantly greater in going from conventional crystalline material to the nanocrystalline form than in going from crystalline to glassy solid. The nature of such changes and their relationship with the underlying material's structure will be clarified only by further research in this interesting and potentially useful new area of materials synthesis and processing.

Nanometer-scale materials have certain distinguishing features that must be characterized in order to understand the relationships between their unique composition and structures and their properties. Since many materials properties (e.g., magnetic, optical, and electrical) depend strongly on the atomic arrangements in the material, whereas others such as mechanical properties can also depend on morphological structure, knowledge of the structure of nanophase materials is important on both atomic and nanometer scales. Among the features that need to be explained are grain and pore size distributions and morphologies, the nature of their grain boundaries and interphase interfaces, composition profiles across grains and interfaces, perfection and the nature of intragrain defects, and identification of residual trapped species from processing.

Because of the ultrafine scale of these nanophase materials, characterization can be a challenge in itself, and some traditional characterization tools are no longer easily applied. For the characterization of the structure and morphologies of nanoscale materials, traditional tools such as electron microscopy and x-ray and neutron scattering are both necessary and useful. However, for microchemical analysis of the materials on the requisite fine scale, further advancements in the state of the art of instrumental capabilities will be necessary to obtain the desired lateral spatial resolution.

A number of recent developments in microstructural and microchemical analysis methods will almost certainly have a significant impact on characterization of nanoscale materials. Among the most promising new methods currently available are the field ion microscope with atom probe capabilities, the scanning tunneling microscope with atomic force probe capabilities, and such analytical methods as electron-energy loss spectroscopy utilizing ultrafine probe sizes. In addition, the various analytical probes based on new high-luminosity synchrotron radiation sources will undoubtedly make significant contributions. Clearly, the ability to synthesize and examine nanophase materials in situ under carefully controlled conditions, such as ultrahigh vacuum, will be necessary to fully explain their unique characteristics.

In exploring research opportunities for materials with ultrafine microstructures, all elements of the materials science and engineering

continuum need to be addressed, including, the synthesis and processing of nanophase materials, their characterization and properties, and potential application areas. Some of these techniques and materials are summarized here.

- Organic molecular composites are polymeric materials consisting of two or more components dispersed at the molecular level. Examples include compatible polymer blends that are noncrystalline, thermodynamically stable single-phase materials as well as blends of components that are processed into a homogeneous state but are not at thermodynamic equilibrium. The latter blends are polymer analogs of nonequilibrium multiphase alloys. Blends of two amorphous polymers can exhibit significant physical attributes through synergistic effects. The field of polymer blends is extremely active, with much current interest centered on synthetic routes to produce "miscibility windows" wherein the blend can be produced and processed. With further research into synthetic methods, efforts directed at producing various copolymers, and exploration of novel processing of both neat materials and various blends, truly outstanding high-performance materials will certainly be realized.

- Metallic composites are produced by mechanical reduction of two-phase starting materials, which are either mixtures of powders or castings of phases that are mutually insoluble in the solid state. The resulting microstructure has a very dense and uniform dispersion of ultrafine phases. The mechanical reduction technique has the advantage over conventional techniques for forming in situ composites in that it is less dependent on limitations of the phase diagram. Cryomilling, a recent innovation in this field, dispenses with the need to add the dispersed phase and relies on in situ liquid-solid reactions to produce the desired dispersion.

- Metal-ceramic composites (the so-called cermets) are usually synthesized by traditional powder metallurgy methods. Because of the limitations in such methods, it has not yet been possible to extend the range below 1  $\mu\text{m}$  particle size, much less below 100 nm. Thus the challenge is to devise new processing routes for significantly reducing the scale of bicontinuous metal-ceramic composite structures. A promising approach is the controlled decomposition of molecular precursors that encompass within their molecular architecture the correct atomic fractions of the elemental species. This new approach is widely applicable and is limited only by the constraints imposed by molecular design of the precursor solutions. Another approach is the gas-condensation method for synthesizing nanophase materials from mixed ultrafine powders of metals and ceramics. Such ultrafine structures present the opportunity to synthesize a new class of cutting-tool materials that will have the ability to form and maintain a very fine cutting edge that is resistant to chipping. For this reason, it is believed that nanophase composite cermets will find great utility for such high-value-added applications as microtome blades and surgeon's scalpels.

- The ultimate goal of synthetic chemists is to approach the specificity exhibited by nature in controlling the macromolecules of biology, which have extremely well-defined, yet complex, composition and stereoregularity and accomplish a wide variety of functions in a most elegant manner. Researchers in synthetic polymer chemistry are only just beginning to utilize biotechnological approaches to produce synthetic polymers of heretofore never-achieved specificity.

- Progress in nanoscale materials science can also produce advances in ultrafine-scale semipermeable membranes. Membrane microstructures need to be combined with membrane properties, such as flexibility and environmental tolerance. Either man-made assemblies or self-assembled composite materials, in which one phase possesses selective high transport or for which methods are available to selectively remove one of the phases, can provide suitable membranes. The exploitation of polymer gels is also an avenue toward new membrane materials. In particular, gels formed from rod-like macromolecules show promise as interesting materials. Indeed, the general area of phase separation of multicomponent polymer materials to provide ultrafine-scale composites is promising, since the length scale of phase separation can be readily controlled by synthesis of well-defined starting materials and time and temperature processing history.

- Detailed understanding of the relationships between catalyst structure and properties has in the past been hampered by limited structural information on catalysts. New and improved characterization techniques combined with the potential for synthesizing catalysts with controlled microstructures hold potential for making connections between structure and properties in model catalyst systems that closely mimic real catalysts. Such studies also hold potential for synthesizing materials with improved catalytic properties. The application of new catalysts that replace current catalysts will be based primarily on performance criteria. New applications will be based on the potential for new product schemes and the economics for the entire process, of which the catalyst is just one part. Broad classes of catalytic reactions that make use of ultrafine catalytic particles include emission control catalysis, catalytic reforming, synthesis gas catalysis, Ziegler process for polyethylene, and oxidation catalysis. Possible future catalytic processes include catalytic activation of fuel for energy conversion. Since the performance of a catalyst is determined by measuring product yield, testing the activity for a particular reaction is the best way to choose a catalyst. Moreover, important discoveries are made doing kinetic measurements, where serendipity can play a role. Catalyst characterization that is not related to performance is ancillary if the concern is economics.

- Composite materials made up of single-domain and superparaelectric particles have yet to be investigated in a systematic way with proper control of the connectivity and surrounding environment. The controlled synthesis of ultrafine ferroelectric grains will do much to stimulate research in this area. Surface treatment of the ferroelectric phase allows control of the



mechanical boundary conditions. Since polymers are about a hundred times more compliant than ceramics, if a ceramic grain is surrounded by polymer, the mechanical constraints are relatively small. Electrical boundary conditions can also be controlled by adjusting the dielectric constant and conductivity of the surrounding phase.

- Periodicity and scale are important factors when composites are to be used at high frequencies where resonance and interference effects occur. When the wavelengths are on the same scale as the component dimensions, the composite no longer behaves like a uniform solid. Multidomain crystals and ceramics have been used as acoustic phase plates and high-frequency transducers. The extension of this thinking to phenomena associated with optical excitations automatically focuses attention on equivalent nanoscale structures. A wide range of potential property modifications, including shape-induced optical birefringence, shape-controlled optical nonlinearity, and potential modes for inducing optical bistability, remain to be explored. It is clear that there will be corresponding magnetic nanocomposites and that for these materials additional versatility can be expected because of nanoscale interaction with the transport phenomena and the associated optical absorption.

- Many applications for nanophase materials have been identified, but progress has been hampered by lack of sufficient quantities of material for performance evaluation studies and field testing. Thus, in addition to significantly augmenting the current level of support for basic research in the field, there is a need also to support work dedicated to the scale-up and manufacture of nanophase materials.

Although the study of nanophase materials is still in its infancy, it is clear that an exciting new area of research has been opened up and that new materials with novel and useful properties will emerge. Just which avenues of endeavor will be most profitable, however, is not clear. The demonstrated success in synthesizing nanophase metals, single-phase and multiphase alloys, and ceramics with different and sometimes improved properties over those previously available indicates that the possibilities are very promising.



## INTRODUCTION

Materials synthesis--the preparation of materials from atomic or molecular precursors--and materials processing--the manipulation of microstructures to effect desired properties--are both critical to the development of advanced materials with engineered properties. From a historical viewpoint, this concept received its initial impetus in the fields of ceramics and polymeric materials, because traditional methods of materials processing were not applicable. Examples of recent innovations in ceramics (including glass) are laser-pyrolysis of monodispersed particles and hydrothermal synthesis of composites. Of recent interest in polymeric materials has been the development of rigid-rod polymers, self-assembled polymer architectures, polymer blends and alloys, and block copolymers. Developments of comparable significance have occurred in the semiconductor and structural materials fields. Chemical vapor deposition, reactive sputtering, ion-beam processing, and other vapor-phase methods have become the enabling technologies for surface processing in the thin-film device and integrated-circuit industries. These same technologies have recently been adapted to structural applications, such as wear-resistant coatings for bearings, cutting tools, and mirrors. A long history also exists in the area of synthesis of multilayered structures by vapor-deposition methods. These materials have been found to exhibit striking properties, such as a supermodulus effect.

Current research is focused on the design, synthesis, and processing of ultrafine material microstructures, extending into the nanoscale (less than 100 nanometer) regime. This research has been inspired by the realization that significant beneficial changes in the properties of materials can be achieved by progressively reducing the scale of their microstructure while maintaining chemical and microstructural uniformity. Another incentive has been the discovery of novel materials properties when the scale of the microstructure approaches nanoscale dimensions. Birringer and coworkers (1986) tabulated a number of properties measured on nanocrystalline metals and

compared them with values for their coarse-grained counterparts and similar glassy materials. Some of these comparisons are shown in Table 1. The changes in this variety of materials properties are significantly greater in going from conventional crystalline material to the nanocrystalline form than are observed in going from crystalline to glassy solid. Prepared by conventional techniques, these latter changes are generally less than 10 percent.

A series of symposia have addressed the synthesis and processing of nanoscale ceramics and polymers (Hench and Ulrich, 1984; Karasz, 1985; Hench and Ulrich, 1986; Mackenzie and Ulrich, 1988). The materials research community has responded by initiating a new series of symposia at Materials Research Society meetings that extended submicron-scale microstructure concepts beyond nonmetallics to the full range of materials.

TABLE 1 Properties of Nanocrystalline Materials Compared With Their Conventional Coarse-Grained Counterparts\*

Property	Material	Nanocrystal	Conventional Polycrystal
Thermal expansion [ $10^{-6}$ K <sup>-1</sup> ]	Cu	31 (+80%)	17
Density [g/cm <sup>3</sup> ]	Fe	6 (-25%)	7.9
Saturation magnetization @ 4 K [emu/g]	Fe	130 (-40%)	222
Susceptibility [ $10^{-6}$ emu/Oe g]	Sb	20 (+2000%)	-1
Fracture stress [kp/mm <sup>2</sup> ]	Fe (1.8% C)	600 (+1000%)	50
Superconducting T <sub>c</sub> [K]	Al	3.2 (+160%)	1.2

\*The percentages in parentheses represent changes from the reference crystal value (Birringer et al., 1986).

The present report gives a state-of-the-art assessment of activity in this exploding field of research and attempts to identify new areas of research opportunity and some potential application areas for the future. The

focus is on materials with submicron-sized microstructure (with a characteristic length scale less than 100 nanometers), irrespective of the specific type of material or materials being considered.

The scope of the present study includes what is known about metal, ceramic, and polymeric materials and their composites, but it deliberately avoids significant discussion of semiconductor and superconductor materials, electronic and optical properties of multilayers, and rapidly solidified materials, all of which have been adequately treated in previous NMAB publications (National Materials Advisory Board, 1980, 1983, 1988).

#### REFERENCES

- Birringer, R., U. Herr, and H. Gleiter. 1986. Suppl. Trans. Jpn. Inst. Met. 27:431.
- Hench, L. L., and D. R. Ulrich, eds. 1984. *Ultrastructure Processing of Ceramics, Glasses, and Composites*. New York: John Wiley & Sons.
- Hench, L. L., and D. R. Ulrich, eds. 1986. *Science of Ceramic Chemical Processing*. New York: John Wiley & Sons.
- Karasz, F. E. 1985. International Conference on Ultrastructure in Organic and Inorganic Polymers. Final Report AFOSR 85-0314 (15 Sept. 1985-14 Feb. 1986).
- Mackenzie, J. D., and D. R. Ulrich, eds. 1988. *Ultrastructure Processing of Advanced Ceramics*. New York: John Wiley & Sons.
- National Materials Advisory Board. 1980. *Amorphous and Metastable Microcrystalline Rapidly Solidified Alloys: Status and Potential*. Report NMAB-358. Washington, D.C.: National Academy Press.
- National Materials Advisory Board. 1983. *The Reliability of Multilayer Ceramic Capacitors*. Report NMAB-400. Limited distribution, available from DTIC, Washington, D.C.
- National Materials Advisory Board. 1988. *Process Challenges in Compound Semiconductors*. Report NMAB-446. Washington, D.C.: National Academy Press.



## SYNTHESIS AND PROCESSING: GENERAL METHODS

## MOLECULAR SYNTHESIS

The focus of much of present polymer chemistry is on improving synthesis methods for better control of the composition and structure of existing as well as new materials. The basic premise is that specificity in molecular structure rules molecular self-assembly and morphology, which in turn dictates properties.

Precise control of the composition and structure of novel macromolecules (molecular weights of  $10^4$  to  $10^6$ ) to achieve a well-defined synthesis of a particular macromolecule is extremely difficult. Normally, only average quantities are specified: chain length, composition, end groups, stereoregularity, branching, and, most importantly, sequencing.

In the mid-1950s the discovery of certain catalysts that controlled the tacticity (stereoregularity) of  $\alpha$ -olefins permitted the introduction of isotactic polypropylene, currently a 100-million-pound product worldwide. Previous production methods resulted in a mixed-tacticity material with low melting point and poor physical and mechanical properties. Another example is anionic polymerization, which enabled the width of the molecular weight distribution to be significantly narrowed and afforded the polymer chemists standard reference materials for determining a host of physical properties that were known to depend on molecular weight (but not precisely how they depended). Recent advances include group-transfer polymerization (Webster et al., 1983), aluminum-catalyzed ring-opening polymerization (Aida and Inoue, 1981), and cationic polymerization of vinyl ethers (Higashimura, 1986). These techniques provide versatile chemistry to synthesize well-defined macromolecules and efficient routes to the rich varieties of molecular architecture (e.g., diblocks, stars, multiblock, and functionalized end groups) available with macromolecules.

The ultimate goal of synthetic chemists is to approach the specificity of nature in controlling the macromolecules of biology, which have extremely well-defined, yet complex, composition and stereoregularity and accomplish a wide variety of functions in a most elegant manner. As an example, consider the bacteriorhodopsin molecule (Figure 1). This macromolecule provides for light-activated proton transport across the cell membrane as part of the synthesis process of adenosine triphosphate (ATP). Every chain possesses just the correct group of residues to provide the necessary structure and chemical environment for its function. Researchers in synthetic polymer chemistry are only just beginning to utilize biotechnological approaches to produce synthetic polymers of heretofore never-achieved specificity. Thus far, molecular biologists have directed their efforts exclusively toward natural products. An initiative to focus the tremendous power of biotechnological techniques in the area of synthetic macromolecules is quite promising.

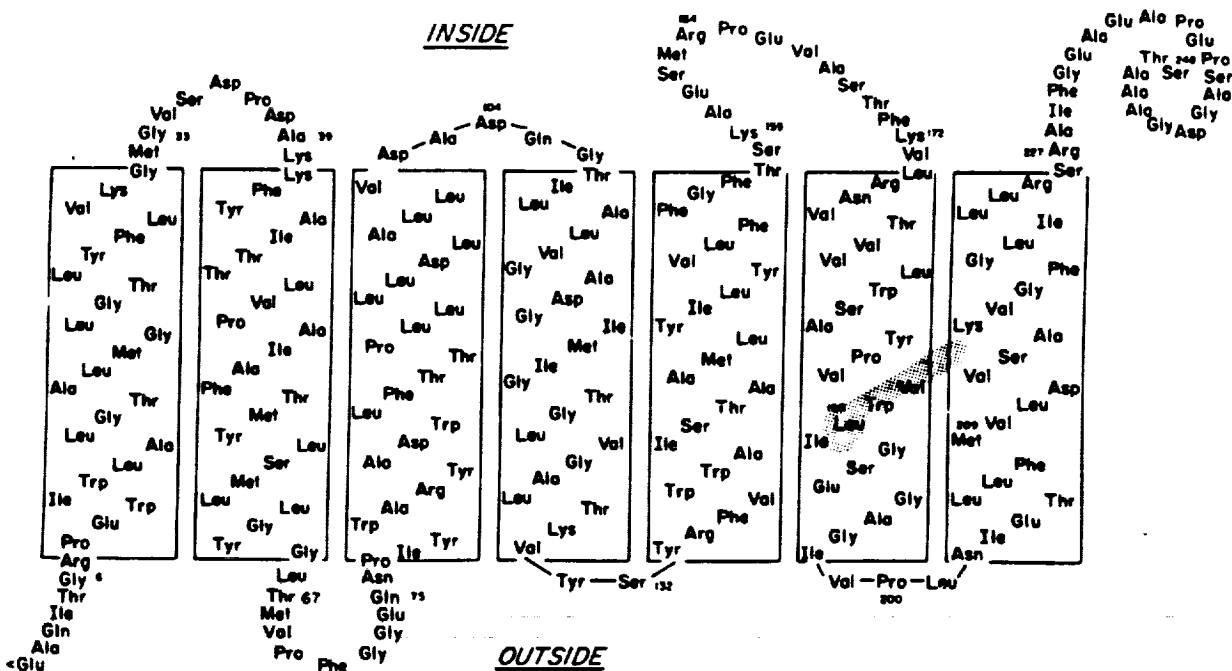


FIGURE 1 Schematic of the bacteriorhodopsin macromolecule, which provides light-dependent proton transport from the inside to the outside of the cell (Khorana, 1987).

Once a macromolecule has been synthesized, consolidation into a material depends, of course, on the detailed processing history. Polymers have characteristic relaxation times that are orders of magnitude slower than other substances, such that they have a long memory of their previous deformation



and temperature history. There is an enormous variety of methods to process polymers, most of which aim at influencing overall texture (extrusion, injection molding, etc.). Of recent interest are various thin-film applications (lithography, dielectrics, optical coatings, etc.) where the polymer may be cast from an initially dilute solution or produced in situ by polymerization of a thin monomer film (both by liquid-phase and vapor-phase methods). Chemical and structural modification of polymer surfaces is also possible. In addition, reactions occurring in the two-dimensional environment of a surface can yield exciting possibilities for novel materials synthesis (e.g., the formation of polyacetylene on catalytic surfaces). Another example of much current interest involves the field-induced crystallization of PVF<sub>2</sub> to create superior piezoelectric, pyroelectric, and ferroelectric materials.

The use of polymers for nonlinear optical (NLO) processes is gaining considerable attention because of the ability to synthesize and tailor molecular structures that have inherently fast response times and large second- and third-order molecular susceptibilities. Polymers provide processing options not available with other classes of NLO materials. These encompass many options on the ultrastructure and submicron levels, including both main-chain and side-chain liquid crystalline polymers, poled isotropic polymers with functionalized chromophores, guest-host structures, polymer alloys and blends, spin-coated films, Langmuir-Blodgett films, and molecular assemblies (Heeger et al., 1988; Khanarian, 1986; Ulrich, 1987).

The characteristic size of a polymer molecule is proportional to the square root of its length. Typical macromolecules are 5 to 20 nm in size, so that perturbation from the two external surfaces of a thin film on a polymer molecule is already strong at thicknesses in the 10-nm range, and completely new physical behavior is expected at thicknesses at and below the characteristic size. For example, craze microstructure changes dramatically for films less than about 0.1  $\mu$ m thickness. Much work in characterization of polymeric materials in the thin-film regime is needed to explore future opportunities for applications in two-dimensional and particularly three-dimensional device architectures.

## REDUCTIVE PYROLYSIS

The synthesis of metal-ceramic composites, so-called cermets, is usually accomplished by traditional powder metallurgy methods. The prototypical example is Co-WC, which is the workhorse material of the cutting-tool industry worldwide. This material has a bicontinuous structure, with the hard WC phase being the major constituent. It is the continuity of the WC phase in three dimensions that provides the compressive strength and elastic stiffness of the material, whereas the relatively soft and ductile cobalt residing within the interstitial space of the hard phase controls the fracture toughness. Trade-offs in strength and toughness are achieved by control of the relative volume fractions of the two phases. The higher the volume fraction of cobalt, the

greater the toughness, as would be expected. For a fixed volume fraction of cobalt, the compressive strength or hardness of Co-WC increases linearly with decreasing scale of the bicontinuous structure. Because of the limitations in traditional powder metallurgy processing, it has not yet been possible to extend the range of such measurements below 1  $\mu\text{m}$  particle size.

The challenge, therefore, is to devise new processing routes for significantly reducing the scale of bicontinuous metal-ceramic composite structures. A promising approach for achieving this goal is by controlled decomposition of molecular precursors that encompass within their molecular architecture the correct atomic fractions of the elemental species. This has been investigated in the Co-WC system, where the predesigned molecular precursor is a complex water-soluble transition-metal coordination compound (McCandlish and Polizzotti, 1989). An example is  $\text{Co(en)}_3\text{WO}_4$  salt, which gives a 50:50 atomic ratio of W and Co. After heat treatment in  $\text{H}_2$  at  $600^\circ\text{C}$ , the resultant structure is a porous aggregate of clusters (order of 10 nm) of the two species. Consolidation at this stage realizes a Co-W nanocomposite whose properties have yet to be explored. If the porous aggregate is subjected to an additional reaction in a controlled C-activity environment, it is possible to access any point along the tie-line connecting 50/50 Co-W to the C corner of the Co-W-C ternary phase diagram. When the activity of the C is set between 0.52 and 1.00 (at a temperature between  $800^\circ\text{C}$  and  $1000^\circ\text{C}$ ), this fixes the structure in the two-phase field of Co plus WC. Since this conversion process takes place at  $800^\circ\text{C}$ , the material has an ultrafine structure. Powders produced in this way can be consolidated by conventional methods while retaining their submicron-sized microstructure. Examples include rapid liquid-phase sintering, laser glazing, and plasma spraying, where the thermal transient in the liquid phase is so brief that no significant coarsening of the microstructure occurs.

This new approach to cermet synthesis is widely applicable and is limited only by the constraints imposed by molecular design. Chemical precursors have already been formulated for the direct synthesis of a wide variety of metal-carbide, metal-boride, and metal-nitride composites.

## GEL SYNTHESIS

The sol-gel processing of mixed organometallic precursors has been used to form ferroelectric and piezoelectric ceramics (Wu et al., 1984). Optically transparent barium titanate, lead titanate, and other perovskites were crystallized that had uniform nanocrystalline structures of preferred orientation. These nanocrystalline ceramics had near single-crystal-like properties, as shown by the dielectric constant-temperature profiles in Figure 4, in contrast to conventional polycrystalline ferroelectrics and piezoelectrics with grain sizes less than 1  $\mu\text{m}$ , which lose their nonlinearity.

The sol-gel process refers to a room-temperature chemical route that is used for preparing oxide materials. The process involves initially a homogeneous solution of the appropriate alkoxides (Hench and Ulrich, 1984). Alkoxides are the organometallic precursors for silica, alumina, titania, and zirconia, among others. A catalyst is used to start reactions and control pH. The reactants are first hydrolyzed to make the solution active, followed by condensation polymerization along with further hydrolysis. These reactions increase the molecular weight of the oxide polymer. The pH of the water-alcohol mixture has an influence over the polymerization scheme such that acid-catalyzed solutions remain transparent and base-catalyzed solutions become opaque. Eventually the solution reacts to a point where the molecular structure is no longer reversible. This point is known as the sol-gel transition. The gel is an elastic solid filling the same volume as the solution. When dried, the gel gradually shrinks and transforms to a rigid oxide skeleton. The oxide skeleton has interconnected porosity. The nature of the porosity is determined by the processing steps. As a result, the porosity can be tailored in terms of size, shape, and volume. This controlled porosity can be exploited in many ways. One way is by infiltration of a second phase to form submicron-scale composites.

Hypercritical evacuation of the solvent from the pores results in aerogels, and natural evaporation results in xerogels (Klein, 1987). Xerogels may have water and alcohol in the pores or solvent substituted in various proportions with a drying control chemical agents (DCCA). In aerogels the pore size is on the scale of 10 to 50 nm, approaching sizes of those pores in samples prepared by colloidal techniques. In xerogels, the pore size is on the scale of 2 to 5 nm. Aerogels dry much faster than xerogels. This is significant in forming monolithic shapes without cracks. In fibers and thin films, drying is less of a problem.

DCCAs make it possible to optimize gelation, aging, and drying of gels to produce large-scale, fully dried monolithic gels (Ulrich, 1988a). They also make it possible to control the size and shape of the pore distribution. Addition of a basic DCCA such as formamide produces a large sol-gel network with uniformly large pores (see Figure 2). An acidic DCCA, such as oxalic acid, in contrast, results in a somewhat smaller-scale network after gelation, but also with a narrow distribution of pores.

The DCCAs minimize differential drying stresses by minimizing differential rates of evaporation and ensure a uniform thickness of the solid network that must resist the drying stress. Achieving a uniform scale of structure at gelation also results in uniform growth of the network during aging, which thereby increases the strength of the gel and its ability to resist drying stresses.

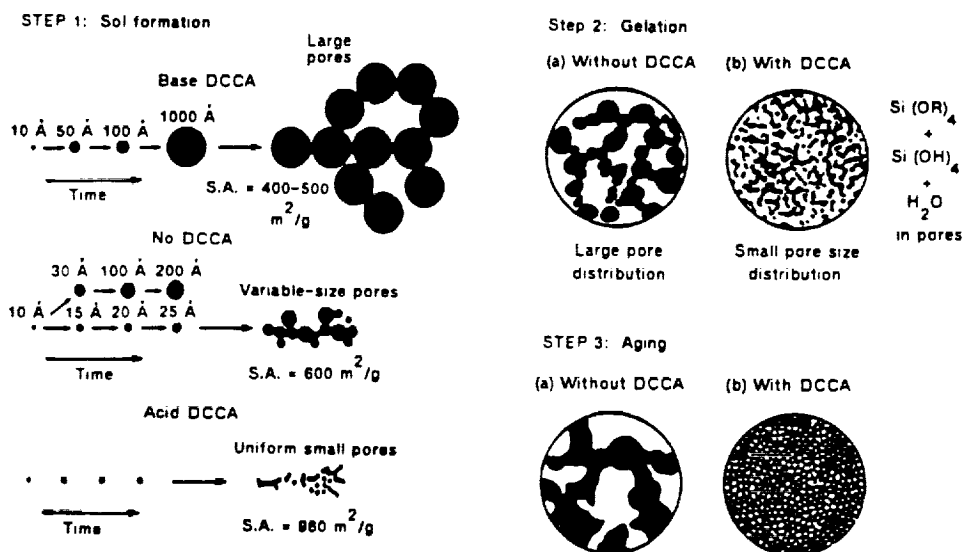


FIGURE 2 Control of sol-gel processing with organic acid DCCAs (Hench and Ulrich, 1986).

Recently, the sol-gel process has been investigated widely for the synthesis of a variety of glasses and crystalline materials suitable for ceramic matrix composites (Hench and Ulrich, 1986). In all cases the advantages of the process are purity and low-temperature processing (see Figure 3). By far the most common system is that composed of

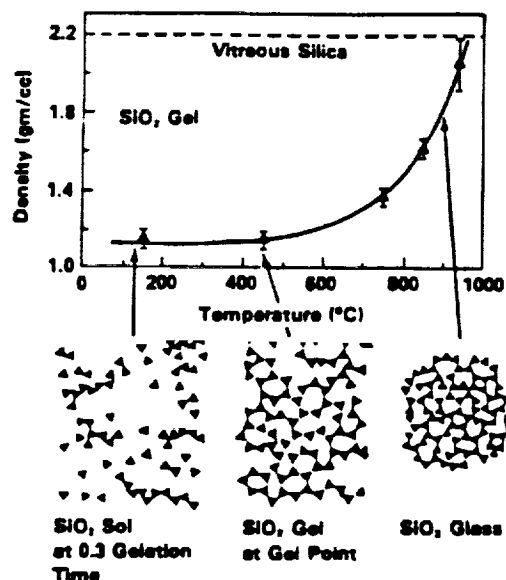


FIGURE 3 Densification microstructures for  $\text{SiO}_2$  gels. (Reprinted by permission of the publishers, Butterworth & Co. (Publishers) Ltd.®, from Polymer 28, 533, D. Ulrich, 1987)

tetraethoxysilane-water-alcohol. Various studies have elucidated the influence of the ratios of the starting species, the catalyst, and other additives on the structure of the final gel or ceramic. Depending on these conditions, powders, fibers, films, and monolithic pieces of transparent or opaque oxide can be produced (Figure 4).

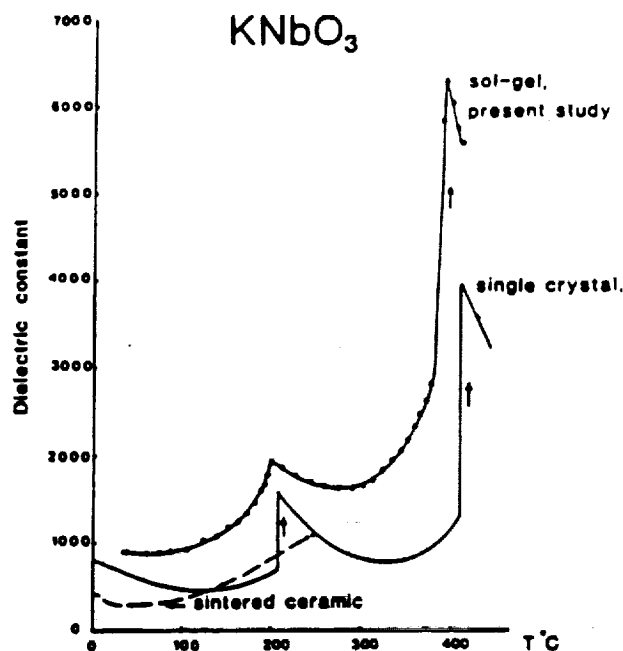


FIGURE 4 Superior properties of sol-gel samples.

(Reprinted by permission of Elsevier Science Publishing Co., Inc. Ferroelectric Ceramics--The Sol-gel Method Versus Conventional Processing, by E. C. Wu, K. C. Chen, and J. D. Mackenzie, Better Ceramics Through Chemistry III: Materials Research Society Proceedings, Vol. 32, 1984.)

### In Situ Composites

There are several published reports on the sol-gel process applied to in situ composites (Figure 5). In one case, short and long ceramic fibers were embedded in an alumina gel. In another case, a carbon-containing composite was prepared in situ by pyrolyzing an organometallic gel precursor. More recently, a class of materials called diphasic gels has been developed. These materials are a gel host for the precipitation of a second phase on an extremely fine scale. Although these approaches produce unusual composite materials, none of them addresses specifically the fabrication of monolithic composites. While a relevant patent exists for carbon fibers, what is needed is a practical demonstration of a sol-gel matrix rigid composite with thermal stability. When it comes to evaluating a composite, the important parameters are mechanical behavior and thermal stability. The question is whether they can be achieved from a sol-gel process.

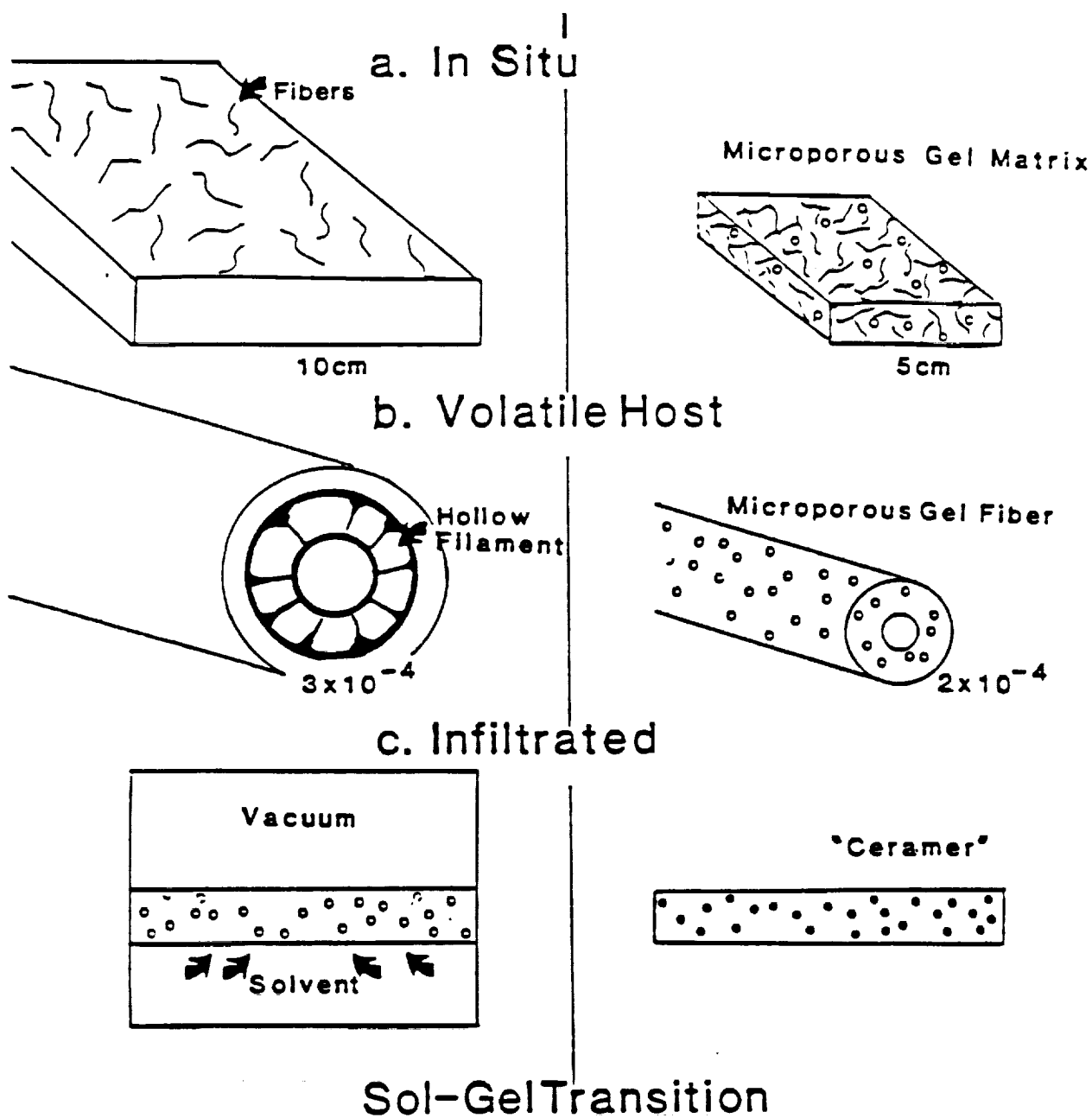


FIGURE 5 Schematic of composite structures (Klein, 1987).

### Porous Sol-Gel Composites

An important characteristic of sol-gel-derived materials is the very large percentage (30 to 70) of microporosity in the materials after drying. Consequently, a wide range of physical properties and microstructural control can be achieved with materials of the same chemical composition by varying the volume fraction, size distribution, and connectivity of the microporosity. Microporous structures can be impregnated with passive and active organic, polymeric, and inorganic materials to produce a wide range of structural, optical, and electromagnetic composites with submicron dimensions (Ulrich, 1988a).

Porous gel glass-organic polymer composites reveal significant differences between nanoscale and bulk polymers. For example, it is well known that as the size of a particle decreases, the surface area-to-volume ratio increases, such that a 10-nm particle has a surface area-to-volume ratio 10,000 times that of a 0.1-mm particle. The thermodynamics of surfaces differ significantly from that of the interior of a material, raising the question as to whether differences can be observed between the bulk polymer and the polymer impregnated into 10-nm pores of the silica gel. In Table 2, data for polymethylmethacrylate (PMMA) prepared under identical conditions are shown with one difference. In the second case the porous gel was impregnated with monomer and PMMA polymerized in the gel. A significant reduction of the glass transition and curing temperatures was observed. The density of the polymer phase was measured to be the same in both cases. These transparent composites have relatively high strengths and elastic modulus as well as low densities (Pope and Mackenzie, 1985, 1986).

TABLE 2 Glass Transition and Curing Temperature for PMMA

<u>Sample</u>	<u>Glass Transition Temperature (°C)</u>	<u>Curing Temperature (°C)</u>
PMMA (bulk)	97.2	157.1
PMMA (in silica gel)	81.9	120.5

### Volatile-Host Method

Another approach for near-net-shape processing requires an organic polymer as well as an inorganic polymer. In one method, known as the volatile-host method, a plastic filament is dipped into an alkoxide solution

and a thin film of liquid adheres to the filament. Upon exposure to atmospheric moisture, the film gels. The filament may be dipped repeatedly to build up a series of films. At this point, a rigid, continuous shell runs the length of the filament.

Further work is in progress to optimize the processing steps so that a crack-free fiber can be collapsed to glass at around 1000°C in containerless conditions. In addition, the volatile host, being flexible, can be used to facilitate conformal coatings on complex shapes.

In some cases, the organic polymer is left in the ceramic matrix when the composite is intended for use at low temperatures. The name *ceramers* has been coined for such materials (Klein, 1987).

### Infiltrated Composites

The third experimental technology with respect to composites involves infiltration (Klein, 1987). In this case the objective is to use sol-gel processing to create a nanoporous matrix that can be infiltrated by a second phase. The second phase is intended to improve the thermal shock resistance of the composite.

The product of the sol-gel process is by its very nature two-phase. At the time the oxide polymer condenses, the second phase is the rejected solvent. When the solvent is removed during drying, the second phase is the interconnected porosity. The channels where gas replaces liquid are typically 2 to 20 nm, uniform in cross section, and narrowly distributed in size. In the case of silica, this porosity does not interfere with transmission of visible light despite measured surface areas in the range of 200 to 500 m<sup>2</sup>/g. Since the porosity in silica is interconnected until temperatures around 800°C, the pore channels provide a means for distributing a second phase with high uniformity. The second phase may be introduced by a solvent-exchange process or by liquid intrusion.

The thermal expansion, thermal conductivity, and oxidation behavior at elevated temperatures are the important physical properties of ceramic matrix composites. In the long run, the projected advantages for the sol-gel approach to composite fabrication are the simple processing steps, the flexibility of solution chemistry, the low-temperature treatments, and the small investment in equipment. There is a need for innovative thinking to adapt sol-gel processing to ceramic matrix composite fabrication.

### **SUPERCritical FLUID PROCESSING**

Dense gases and liquids at conditions above their respective thermodynamic critical points are known as supercritical fluids. The



supercritical regime is illustrated in Figure 6. A supercritical fluid behaves as a high-density gas with liquid-like density. At moderate temperature and pressure, such fluids have high solubility for other materials and exhibit no surface tension.

### Supercritical Fluid Characteristics

- Liquid-like density
- No surface tension
- Moderate temperature and pressure  
(propane critical point 97°C and 42 bar)

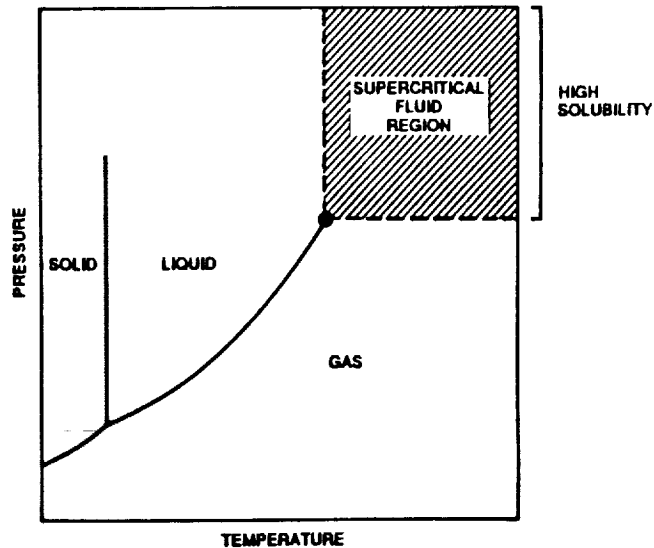


FIGURE 6 Supercritical fluid characteristics (R. A. Wagner, private communication).

The technique offers several opportunities for the processing of submicron-level particles, structures, and coatings. One recent example demonstrated this potential (Wagner, 1988). Current oxidation protection for carbon-carbon composites relies on outer coatings of silicon carbide ceramic and glassy sealers. Thermal expansion mismatch between the silicon carbide and the composite results in coating cracks and oxidation at temperatures below 800°C. Using supercritical fluid impregnation, both oxidation resistance and bend strength of the coated carbon-carbon composite were substantially improved.

There is a broad range of applications for this approach (Smith et al., 1987). These include powder preparation, surface modification, thin film deposition, and, as shown by the above example, composite impregnation.

### LASER PYROLYSIS

Laser-initiated gas phase synthesis methods have been developed for making powders and thin films of ceramic materials. Powders have been synthesized with crossflow and counterflow gas stream-laser beam configurations and with both static and flowing gases (Cannon et al., 1982).

In the crossflow configuration, the laser beam having a Gaussian shaped intensity profile orthogonally intersects the reactant gas stream possessing a parabolic velocity profile. The laser beam enters and exits the cell through KCl windows. The premixed reactant gases, under some conditions diluted with an inert gas, enter through a stainless steel nozzle located below the laser beam. A coaxial stream of Ar is used to entrain the particles in the gas stream. Cell pressures are maintained between 0.08 and 2.0 atm with a mechanical pump and throttling valve. The powder is captured in a microfiber filter located between the reaction cell and vacuum pump.

The counterflow geometry, with laser beam and reactant gas streams impinging on each other from opposite directions, has the important advantages of exposing all gas molecules to identical time-temperature histories and absorbing all of the laser energy. However, the achievement of a stable reaction requires that the reaction and gas stream velocities must be equal and opposite to one another. This is readily accomplished once process conditions are defined.

Principally, Si,  $\text{Si}_3\text{N}_4$ , and SiC powders have been made from appropriate combinations of  $\text{SiH}_4$ ,  $\text{NH}_3$ , and  $\text{C}_2\text{H}_4$  gases.  $\text{B}_2\text{H}_6$  has been used to add boron to the Si and SiC powders as a sintering aid.  $\text{TiB}_2$  has been successfully synthesized from  $\text{TiCl}_4 + \text{B}_2\text{H}_6$  mixtures. Boron powder has been made from both  $\text{BCl}_3$  and  $\text{B}_2\text{H}_6$ .  $\text{TiO}_2$  and  $\text{Al}_2\text{O}_3$  have been made from alkoxides and reactants like  $\text{Al}(\text{CH}_3)_3$ . While most of this process research has been focused on a limited set of compounds and reactants, it is apparent that laser-induced reactions are applicable to a broad range of materials.

The Si,  $\text{Si}_3\text{N}_4$ , and SiC powders all exhibit the same general features and match the idealized characteristics sought. The particles are spherical and uniform in size ranging from about 20 to 300 nm. The  $\text{Si}_3\text{N}_4$  and SiC powders are smaller and have a narrower size distribution than the Si powders.

For making thin films by the laser-induced CVD process, the laser beam passes parallel to the substrate through an optically absorbing gas that is heated by the laser. Thin films of amorphous hydrogenated silicon ( $\alpha\text{-Si:H}$ ) and  $\text{Si}_3\text{N}_4$  have been made by operating under conditions where heterogeneous rather than homogeneous nucleation occurs. The virtually unique combination of high gas temperature and low substrate temperature permits rapid deposition rates and controlled film properties. Resulting films have demonstrated superior electrical, optical, structural, and mechanical properties.

## COLLOIDAL SYNTHESIS

In the shape-forming of ceramics, a desirable goal is to achieve near-net-shape processing of complex monoliths with precise control of structural features at the submicron level. There are three basic steps that are closely linked in the conventional processing sequence: (1) synthesis or selection of

the raw materials in powder form, (2) consolidation of powders either with the use of a liquid medium or by dry-pressing techniques, and (3) densification of the powder compacts by sintering. The importance of establishing a strong correlation between these three process steps is well recognized (Aksay, 1988).

Colloidal techniques are useful in avoiding problems associated with uncontrolled agglomerate formation during the synthesis of powders and also in obtaining very-low-viscosity powder and fluid systems that are suitable for near-net-shape forming. A desirable goal is to work with systems containing submicron-size particles at solid contents of greater than 70 volume percent and viscosities of less than 1 Pa-s. With the use of polymeric additives and polydisperse particle size systems, this goal can be achieved in the micrometer range. When the particle size is reduced to the nanometer range, it becomes increasingly difficult to accomplish this goal via these conventional methods. However, with the use of lubricating surfactants, it is also possible to form dense (greater than 60 volume percent) nanoscale structures.

Processing steps leading to the formation of colloiddally consolidated compacts first start with the dispersion of particles in a liquid medium. This dispersion stage is useful for various reasons: (1) when the particle concentration is low, dispersed colloidal suspensions can be used to eliminate flow units larger than a certain size through sedimentation or centrifugal classification; (2) the surface chemistry of the particles can be modified through the adsorption of surfactants; and (3) the mixing of multiphase systems can be achieved at the scale of the primary particle size. Once the desired modifications are achieved, transition from a dispersed to a consolidated structure is accomplished either by increasing the particle-to-particle attraction forces (i.e., flocculation) or by increasing the solid content of the suspension (i.e., forced flocculation). Experimental observations have shown that colloiddally consolidated systems always display hierarchically clustered nonequilibrium structures as a result of a nucleation and growth process of particle clusters. The most important consequence of this hierarchical clustering is that, even in monosize particle systems, a monomodal void size distribution is never attained. When the first-generation particle clusters are at a packing density of 75 percent, the packing density of the second-generation clusters drops to an average value of at least 64 percent because of the bimodality of the void size distribution.

Since these hierarchically clustered structures signify the formation of nonequilibrium structures, Aksay (1988) has suggested the form of a nonequilibrium phase diagram in  $V/kT$  versus particle concentration space (Figure 7), where  $V$  denotes the generalized interaction potential,  $k$  is the Boltzmann constant, and  $T$  is the temperature. The high  $V/kT$  region of this diagram outlines the equilibrium transitions observed in highly repulsive systems in electrostatically interacting systems. The onset of fluid-to-solid transition shifts to lower concentrations as the hydrodynamic radius of the

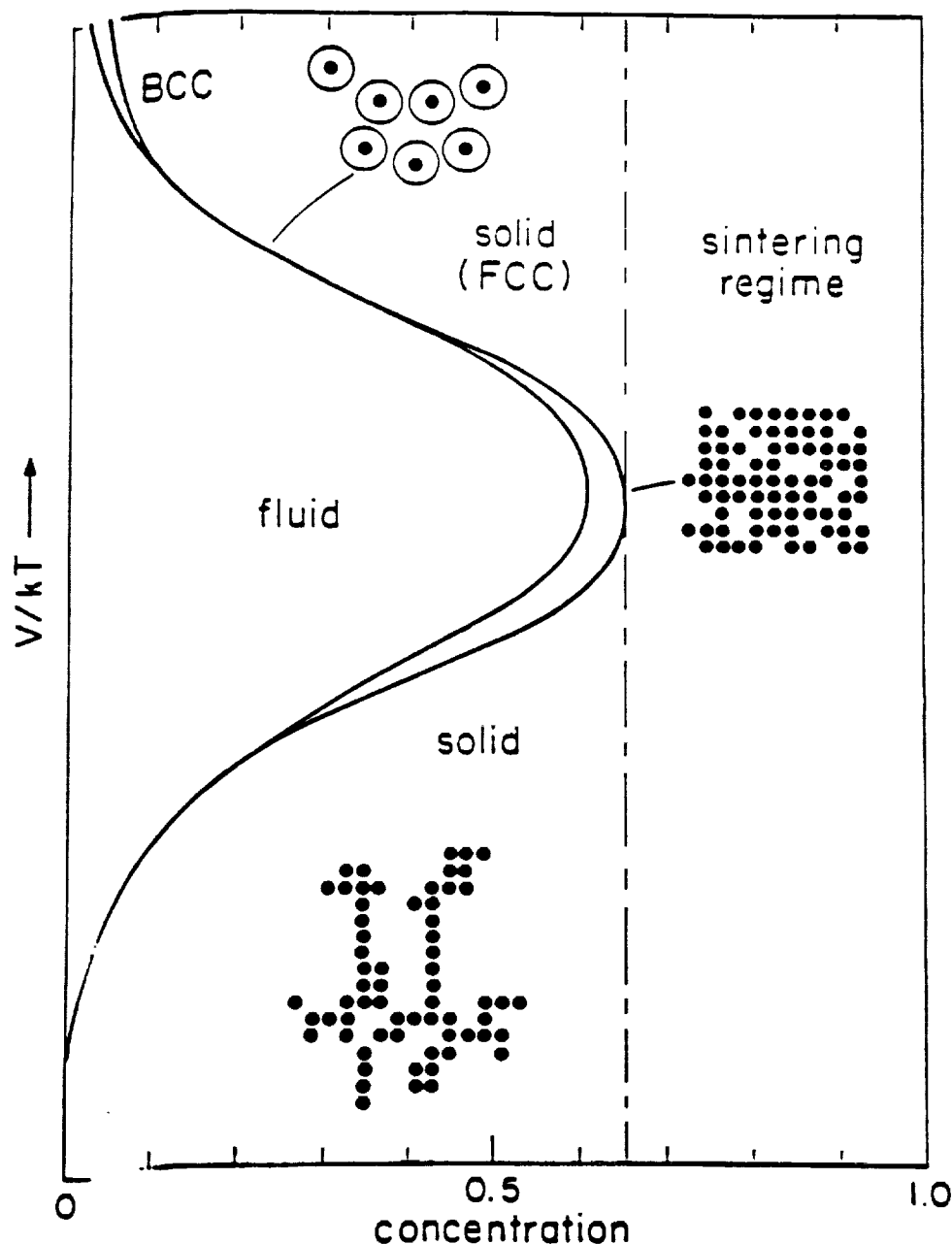


FIGURE 7 Schematic form of the nonequilibrium colloidal phase diagram. In the high  $V/kT$  region, the onset of fluid-to-solid transition shifts to lower concentrations because of increasing hydrodynamic radius. A similar trend is observed at the low  $V/kT$  region because of the formation of low-density fractal clusters. Body-centered cubic (bcc) packing of particles is observed with organic particles, but ceramic systems have been observed only with face-centered cubic (fcc) packing (Aksay, 1988).

particles increases with the development of an electrostatic repulsive barrier around the particles. From a practical point of view, the conditions corresponding to the upper and the lower ends of this diagram must be avoided to obtain high packing densities in the casts and to minimize drying shrinkages. The middle range is the most suitable for the preparation of high-concentration slips that can be converted to high-packing-density casts with a minimum amount of shrinkage.

One effective way of developing sufficient repulsive interaction between particles in concentrated colloidal dispersions without increasing the hydrodynamic radius is through the steric repulsion of polymeric protective coatings. Industrial practice has shown that polyelectrolytes are especially useful in achieving this goal in aqueous systems.

The nucleation of particle clusters and their networks as hierarchically clustered structures takes place in all size ranges. The extent of the hierarchy determines the overall packing density of the system. Recent studies have shown that, when suspended particles are first coated with lubricating surfactants, it is possible to form close-packed structures (Figure 8). This promising approach needs to be generalized in its applications to a variety of multiphase systems.

To achieve lower sintering temperatures and a minimum amount of grain growth, the size of the voids must be minimized during forming. Some of the most commonly used forming techniques are not suitable for this purpose. Slip- and tape-casting techniques that use filtration as the basic consolidation mechanism fall into this category. In contrast, techniques such as extrusion and injection molding, which result in shear deformation, yield a relatively narrow pore size distribution because of the restructuring of particle clusters during the forming operation. A narrow pore or particle size distribution may not always be the most effective route to densification. Appropriate multimodal size distributions of particles can provide an alternative path toward densification.

## REACTIVE SPUTTERING

Reactive sputtering is a versatile technique capable of synthesizing a broad class of materials. Thin films of virtually any metal (Ag, Ti, Mo, etc.) or elemental dielectric (Si, Ge, etc.) can be deposited by sputtering from a source of the same material using Ar or Kr inert gas.

Addition of a reactive gas such as  $O_2$ ,  $N_2$ , or  $H_2$  to the Ar or Kr permits deposition of oxides, nitrides, and hydrides from metallic or elemental dielectric sources. For example, a Si source can be used with Ar, Ar +  $O_2$ , Ar +  $N_2$ , or Ar +  $H_2$  to deposit thin films of Si,  $SiO_2$ ,  $Si_3N_4$ , and Si:H alloys. Compared to conventional evaporative techniques for depositing thin films, sputtering generally provides improved control over the properties of



FIGURE 8 (a) Fractal clusters of 15-nm gold particles that result in the formation of low-density compacts; (b) the dense packing of the same gold particles after they are first coated with lubricating surfactants. (Reprinted by permission of Elsevier Science Publishing Co., Inc. from Better Ceramics Through Chemistry III, by C. J. Brinker, P. E. Clark, and D. R. Ulrich, eds., Material Research Society Proceedings, 1988.)

conventional coating materials. Sputtering also makes possible the deposition of new coating materials with complex compositions that cannot be made by evaporation.

To allow coating of plastics and other temperature-sensitive substrates, reactive magnetron sputtering can be used. Magnetic confinement of secondary electrons minimizes substrate heating. Increased adatom energy at the substrate plus increased chemical reactivity in a gas discharge allow fabrication of dense, adherent, and fully reacted dielectric compounds without external substrate heating.

By the use of multiple sources, one can control composition and thickness of the ultrafine multilayered structures. Substrate temperature, bias, and deposition rate in the appropriate combination can be utilized to control the microstructures from the microcrystalline to the glassy state. Some examples of magnetron sputtered optical coatings on polymeric substrates are given in Table 3.

TABLE 3 Magnetron Reactively Sputtered Coating Materials and Measured Properties.

Coating Material	Refractive Index at 550 nm	Absorption Edge (nm)
TiO <sub>2</sub>	2.26	350
Nb <sub>2</sub> O <sub>5</sub>	2.22	330
V <sub>2</sub> O <sub>5</sub>	2.20 (700 nm)	475
Ta <sub>2</sub> O <sub>5</sub>	2.13	275
ZrO <sub>2</sub>	2.04	235
SnO <sub>2</sub>	1.93	315
Al <sub>2</sub> O <sub>3</sub>	1.58	<200
SiO <sub>2</sub>	1.46	<200
Si <sub>3</sub> N <sub>4</sub>	1.95	220
AlN	1.94	220

### CRYOCHEMICAL SYNTHESIS

Although a number of methods exist for making ultrafine-grain (diameter <100 nm) starting materials, freeze-drying methods (Schnettler et al., 1968) have several very important advantages. The most prominent advantage is that very little change in technique is required over an unlimited range of materials of varying crystal structure, and control is afforded over particle sizes from very reactive fine-grain materials of 5 nm

sizes to less reactive micrometer sizes. The freeze-drying process for producing metal or ceramic powders is very simple in concept. It involves the dissolution of salts containing cations of interest, flash freezing of the resulting solution, and sublimation of the solvent, followed by conversion to the desired product. The conversion can be effected by calcining to the appropriate oxide or metal form. Alternatively, conversion may be to a compound--for example, by reacting with a carburizing gas to form a refractory carbide. The initial step of the process (that is, the dissolution of the salt or salts) produces a homogeneous solution that is retained during the low-temperature quenching process. This essentially locks in the cation distribution that had been present in the liquid solution. The homogeneity of the product is retained during the freeze-drying process, since little atomic movement occurs during the low-temperature sublimation process. Because most of the frozen solvent molecules are removed by sublimation, the resulting structure is a very open one. The resulting increased surface-to-volume ratio makes feasible lower calcining temperatures, which in turn leads to a finer particle size after the calcining operation.

#### CHEMICAL VAPOR SYNTHESIS

Submicron-sized powders have been produced by chemical vapor synthesis for many years, using flame or plasma torch reactors. Primary particles produced can range in size from as small as 6 nm to as large as 600 nm, with size controlled primarily by the flame or plasma temperature and rate of cooldown. Often these primary particles are cemented together to form aggregates, which can contain from 10 to as many as 1000 primary particles, depending on the substance and manufacturing conditions. Normally, conditions that produce small primary particles yield aggregates with many particles so that complete control of product morphology is not possible.

With the exception of carbon black, flame reactors are normally employed to produce oxides--the largest volume commercial products being fumed silica and titanium dioxide. Fumed alumina, zirconium dioxide, and mixed oxides have been produced on a developmental basis. Plasmas permit temperatures well above those attainable with combustion or chemical flames and also allow independent control of the operating atmosphere. Diverse ceramic raw materials such as titanium diboride, carbides, and nitrides have been produced in these systems, and some of these operations are at the commercial prototype scale.

Generally, chemical vapor synthesis requires moderately expensive volatile metal chlorides or fluorides as the raw material, but the simplicity of the process (e.g., product isolation) often compensates for this cost.



## ION-BEAM PROCESSING

Ion implantation is a method of introducing elements into a target material to form a controlled mixture up to 1  $\mu\text{m}$  in depth, with a high degree of precision and without having to heat the material.

The ion implantation process begins by forming a plasma of ions containing the elements to be implanted. Ions are then extracted from the plasma, focused, and accelerated to an energy about 10 to 30 keV. The desired ion species is then selected by a magnet and is further accelerated up to many MeV before reaching the surface of the solid. Upon entering the surface of the solid, the incident ion loses its initial kinetic energy by collision with the atoms and excitation of the electrons in the solid. The final distribution of the ions can be accurately predicted by either analytical theories or computer simulations. The penetration depth of the ions is controlled by the energy to which they are accelerated, and the final composition is determined by the depth profile and total number of ions implanted.

Since the ion depth is typically less than 1  $\mu\text{m}$ , ion implantation is suitable for surface engineering on the submicron scale. In addition to the high degree of precision and control of the distribution of the implanted species, which may be any element in the periodic table, ion implantation is a nonequilibrium process that can be used to make new materials, including metastable crystalline and amorphous materials on surfaces. An increasing effort is being directed toward applications of ion implantation to the fabrication of semiconductor devices, corrosion and wear-resistant surfaces, and high-temperature superconducting thin films. Clearly, the development of micron- or submicron-sized ion beams for patterning will have considerable future impact in these areas.

Ion-beam mixing is a mechanism whereby energetic ions bring about the intermixing of layers during ion irradiation. A variety of submicron surface structures, which may be either amorphous or crystalline, can be formed, depending on the chemical composition of the surface layers and the ion-beam irradiation conditions.

In many ways ion-beam mixing is analogous to ion implantation. They differ principally in emphasis. In ion implantation, the interest focuses on modifying the solid by the addition of the implanting species. But the maximum concentration of the implanted species in a solid can be severely limited by the process of sputtering that occurs during ion implantation. The highest concentration of the implanted species is typically less than 30 percent.

Ion-beam mixing does not suffer from the limitation of sputtering to the extent that ion implantation does. In ion-beam mixing the desired species is first deposited onto the surface of a sample by some conventional means such as evaporation deposition or sputter deposition. An ion beam of sufficient

energy is then used to bombard the interface between the overlayer and the substrate, resulting in the "mixing" of the two. Unlike the ion implantation process, the primary function of the incident ion beam in ion-beam mixing is to induce collision cascades at the interface.

Similar to ion implantation, ion-beam mixing is suitable for surface engineering on the submicron scale and is also a nonequilibrium process. Because the composition of the mixed layer is not limited by sputtering, ion-beam mixing can produce new materials at compositions difficult to achieve by ion implantation. Therefore, ion-beam mixing is a powerful alternative to conventional ion implantation. In addition, it has been shown that ion-beam mixing is a valuable research tool in studying the "chemical effect" on atomic diffusion induced by ion bombardment and the formation of quasicrystalline materials.

## MECHANICAL PROCESSING

Metallic composites can be produced by mechanical reduction (Bevk, 1983) of two-phase starting materials, which are either mixtures of powders or castings of phases that are mutually insoluble in the solid state. The reduction may be performed by swaging, extrusion, wire drawing, or rolling. Both phases must be sufficiently ductile to allow large reductions. In most cases, the matrix has an fcc structure, whereas the second phase is either fcc or bcc. The resulting microstructure has a very dense and uniform dispersion ( $10^6$  to  $10^{10}$  cm<sup>-2</sup>) of very fine (5 to 100 nm diameter) filaments. The mechanical reduction technique has the advantage over other techniques for forming in situ composites, such as directional solidification of eutectics, in that it is less dependent on limitations of the phase diagram. The resulting interfaces usually have a higher structural mismatch, which makes them more effective for interaction with dislocations in strengthening.

This approach has been exploited to fabricate high-strength superconducting wires consisting of Cu wire with thin filaments of the superconductor Nb<sub>3</sub>Sn. The ultrafine structure is produced by repetitive drawing of Cu and Nb, with intermediate anneals, followed by bulk diffusion of Sn to convert the Nb filaments to Nb<sub>3</sub>Sn.

The performance of Cu-Nb<sub>3</sub>Sn superconducting composites is particularly impressive at low and moderate magnetic fields, where the combined effects of very small grain size and interface flux pinning and proximity phenomena result in exceedingly high critical current densities (Bevk, 1983). The self-field critical current densities can be as high as  $1.4 \times 10^7$  A cm<sup>-2</sup>, and the maximum flux primary force at 3T exceeds  $7 \times 10^{10}$  Nm<sup>-3</sup>. These values are comparable to the highest values obtained in thin films and layered composites. This method is being applied to other traditional superconductors as well as the new class of perovskite high-T<sub>c</sub> superconductors.

Mechanical alloying is another approach to the fabrication of inert-particle dispersion-strengthened materials. Typically, ceramic particles are mechanically mixed with metal powders in a high-energy ball mill to produce an intimate mixture of the two phases. The attrition process, by a repetitive particle fragmentation mechanism, gives rise to a fine dispersion (less than  $0.1\text{ }\mu\text{m}$ ) of ceramic particles in a metal matrix. After consolidation by hot extrusion, the resulting grain size of the metal matrix is typically 1 to  $5\text{ }\mu\text{m}$  in diameter, with the dispersed phase in the 10- to 30-nm size range, with comparable interparticle spacings. In optimized systems, the volume fraction of the dispersion ranges from 1 to 5 percent. Such materials have excellent resistance to high-temperature creep and are capable of being used effectively in structural applications up to about  $0.8\text{ }T_m$ .

The most recent innovation (M. J. Luton, private communication, 1989) in this field dispenses with the need to add the dispersed phase and relies on gas-solid reactions to produce the desired dispersion. In one preferred methodology, the metal particles (e.g., Al) are milled in liquid  $N_2$ . Such cryomilling takes advantage of sluggish reaction kinetics between the clean Al-particle surfaces and the  $N_2$  molecules to produce small AlN clusters, which become embedded within the Al particles during the further mechanical deformation in the ball mill. The resulting microstructure has a grain size less than 50 nm, with a particle size of the dispersed phase of approximately 20 nm, which is the smallest uniform-scale microstructure yet achieved by mechanical working processes. This microstructure has been found to be remarkably resistant to coarsening, even at temperatures approaching the melting point of the material. Obvious extensions of this technology are being considered, such as the synthesis of metal-polymer, polymer-ceramic, and other mixtures with nanoscale dimensions. The synthesis of metastable phases, such as amorphous and quasicrystalline materials, can also be produced by mechanical mixing of crystalline precursors (that are ready glass formers) followed by a low-temperature interdiffusion annealing treatment.

#### GAS-CONDENSATION SYNTHESIS

The gas-condensation method (Granqvist and Buhrman, 1976; Kimoto et al., 1963; Thölén, 1979) for the production of ultrafine metal particles in an inert-gas atmosphere has been extensively studied during the past 25 years. Using this technique, powders with rather narrow size distributions can be produced in technologically significant amounts. The particle sizes can be varied over a wide range by changing the gas pressure, the partial pressure of the evaporating material (i.e., its temperature or evaporation rate), or the inert gas itself. All of these parameters are in principle easily controlled to yield particles in the size range of 5 to 100 nm.

Nanophase materials are synthesized in a two-step process that consists of the production of small powder particles by the gas-condensation method and their subsequent in situ compaction and sintering into a solid material

without exposure to air. The resulting new class of nanophase materials may contain crystalline, quasicrystalline, or amorphous phases; they can be metals, ceramics, or composites with rather different and improved properties than normal coarser-grained polycrystalline materials (Gleiter, 1981; Siegel and Hahn, 1987).

An alternative single-step process (P. R. Strutt, University of Connecticut, private communication, 1989) for the production of thin-film nanophase materials involves laser-induced evaporation of metallic or ceramic species and condensation as a thin film on a cold substrate. When carried out in a highly reducing environment, it is possible to convert a ceramic into primarily metallic material. This transformation is facilitated by the creation of an intense plasma flame, which is typical of the interaction of a high-power-density laser beam with a material surface. Critical to the success of this single-step process is the condensation from a highly excited, fully ionized state of the material.

A specific advantage of the gas-condensation method is the exceptional physical and chemical control available, which permits the particle surfaces to be maintained clean, or to be reacted or coated, allowing subsequent high grain-boundary purity or selective interfacial doping and phase formation. In addition, exceptionally high (rather surface-like) atomic diffusivities along the dense grain-boundary network in nanophase materials allow for efficient doping, and property modification, subsequent to consolidation.

The major components of a system for the synthesis of nanophase materials using the gas-condensation method are shown in Figure 9. The system ideally consists of an ultrahigh-vacuum (UHV) chamber equipped with a turbomolecular pump capable of a base pressure of better than  $1 \times 10^{-6}$  Pa. The starting material or materials from which the nanophase compacts are to be made are evaporated using conventional methods but in a high-purity gas atmosphere introduced after the production chamber has been pumped to better than  $1 \times 10^{-6}$  Pa. During the evaporation in the gas atmosphere (usually an inert gas such as helium), convective gas flow transports the particles, which are formed by homogeneous condensation in close proximity (within a few mm) to the resistance-heated evaporation source, to a liquid-nitrogen-filled cold finger, where the particles are collected. Binary mixtures of powder particles or nanocrystals of different materials can be prepared in the same way by using two evaporation sources simultaneously. To achieve a better mixture in such a case, the cold finger can be rotated during the deposition process. Although resistance-heated evaporation sources have been commonly used in the gas-condensation method, radio-frequency sources, electron-beam, laser, or plasma-torch-heated sources, and ion-sputtering sources are now being used or investigated to allow for greater control of the evaporation and powder-production conditions for a wider range of starting materials. The synthesis of more complex nanophase materials will also be facilitated.

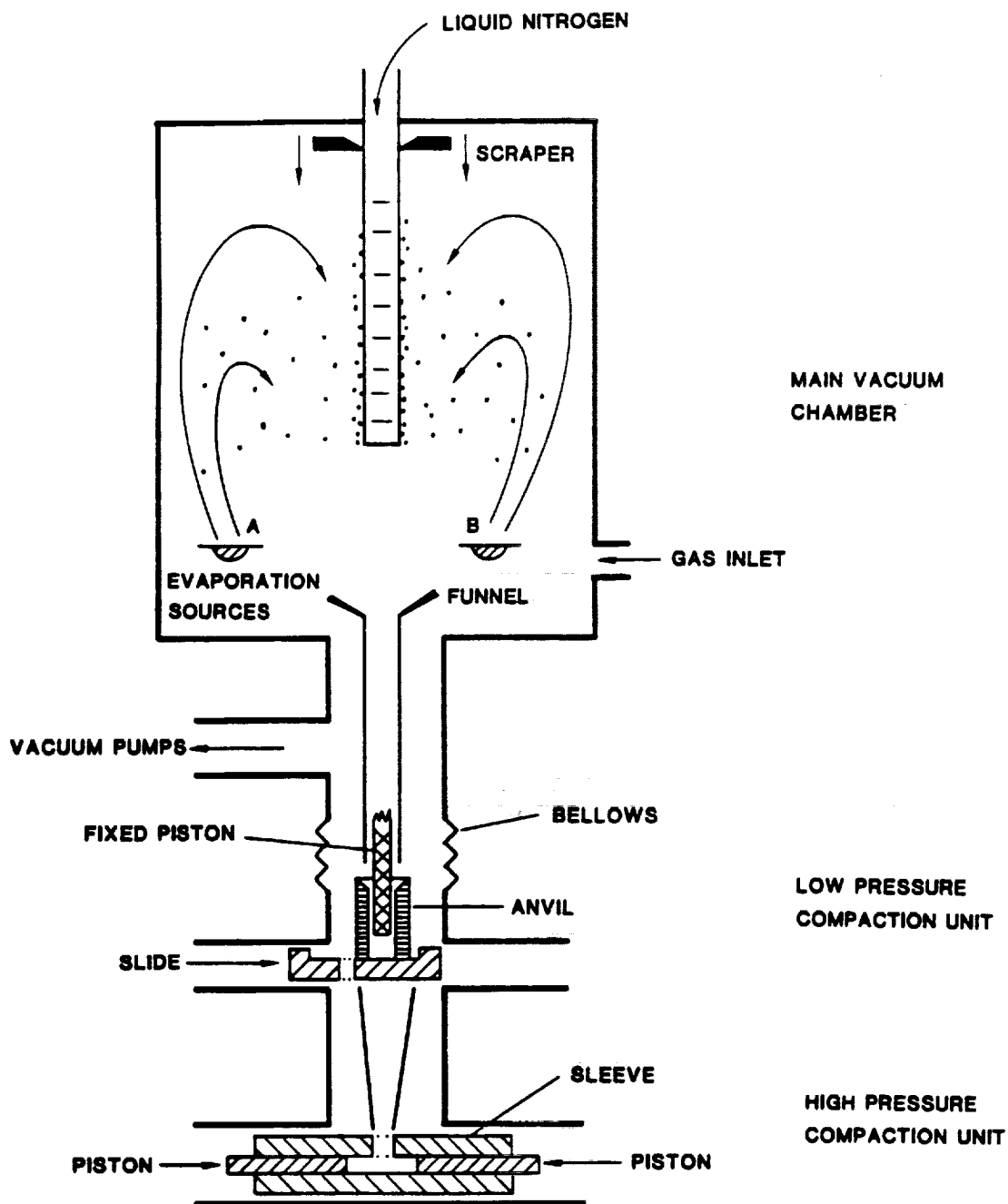


FIGURE 9 Schematic drawing of a gas-condensation chamber for the synthesis of nanophase materials. The material evaporated from source A and/or B condenses in the gas and is transported via convection to the liquid-N<sub>2</sub>-filled cold finger. The powders are then scraped from the cold finger, collected, and compacted in situ (Siegel and Eastman, 1989).

The nanophase compacts are then formed in situ by collecting the powder scraped from the cold finger into a compaction device. The scraping and compaction process is again done under UHV conditions, after removal of the gas atmosphere, to guarantee the cleanliness of the particle surfaces and subsequent nanophase interfaces and also to minimize the amount of any trapped gases. Although the evaporation itself is done in an inert-gas atmosphere, UHV conditions for the production system are favorable, since gas leakage during the deposition should be reduced as much as possible because of the high reactivity of the small particles. However, if a reaction of the particles with a gas is desired, such as the oxidation of a metal to form an oxide ceramic, the gas can be easily added to the inert-gas atmosphere during or after the evaporation. Nanophase ceramics ( $\text{TiO}_2$ , rutile), with greatly increased sinterability over normal coarser-grained ceramics and with no need for compaction or sintering additives, have recently been synthesized using this method (Siegel et al., 1988). This enhanced sinterability appears to result from a combination of the small and relatively uniform particle size available in the gas-condensation method and the clean particle surfaces, and resulting grain boundaries, maintained in the in situ consolidation process.

Particle agglomeration has not been a problem in the synthesis of nanophase  $\text{TiO}_2$  (Siegel et al., 1988) and thus is not expected to be a significant problem in the processing of nanophase ceramics in general. A hint as to why this might be the case can be found in the particle morphology generated by the gas-condensation method. The fractal-like structure of the as-collected  $\text{TiO}_2$  powders indicates that fewer boundaries are formed between individual particles than are normally seen in the three-dimensionally compact particle agglomeration resulting from conventional ceramic processing methods. Hence, less energy is required in the nanophase processing method to break down this one-dimensional, tree-like structure during compaction than would normally be expected. The cleanliness of the small particle surfaces and the resulting high degree of activity lead to the rather dense nanophase ceramic compacts obtained with this method.

#### RAPID SOLIDIFICATION PROCESSING

A well-known method of producing ultrafine microstructures is by rapid quenching from the molten state. It has found its greatest utility in the rapid solidification of metals and alloys. The resulting microstructures exhibit high degrees of supersaturation. The finest microstructures are obtained at the highest cooling rates, corresponding to the highest undercoolings of the molten state. Large undercoolings also promote prolific nucleation and the formation of microgranular materials containing one or more phases. The same can be obtained by thermomechanical treatment of metastable phases.

Techniques are available for producing melt-quenched powders in the size range from 1 to 10  $\mu\text{m}$  by gas- and centrifugal-atomization methods. Electro-

hydrodynamic atomization is a means to generate submicron-size particles. The highest cooling rates are obviously obtained for the smallest particles. Melt spinning is the most widely used technique for producing rapidly solidified ribbons in the 25 to 50  $\mu\text{m}$  range, corresponding to cooling rates in the range of  $10^6$  K/s. Good examples of melt-spun nanophase composite products are the permanent magnet rare earth Fe-B materials (see Chapter 6).

A complete discussion of rapid solidification science and technology is beyond the scope of this study and, as noted in Chapter 1, has been adequately covered in previous National Materials Advisory Board reports.

#### REFERENCES

- Aida, T., and S. Inoue. 1981. *Macromolecules* 14:401162.
- Aksay, I. A. 1988. *Ceramic Transactions, Vol. 1, Part B, Ceramic Powder Science. Proceedings of the First International Conference on Ceramic Powder Processing Science.* Westerville, Ohio: American Ceramic Society.
- Bevk, J. 1983. Ultrafine filamentary composites. *Ann. Rev. Mat. Sci.* 13:319.
- Cannon, W. R., S. C. Danforth, J. S. Haggerty, J. H. Flint, and R. A. Marra. 1982. *J. Am. Ceram. Soc.* 65:324-325.
- Gleiter, H. 1981. Materials with ultrafine grain sizes. Pp. 15-21 in *Deformation of Polycrystals: Mechanisms and Micro-structures*, N. Hansen et al., eds. Roskilde, Denmark: Riso National Laboratory.
- Granqvist, C. G., and R. A. Buhrman. 1976. Ultrafine metal particles. *J. Appl. Phys.* 47(5):2200.
- Heeger, A. J., J. Orenstein, and D. R. Ulrich, eds. 1988. *Nonlinear Optical Properties of Polymers. Materials Research Society Proceedings, Vol. 109.* Pittsburgh: Materials Research Society.
- Hench, L. L., and D. R. Ulrich. 1986. *Science of Chemical Processing.* New York: John Wiley & Sons.
- Hench, L. L., and D. R. Ulrich, eds. 1984. *Ultrastructure Processing of Ceramics, Glasses, and Composites.* New York: John Wiley & Sons.
- Higashimura, T. 1986. *Makromol. Chem., Makromol. Symp.* 3:83.
- Khanarian, G., ed. 1986. *Molecular and Polymeric Optoelectronic Materials: Fundamentals and Applications. Proceedings, SPIE, 682.*

- Khorana, H. G. 1987. Recent work on bacteriorhodopsin. Chapter 1 in *Proteins of Excitable Membranes*, B. Hille and D. M. Farnbrough, eds. New York: Wiley-Interscience.
- Klein, L. C. 1987. Design of microstructures in sol-gel processed silicates. P. 39 in *Design of New Materials*, D. L. Cocks and A. Clearfield, eds. Denver: Cahmus Publishing Co.
- Kimoto, K., Y. Kamiya, M. Nonoyama, and R. Uyeda. 1963. *Jpn. J. Appl. Phys.* 2:702.
- McCandlish, L. E., and R. S. Polizzotti. 1989. Control of Composition and Microstructure in the Co-W-C Ternary System Using Chemical Synthesis Methods. *Solid State Ionics* (in press).
- Pope, E. A., and J. D. Mackenzie. 1985. Porous and dense composites from sol-gel. In *Proceedings of the 21st University Conference on Ceramic Science* (July).
- Pope, E. A., and J. D. Mackenzie. 1986. Oxide-nonoxide composites by sol-gel. Pp. 809-814 in *Better Ceramics Through Chemistry II*, C. J. Brinker, D. E. Clark, and D. R. Ulrich, eds. Pittsburgh: Materials Research Society.
- Schnettler, F. J., F. R. Monforte, and W. W. Rhodes. 1968. A cryochemical method for preparing ceramic materials. *Science of Ceramics*, G. H. Steward, ed., Vol. 4, pp. 79-90. Stoke-on-Trent, England: British Ceramic Society.
- Siegel, R. W., S. Ramasamy, H. Hahn, Z. Li, T. Lu, and R. Gronsky. 1988. *J. Mater. Res.* 3:1367.
- Siegel, R. W., and H. Hahn. 1987. P. 403 in *Current Trends in the Physics of Materials*. M. Yussouff, ed. Singapore: World Scientific Publishing.
- Siegel, R. W., and J. A. Eastman. 1989. P. 3 in *Multicomponent Ultrafine Microstructures*, L. E. McCandlish et al., eds. *Mater. Res. Soc. Symp. Proc.* 132:3.
- Smith, R. D., B. W. Wright, C. R. Yonker, and D. W. Matson. 1987. *Army Research Office Workshop on Supercritical Fluid Technologies*. University of Washington (August).
- Tarasevich, B. J., J. Liv, M. Sarikaya, and I. A. Aksay. 1988. Inorganic gels with nanometer-sized particles. Pp. 225-237, *Better Ceramics Through Chemistry III*, C. J. Brinker, P. E. Clark and D. R. Ulrich, eds. Materials Research Society.



- Thölen, A. R. 1979. Acta Metall. 27:1765.
- Ulrich, D. R. 1988. Nonlinear optical polymer systems and devices. Mol. Cryst. Liq. Cryst.
- Ulrich, D. R. 1988a. Sol-gel processing. Chemtech (American Chemical Society), 18(4).
- Ulrich, D. R. 1987. Multifunctional macromolecular ultrastructures. Polymer, 28:533-542.
- Wagner, R. A. 1988. A New Process for Final Densification of Ceramics. Final Report, Air Force Contract AFOSR F49620-S5-C-0053 (May 13).
- Webster, O. W., W. R. Herter, D. Y. Sagah, W. B. Farnham, and T. J. Rajan Babu. 1983. J. Am. Chem. Soc., 105:5706.
- Wu, E. C., K. C. Chen, and J. D. Mackenzie. 1984. Ferroelectric ceramics-- The sol-gel method versus conventional processing. In Better Ceramics Through Chemistry, Materials Research Society Symposia Proceedings, Vol. 32, C. J. Brinker, D. E. Clark, and D. R. Ulrich, eds. New York: Elsevier.



## SYNTHESIS AND PROCESSING: MORPHOLOGICALLY SPECIFIC METHODS

## FILAMENTARY STRUCTURES

The growth of filamentous carbon by the catalytic decomposition of hydrocarbons has been the subject of intensive research worldwide for more than a decade. Most of the work, regardless of its source, has centered on the use of Fe, Ni, or their oxides as hydrocarbon decomposition catalysts. The preferred hydrocarbons are the C1-C3 alkanes and benzene. The primary motivation for this research has been the potential for the low-cost synthesis of carbon filaments for use in filament-reinforced composites (e.g., carbon-epoxy and carbon-carbon composites).

Growth mechanisms have been established by electron microscopy observations. The most revealing studies have been performed by controlled-atmosphere electron microscopy, in which a gas reaction cell is incorporated within an electron microscope to permit the continuous observation of the gas-solid reactions as they occur (Baker and Harris, 1978). Much of this work has involved filament synthesis from the decomposition of acetylene at temperatures between approximately 500 and 975°C in the presence of iron, cobalt, and chromium catalysts. Each of the filaments was observed to have a catalyst particle at its growing end, with the diameter of the filament fixed by that of the catalyst particle (Figure 10). The filaments varied from 0.01 to 0.15  $\mu\text{m}$  in diameter and from 0.5 to 8.0  $\mu\text{m}$  in length. Filament growth followed random paths, thereby forming loops, spirals, and interconnected networks. Growth rates varied inversely with catalyst particle size. A filament stopped growing when its catalyst particle became completely covered with a carbon layer (Figure 10).

In studies (Baker et al., 1982) of the effect of pretreatment of iron surfaces on filament formation, it was observed that heating in steam at 700°C to form FeO produced an extremely active filament-forming catalyst when

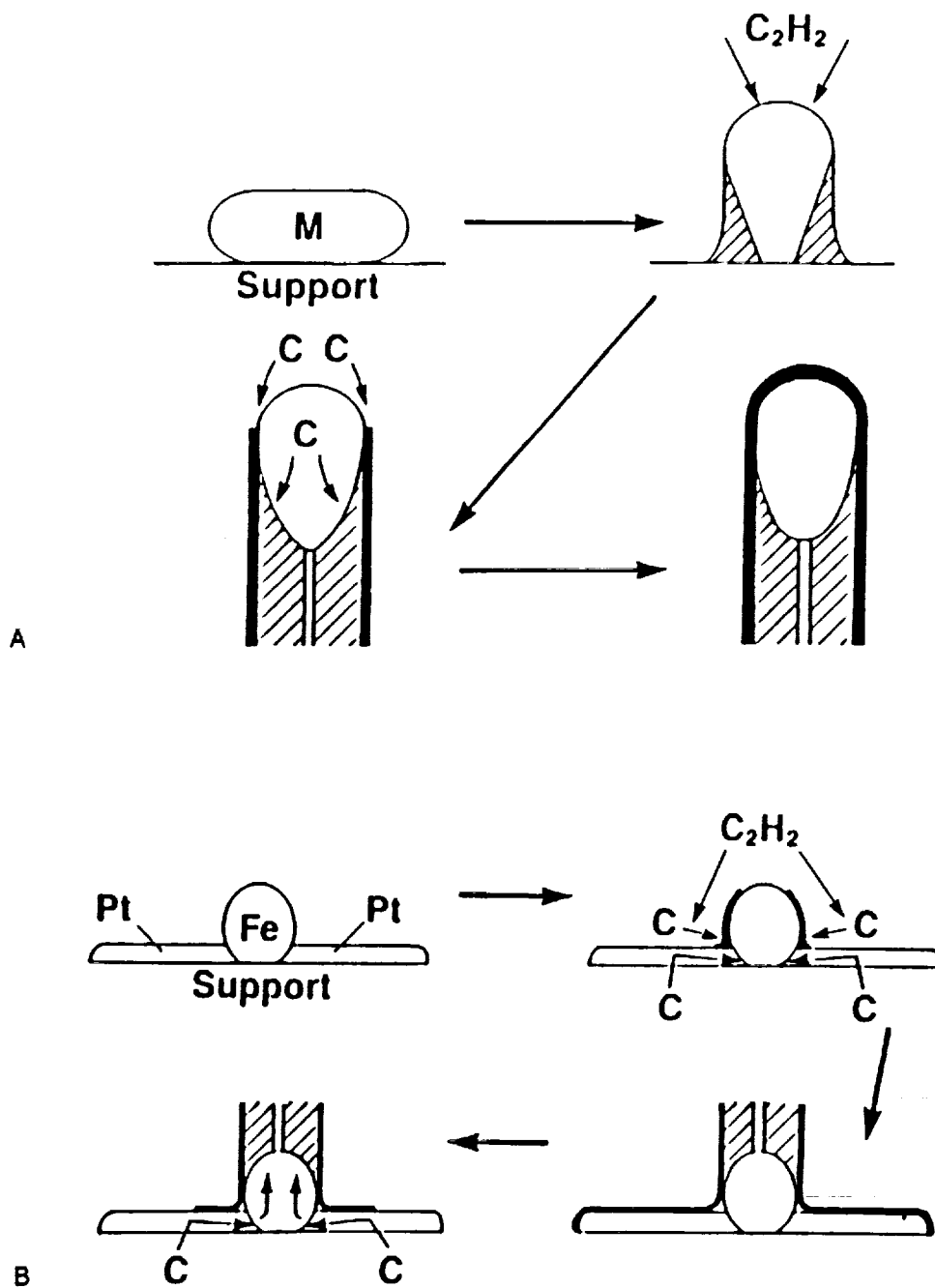


FIGURE 10 Baker mechanisms for filamentous carbon growth: (A) particle at the tip mechanism; (B) particle at the base mechanism (Baker and Harris, 1978).

reacted with acetylene or ethane. The key to the high activity of FeO is its role as a precursor for the formation of a high-surface-area Fe catalyst. More recently, the performance of transition metal-based alloy catalysts has been examined (H. Witzke and B. H. Kear, private communication, 1989). The behavior of the alloy catalysts is distinguished from that of pure Ni by the directionality and the rate of filamentous carbon growth. Filaments formed on pure Ni typically grow in a single direction, with the particle located at the tip of the filament. Alloy particles generally exhibit bidirectional or multidirectional growth, with the particle positioned in the middle of the filaments. Alloy particles also yield significantly higher filament growth rates than Ni alone. High-resolution lattice imaging studies of the filaments have revealed a bimodal structure consisting of a graphitic skin and amorphous core.

Attempts to exploit this filamentary growth mechanism have been frustrated by the inability to obtain as-grown carbon filaments of sufficient strength and stiffness to qualify them as reinforcing elements in composites. The problem seems to be that the preferred temperature range for catalytic growth of ultrafine filamentary carbon networks (500 to 900°C) is well below that necessary for producing fully graphitic material of high strength and stiffness. To overcome this problem, several different approaches are being investigated (Tibbets and Devour, 1986; Endo and Koyama, 1976). Heat treatments at temperatures above 2500°C are reported to give fully graphitized filaments of high strength and stiffness. After heat treatment at 2500°C, the tensile strength and elastic coefficient of the resulting fibers were, respectively, 1 GPa and 14 GPa.

Graphite fibers have also been grown directly on a ceramic surface pretreated with a ferric nitrate solution by a two-stage process. At the start of the two-stage growth process a mixture of methane (5 to 15 volume percent) and hydrogen is passed over the surface of the ceramic heated to between 600 and 1200°C. In the presence of this reducing atmosphere, the iron compound decomposes to form micron-sized iron particles, which act as the nucleation sites for the fibrous carbon growth. Filament formation is completed in a relatively short time after nucleation. The second growth stage is then initiated by increasing the methane concentration in the gas to 15 volume percent or higher. The methane-enriched gas results in the thickening of the filaments into fibers with diameters between 5 and 15  $\mu\text{m}$ .

It is expected that these different approaches to the synthesis of ultrafine carbon filaments from gaseous precursors will in due course yield filaments with the desired mechanical properties, in which case the emphasis will shift to matrix infiltration processes and the control of matrix-filament adhesion for optimizing composite properties. The long-term goal of General Motors Corporation, for example, is to commercialize the technology for producing carbon fibers at a cost competitive with that for glass fibers currently used in fiber-reinforced plastic automotive bodies.

## MULTILAYER STRUCTURES

Synthesis of multilayer structures with nanometer-scale thicknesses has been achieved by various atomic and molecular deposition processes, such as evaporation, sputtering, molecular-beam epitaxy, electrodeposition, chemical vapor deposition, cluster beam deposition, and gas-condensation methods.

### Molecular-Beam Epitaxy

Molecular-beam epitaxy (MBE) is an extremely well-controlled deposition technique to grow single-crystal films on selected substrates at relatively low temperatures in ultrahigh vacuum. Undesirable impurities can be reduced to below  $10^{14}$  atoms  $\text{cm}^{-3}$ , and desirable dopants can be tailored to achieve atomically sharp junctions. Both line and plane defects can be eliminated, provided that the lattice mismatch and the epilayer thickness are not too large. Because of the control that can be achieved in both lattice structure and composition at the atomic level, many artificially structured materials with submicron dimension along the growth direction have been produced, as well as ordered compounds with atomic periodicities. MBE has been most successful in its application to III-V compounds because of the great flexibility it offers in control of alloy composition and lattice match. More recently, first attempts have been made to fabricate metal-ceramic and metal-metal multilayers. One example is the synthesis of a Co-WC carbide multilayer with periodicity in the 2 to 10 nm range. Such a layered structure exhibits a supermodulus effect, with a peak in the modulus occurring at a composition-modulation wavelength of about 2 nm. Use of reactive gas phase etching in conjunction with microlithography can create extremely high-surface-area materials for catalytic applications.

### Electrodeposition

Artificially layered materials can also be made in a single electroplating bath by modulating either the cathodic current or potential. Ag and Pd multilayers have been produced by this technique. The layer thicknesses, however, were rather large--only composition modulations with a repeat length greater than 100 nm could be made because of electrokinetic limitations. Recently, multilayers with modulation as small as 5 nm have been obtained.

A two-bath technique has been adapted successfully to the production of metallic multilayers (Goldman et al., 1986). By rotating a substrate either in front of two windows connected to baths of different compositions or above two jets of solutions with different composition, multilayers with composition-modulation wavelengths as small as 2 nm have been produced.

### Cluster Beam Deposition

Although multilayer materials are usually prepared using chemical deposition methods or by effusion from a thermal evaporative source, another alternative involves preparation from clusters. Clusters have been used to prepare thin films of metals, insulators, and semiconductors. The clusters may be prepared by a number of methods, with the inert gas condensation and free jet expansion method being the most viable. The general subject of clusters and cluster-assembled materials, beyond the application to multilayer structures, has been recently considered in some detail elsewhere in a Department of Energy panel report (Andres et al., 1989).

A great variety of source designs have been developed to produce cluster beams. Figure 11 shows schematically four generic types of sources: free jet source, pulsed laser vaporization source, continuous thermal vaporization source, and supercritical solvent extraction source. The free jet source is the most widely studied cluster source because the flow field is fairly well understood and some reasonable cluster kinetic models have been developed. Pure or mixed species can be expanded; as they cool in the rapid expansion, they form clusters.

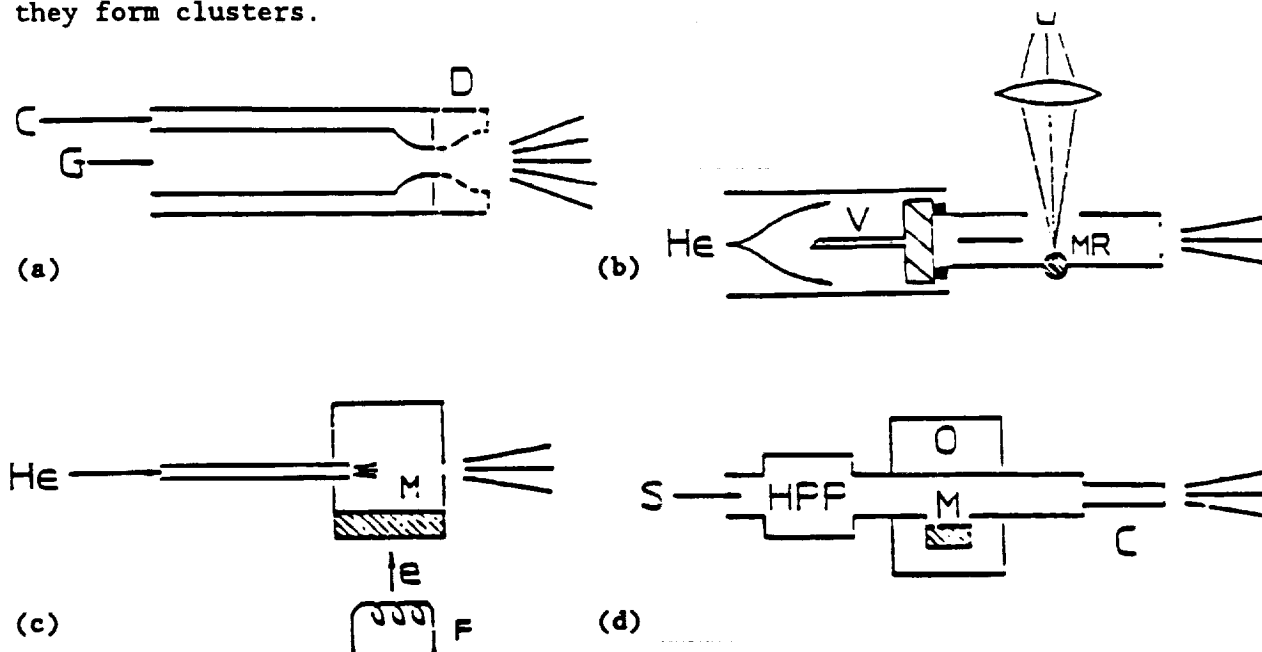


FIGURE 11 Cluster sources: (a) standard free jet source (G = gas, C = coolant, D = divergent section); (b) pulsed laser vaporization source (V = pulsed valve, L = laser, MR = rod of material); (c) thermal vaporization into helium carrier source (M = material inside graphite source, F = electron bombardment filament); (d) supercritical solvent extraction source (S = solvent, HPP = high-pressure pump, O = oven, M = material, C = capillary) (J. M. Weare, D. R. Miller, and J. E. Crowell, 1988, private communications).

By cooling the source and/or adding a divergent section, very large cluster species can be obtained. The pulsed-laser vaporization source is ideal for forming nonvolatile material clusters from dimers to 100 atoms. The helium or other inert carrier is pulsed over the rod source that is in turn pulsed by a laser, causing material to vaporize into the carrier gas. In the continuous thermal source the graphite oven (or tungsten oven) can be heated resistively or by electron bombardment. The supercritical solvent-extraction source allows for molecular species of low volatility to be transferred to the gas phase (J. M. Weare, D. R. Miller, and J. E. Crowell, private communication, 1988). This method has been used to grow films of silica, organic polymers, and  $\text{Al}_2\text{O}_3$ . In practice, the material of interest is dissolved in a supercritical fluid and expanded into a vacuum through a small capillary. The solvent evaporates, leaving the solute material to form clusters. Supercritical water is a convenient solvent for ceramic materials. One of the most important properties of a supercritical fluid, especially for making a wide range of cluster sizes, is the continuously variable solvating power of the fluid obtained by adjusting temperature, pressure, and composition (e.g., electrolytes).

It is apparent that cluster properties are extremely important in the morphology and nature of the thin films produced by these methods, since the size of the clusters deposited is quite sensitive to the source temperature and pressure. Furthermore, by varying the composition of the solvent (e.g., by adding trace amounts of electrolytes), it is expected that the chemistry of the clusters may be altered. In addition, species may be added externally to the clusters prior to deposition by crossing the nozzle cluster beam with a second molecular beam. Catalytically active atoms such as Pt and Rh can be selectively added to the clusters by these methods. The extension of this technology to include excitation of gaseous species in corona-discharge free jets is being considered.

#### DISPERSED-PHASE STRUCTURES

The dispersed-phase composites listed in Table 4 have been prepared by chemical vapor deposition. In general, these materials have been deposited using conventional equipment and processes, with the exception that one or more additional reactant gases were added to the inlet gas stream. Some examples are taken from Lackey and coworkers (1987).

#### Carbon + SiC

The structure and properties of pyrolytic carbon can be varied by alternating the deposition conditions. An even broader range of properties is afforded by the addition of a dispersed SiC phase. Carbon and SiC have little solid solubility in one another; carbon containing from 0 to 72 weight percent



SiC has been codeposited and characterized. Chemically vapor deposited carbon coatings containing 7 to 17 weight percent SiC have been used commercially for heart valves for several years.

TABLE 4 Dispersed-Phase Ceramic Composites Prepared by CVD (Lackey et al., 1987)

Matrix	Dispersoid
Carbon	SiC, TiC, B <sub>4</sub> C, BeO
Si <sub>3</sub> N <sub>4</sub>	C, TiN, BN, AlN, or SiC
SiC	TiSi <sub>2</sub>
Ti-Si-C	Ti-Si-C
Ti-Ge-C	Ti-Ge-C
Al <sub>2</sub> O <sub>3</sub>	ZrO <sub>2</sub>

#### Si<sub>3</sub>N<sub>4</sub> Matrix Composites

Dispersoid-type composites having a Si<sub>3</sub>N<sub>4</sub> matrix have been prepared by Hirai (1982). The dispersed particles were TiN, C, BN, or SiC. Dispersoid concentrations were and have been as high as 32, 10, and 83 weight percent for TiN, C, and BN respectively. The thermal conductivity of  $\alpha$ -Si<sub>3</sub>N<sub>4</sub> containing less than 10 volume percent of 10-nm TiN particles was a factor of 10 less than for pure Si<sub>3</sub>N<sub>4</sub>. It appears that the TiN particles resist phonon transport. The morphology of the dispersed phase and crystallinity of the matrix can be varied by control of deposition temperature and pressure. Deposits containing TiN whiskers in Si<sub>3</sub>N<sub>4</sub> matrix have been codeposited.

#### SiC + TiSi<sub>2</sub>

Stinton and Lackey (1985) have deposited SiC coatings containing TiSi<sub>2</sub> as a dispersed phase. Coatings were deposited on graphite substrates, some of which were suspended in a particulate fluidized bed. For nonfluidized bed coatings, the TiSi<sub>2</sub> particles were columnar, whereas fluidized bed coatings produced smaller, nearly equiaxed particles and the coatings were more uniform. The composite coatings, compared to single-phase SiC, were more adherent and possessed significantly greater fracture toughness.

### Composites in the Ti-Si-C and Ti-Ge-C Systems

Nickl et al. (1972) have investigated composite formation in the Ti-Si-C and Ti-Ge-C systems as a function of reactant concentration and temperature. They have shown that virtually all of the dozen or more two- and three-phase assemblages possible can be prepared by CVD. Some of the composites prepared were SiC + TiC, SiC + TiC + C, and  $Ti_5Si_3C_x$  +  $TiSi_2$ . During extensive microstructural characterization it was observed that either of the ternary phases  $Ti_3SiC_2$  and  $Ti_5Si_3C_x$  tend to deposit as lamellae when codeposited with binary phases such as TiC or  $TiSi_2$ . The boundaries between ternary and binary phases were coherent or semi-coherent. The tendency for ternary phases to form alternating layers with binary phases was also observed in the Ti-Ge-C system.

### MACROMOLECULAR COMPOSITE STRUCTURES

A molecular composite is a polymeric material consisting of two or more components dispersed at the molecular level. Examples include compatible polymer blends that are noncrystalline, thermodynamically stable single-phase materials, and blends of components that are processed into a homogeneous state but are not at thermodynamic equilibrium. The latter blends are polymer analogs of metastable multiphase alloys. An example of the synergistic effects that result is General Electric's Noryl--a blend of poly(styrene) and poly(phenylene) oxide that has excellent mechanical properties, especially toughness. The field of polymer blends is extremely active, with interest centered on synthetic routes to produce "miscibility windows" wherein the blend can be produced and processed. The material is then quenched to room temperature, where it maintains its single-phase character because of the lack of molecular mobility below the glass transition.

The possibility of tailoring the macroscopic properties of macromolecular systems by varying the nanoscale morphology of the bulk polymer is being shown by research on blends of high-performance systems (Karasz, 1986; DeMuese et al., 1988; Guerra et al., 1988). Polymer blends may or may not be miscible (i.e., forming a true thermodynamic solution). Miscibility is a relatively uncommon phenomenon in homopolymer-homopolymer systems because of the absence of a significant configurational entropy of mixing. In contrast, blends containing random or near-random copolymers are much more likely to form miscible systems, because of the possibility of a net lowering of the overall free energy caused by the presence of intramolecular repulsive interactions in the copolymer.

The copolymer route allows three morphological types to be processed into the polymer alloy (Figure 12): a homogeneous single phase between the phase boundary and the glass transition temperature ( $T_g$ ); two-phase nucleation morphologies; and two-phase spinodal decomposition. By

changing the copolymer composition only slightly, the  $T_g$  will show minimal change, but the lower critical solution temperature (LCST) shows considerable change, allowing the selection of morphology.

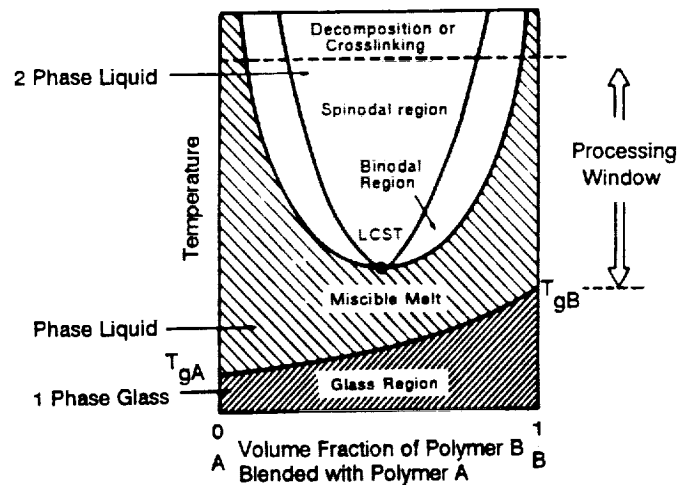


FIGURE 12 Schematic phase diagram for polymer blends (Karasz, 1986).

While compatible polymer alloys are of interest, the focus here is on the area of self-reinforcing alloys, the so-called molecular composites. The term molecular composite is adapted from the field of macro composites such as fiberglass-epoxy materials, where one component is a rigid reinforcement for a ductile matrix of the other. If one could disperse individual rod-like macromolecules in a flexible-coil matrix, then the intrinsically large length-to-diameter ratio ( $L/D$ ) inherent to such rigid macromolecules (easily in excess of 100 for reasonable molecular weights) coupled with the strong nonbonded interactions of the reinforcing molecules to the matrix molecules would provide essentially an ideal reinforced composite. It should be possible to use various processing flow fields to tailor the orientation of the rod-like molecules and produce a high degree of mechanical anisotropy. In practice, however, because these systems consist of two rather dissimilar components, they are highly likely to phase-separate, forcing a nonequilibrium approach to their production.

The first attempts to produce such materials originated at the Materials Laboratories at Wright-Patterson Air Force Base (Helminiak et al., 1978) but failed to achieve a single-phase material because slow evaporation of the solvent allowed macro-phase separation to occur (Husman et al., 1980). Takayanagi (1983) employed a wet-spinning process to produce an oriented fiber of nylon 6 or nylon 6,6 and poly(p-phenylene terephthalamide) (PPTA). Although solid formation during coagulation of the wet-spun fiber was considerably faster than the solvent evaporation method, Takayanagi found that phase separation did indeed occur at a fine scale, producing oriented 30-nm microfibrils of the rigid-rod macro-

molecules in the semicrystalline flexible chain nylon matrix. Lately, researchers have sought various ways to overcome the tendency to phase-separate. The approach is to employ dilute solutions at a concentration below the critical concentration for phase separation so that the rod, coil, and solvent molecules form a homogeneous isotropic phase. This solution is then wet-spun into an oriented fiber and rapidly coagulated to capture the mixture in a homogeneous solid state. As applied to the poly(p-phenylene benzobisthiazole) PBZT/poly-2,5(6) benzimidazole (ABPBI) system, such processing results in a solid with no detectable phase separation above the 3-nm level. The 30/70 PBZT/ABPBI fibers thus produced have outstanding mechanical properties (modulus 120 GPa, strength 1300 MPa, strain to break 1.4 percent) (Krause et al., 1986). Another standard approach to control molecular dispersion of different macromolecular components is, of course, to utilize block copolymers. Triblock ABPBI/PBZT/ABPBI materials have recently been synthesized containing the same 30 percent PBZT to 70 percent ABPBI composition (Tsai et al., 1985). The advantage here is that the built-in chemical connections between the dissimilar segments significantly raise the critical concentration at which phase separation takes place; moreover, the scale of this phase separation is dictated to be on the order of the respective block radii of gyration, thus preventing macroscale segregation and loss of physical properties. The mechanical properties of the considerably more easily processed PBZT/ABPBI block copolymer fiber are comparable to those of the physical blend.

As indicated previously in the section entitled Reductive Pyrolysis, properties of biphasic materials are particularly synergistic for bicontinuous microstructures. It has been demonstrated theoretically that a bicontinuous structure has an intrinsic thermodynamic stability at the 73:27 volume percent ratio of the constituent phases (Thomas et al., 1988). Such a structure has been observed in block copolymers (Figure 13), but so far not in metal-ceramic composites. A rationalization for the morphologies of two-phase structures has been given by Newnham et al. (1978). Four types of microdomain morphologies have been identified for biphasic block copolymers (Figure 14). The triply periodic bicontinuous morphology has the special virtue of generating three-dimensional, near-isotropic reinforcement. Other properties will be influenced as well by such structurally symmetrical composites.

With further research into synthetic efforts and exploration of novel processing methods, truly outstanding high-performance materials should certainly be realized.

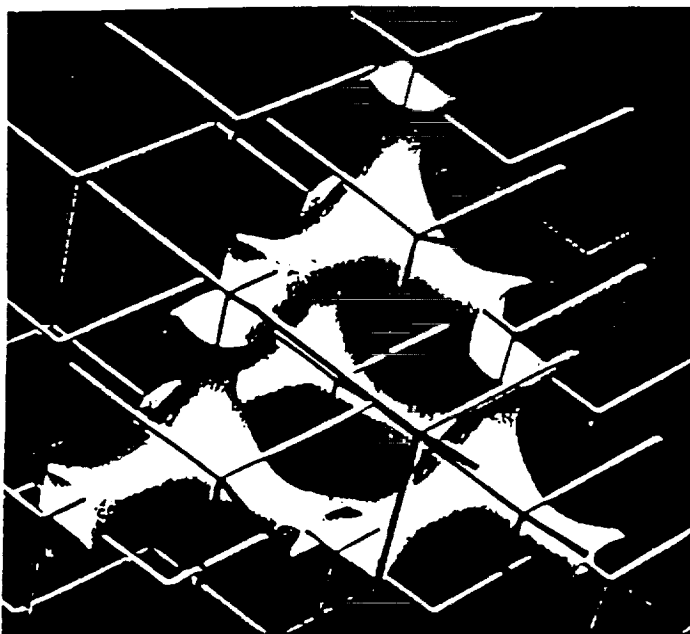


FIGURE 13 Computer-generated image of triply periodic surface of constant mean curvature; see also Figure 14c (Thomas et al., 1988).

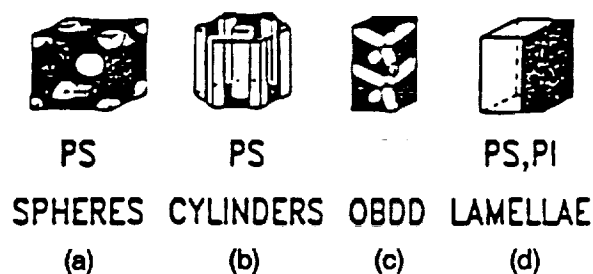


FIGURE 14 The four types of ordered microdomain morphology of diblock copolymers: (a) bcc spheres of A in B matrix, (b) hexagonally packed cylinders of A in B matrix, (c) bicontinuous double-diamond network, and (d) lamellae of A and B phases (Thomas et al., 1988).

#### HETEROGENEOUS NANOCOMPOSITES

The sol-gel route can be used to make heterogeneous materials with a high degree of interpenetration (Roy, 1985, 1987). A wide range of high-

temperature ceramic examples of the sol-gel route has been demonstrated using two or more phases lying in the range of 1 to 10 nm derived from multiphasic xerogels. The multiphases may differ in either composition or structure or both.

There are several varieties of reliable and unique high-temperature structural and electromagnetic ceramics made from this low-temperature process. Figure 15 shows the design of high-temperature calcium strontium zirconium phosphates with zero thermal expansion. This nanocomposite has zero thermal expansion from 0°C to at least 500°C.

These materials can be designed to have electrically conducting or insulating properties, ferromagnetic properties, or low-frequency damping properties concurrently with ultralow thermal expansion. One series based on sodium zirconium silicate and yttrium iron garnet provides a high-temperature, low-thermal-expansion magnetically absorbing nanocomposite.

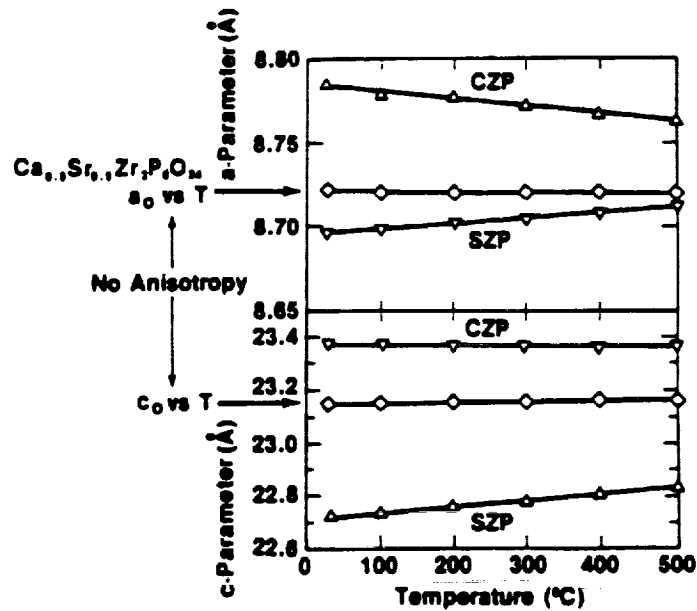


FIGURE 15 Sol-gel design of zero-expansion nanocomposites.

## HIGH-SURFACE-AREA MATERIALS

Most of the synthesis methods discussed previously produce initially high-surface-area particulate materials that if left uncompacted may yield materials exhibiting novel catalytic properties or may be suitable for physical and/or chemical separation purposes. An example is the high-surface-area Co-WC produced by reductive pyrolysis or by lithographic etching of multilayer structures.

Methods already in use for the synthesis of supported metal catalysts are well known. Metals are normally dispersed as small particles on the surface of catalyst supports in order to increase the metal surface exposed per unit mass of metal. For a dispersion exceeding 50 percent (more than 50 percent of the metal atoms on the surface of particles), the metal particle size must be less than 2 nm in diameter. Metal clusters of interest as catalysts are generally smaller than 10 nm and are commonly 1 to 5 nm.

Commercial catalyst preparation generally consists of a series of unit operations, which depend on the type of catalyst being prepared. For example, precipitation may be used for the manufacture of oxide-based catalysts, gel formation for making silica and alumina, and coating for the preparation of catalysts with low surface area. Procedures used for the preparation of supported metal catalysts with submicron-sized particles include impregnation, ion exchange, and adsorption-precipitation.

The role of the catalyst support in determining catalytic properties has received wide recognition in the past few years. Catalyst supports are selected on the basis of their effectiveness in dispersing and "anchoring" the metal particles, their chemical and thermal stability, and their stability in the reaction environment. Interactions between the support and the catalyst particles can influence the catalytic properties of the metal particles. Other factors are the surface area of the support, its pore structure, the affinity of the support for catalyst poisons, crush strength, and attrition resistance. Typical supports are alumina, silica, silica-alumina, zeolites, titania, magnesia, and carbon. Typical configurations for catalyst supports are powders, pellets, spheres, tablets, granules, extrudates, and monoliths. Molecular-level information of the details involved in the synthesis is not readily available for highly dispersed systems with particles of interest buried within the porous support.

Widely used as well as new catalyst-preparation techniques of interest for preparing submicron-sized metal particles are summarized in the following sections.

### Impregnation and Ion Exchange

Two techniques commonly used to prepare supported metal catalysts are impregnation and ion exchange, which yield submicron-sized catalyst particles in the form of small metal crystallites dispersed on the porous surface of preformed supports. For impregnation, the support in either a wet or dry state is treated with a solution containing a compound of the desired catalytic constituent. The liquid is removed by drying, leaving catalytic materials on the surface of the support. Supports such as alumina or silica that have a high surface-to-volume ratio stabilize the dispersion of the metal over a large area. Research studies on catalyst preparation have provided understanding of the impregnation process and how to control the amount and location of the metal particles on the support (D'Aniello, 1981; Komiyama, 1985). The strength of the interaction of the metal-containing anion and cation with the support influences the penetration of the metal into the support matrix. Preparation of supported catalysts by impregnation produces a distribution of metal particle sizes. As a result, precise information on the consequences of molecular structure is not available for highly dispersed systems.

Other catalyst-preparation techniques that make use of preformed supports include vapor-phase methods in which metal atoms, preformed metal clusters, or a vapor-phase compound of the metal such as a carbonyl complex are deposited on the support.

### Decomposition of Metal Carbonyls

Metal carbonyls can also be used to produce small supported metal particles. Thermal decomposition of metal carbonyls on hydroxylated supports, such as alumina, results in the formation of highly dispersed oxide species. These catalysts are of interest as model systems to probe support effects and as a means to prepare materials with precisely controlled characteristics. Provided that the temperature is kept below 400 K, metal carbonyls can be used to form zero valent subcarbonyl species, which are analogs of metal carbonyl clusters with one of the CO ligands replaced by the interaction of the metal with the support. These catalysts have been studied as potential replacements for homogeneous catalysts.

### Bare Metal Clusters

Recently, a significant development in the preparation of new materials with potential significance to the field of catalysis is the ability to prepare bare metal clusters of variable size. These clusters are generally prepared by the vaporization of a metal into a gas, supersonic expansion to promote nucleation, introduction of a reactant gas if desired, and finally mass selection. Cluster-size-dependent variations



in reactivity have been observed (Kaldor et al., 1986). Photoionization threshold measurements are sensitive to cluster electronic structure as a function of cluster size; shifts in the photoionization thresholds induced by chemisorption provide information on the adsorbate-cluster bonding. The reaction of gas-phase platinum clusters with benzene and several hexanes have shown extensive evidence of dehydrogenation and size-dependent chemisorption (Trevor et al., 1985).

#### Microporous Solids: Pillared Clays

The intercalation of metal complexes in smectite clay minerals has recently led to the development of a new class of catalyst materials. These clays have layer lattice structures with oxyanions separated by layers of hydrated cations. The intercalation of polynuclear hydroxy metal cations and metal cluster cations can be used to form catalysts with pore sizes greatly exceeding those of typical zeolite catalysts. The size and shape of the catalyst substrate can be an important factor in determining the selectivity of the catalyst (Pinnavaia, 1983).

#### Zeolites

Zeolites are porous crystalline materials. The geometry of the pores determines the size of the molecules that can pass through the rigid structure and thereby imparts a shape-selective constraint on the chemical reactions promoted. For some time, zeolites have been recognized as promising supports for the preparation of very small metal clusters, and an extensive body of literature exists on the metal-zeolite system. Metal particles in the supercages of zeolites of faujasite are of submicron size. Their synthesis generally follows this sequence: ion exchange, calcination (to destroy the ligands), reduction in hydrogen. Almost all elements with electrochemical potential more positive than Fe(II) have been examined. For some metals, these procedures do not lead to the desired result because metal ions that lose their ligand shell tend to migrate into smaller zeolite cavities. Reduction to the metal in these locations requires high temperatures and can result in large particles at the external surface of the zeolite.

Recent research has yielded ways to avoid migration of the metal particles and achieve complete reduction and high dispersion. The common element of several strategies to achieve this result is to incorporate into the same zeolite a second metal that is unreducible under the conditions where the first metal is reduced. For example, Fe<sup>4+</sup> ions exchanged in zeolite Y appeared to increase the interaction of platinum with the zeolite framework and thereby enhance dispersion at high temperature (Tzou et al., 1986). The electronic structure and stability of transition metal ions in zeolites has been reviewed by Klier and coworkers (1977).

## MEMBRANES

Broadly, membranes are structural materials involved with the process of permeation. The membrane may be used for separations, to conduct electrical current, to conduct protons, to prevent permeation (packaging), or to chemically modify the permeating species (e.g., ion exchange membranes) (Lloyd, 1984). Structurally, membranes can be classified as porous (containing void space) or nonporous. The tremendous diversity in type and use precludes a systematic approach, so that here we shall only be concerned with semipermeable membranes as illustrative of the opportunities in ultrafine-scale structural design.

A semipermeable membrane is defined as a material structure through which one or more substances in a mixture may pass, but not all. An ideal membrane would selectively pass a specific substance or substances at a high rate and at the same time be impervious to one or all of the other substances in the mixture. The structure of such a membrane would be one of intricate uniformity, consisting of identical pores (or channels of a second phase if the membrane is nonporous) in a geometrical array. For example, the simplest type of sieve is a two-dimensional woven mesh. The pores consist of the regions between the spanning weaves, the selectivity of separation being controlled only by the pore size. A more complex membrane could consist of three-dimensional periodically interconnected pore space with specific chemical groups lining the pores, providing both size and compositional selectivity.

Current technological goals are toward ever-finer pore spaces (channels) with ever-higher overall porosity (channel volume fraction) for high throughputs. Such advances must also provide controlled pore geometry and interconnectivity (topology) as well as uniformity. Interconnectivity is important because the clogging of one-dimensional channels results in the stoppage of flow, whereas, if the pores are interconnected with a high coordination number, there are many routes for flow, and such materials can sustain considerable contamination before needing replacement. Pore uniformity is critical for high selectivity. Such membranes can be used in reverse osmosis, microfiltration, and ultrafiltration. There is a vast number of growing applications of semipermeable membranes (e.g., the removal of pollutants from all types of industrial and agricultural waste). In many cases, the availability of an improved membrane material could significantly affect the viability of a given industrial process.

Some examples of submicron-scale membrane materials are sintered-particle membranes, solution-cast polymeric filters, and molecular sieves (dehydrated crystalline zeolites). The sintered particle membranes usually have a quite nonuniform pore space with a highly polydisperse pore size distribution and contorted three-dimensionally interconnected channels. At present, their size selectivity extends down to only

slightly below 1  $\mu\text{m}$ . Solvent-cast cellulose acetate membranes were a breakthrough in membrane technology in the early 1960s as desalination membranes (Kesting, 1985). Zeolites feature extremely small and uniform pores (0.3 to 1 nm) with several types of periodic three-dimensional interconnectivity and reasonable porosity (50 percent). Because of their polar nature, they selectively absorb polar molecules.

Advances in ultrafine-scale semipermeable membranes can arise from progress in nanoscale materials science. Membrane microstructures need to be combined with membrane properties, such as flexibility and environmental tolerance. Either man-made assemblies or self-assembled composite materials, in which one phase either possesses selective high transport or for which methods are available to selectively remove one of the phases, can provide suitable membranes. For example, spinoidally-decomposed borosilicate glass after acid leaching yields a high-porosity hyperfiltration material. Well-controlled ceramic precursor materials with nearly monodisperse particle size (Bowen, 1986) could, under appropriate sintering conditions, yield a highly uniform, three-dimensional interconnected fine-scale membrane with the inherent advantages afforded by ceramics--namely, thermal and chemical resistance and strength. The exploitation of polymer gels is also an avenue toward new membrane materials. In particular, gels formed from rod-like macromolecules show promise as interesting structural materials because of their mechanical anisotropy and low density. In addition, these materials can be coagulated from an oriented precursor state, thus providing an anisotropic porespace (Cohen and Thomas, 1985). Indeed, the general field of phase separation of materials to provide fine-scale composites is a fertile area, since the length scale of phase separation can be readily controlled by synthesis of well-defined starting materials and time and temperature processing history.

Recent work has utilized the microphase separation of block copolymers to form regularly arrayed and uniform-sized channels. For example, 10-nm diameter one-dimensional cylindrical channels oriented normal to the membrane surface were formed by temperature and solvent gradient phase separation of a polystyrene-isoprene diblock copolymer. This membrane material is a competitor for current nuclear track filters that consist of parallel cylindrical pores formed by the chemical etching of high-energy radiation tracks. Porosity is, however, low because of the need to avoid overlap of tracks. Elegant work utilizing a four-component pentablock copolymer to form a charge mosaic membrane builds on the rational manipulation of controlled synthesis and phase separation (Fujimoto et al., 1984). These membranes contain an alternating lamellar structure with the normal to the lamellae parallel to the external film surface. One of the polymeric phases (vinylbenzyl dimethyl diamine) can be quarternized, which then provides ionically charged layers passing completely across the film thickness separated by 20-nm dielectric insulating layers. Such films have demonstrated both high transport and

good selectivity for electrolytes, which makes them promising candidates for reverse osmosis and electrodialysis applications.

#### REFERENCES

- Andres, R. P., R. S. Averbach, W. L. Brown, L. E. Brus, W. A. Goddard III, A. Kaldor, S. G. Louie, M. Moskovits, P. S. Peercy, S. J. Riley, R. W. Siegel, F. Spaepen, and Y. Wang. 1989. Research opportunities on clusters and cluster-assembled materials: A Department of Energy-Council on Materials Science Panel Report. *J. Mater. Res.* 4:704.
- Baker, R. T. K., and P. S. Harris. 1978. The formation of filamentous carbon. *Chem. Phys. Carbon* 14:83-165.
- Baker, R. T. K., J. R. Alonzo, J. A. Dumesio, and D. J. C. Yates. 1982. *J. Catalysis* 77:74-84.
- Bowen, H. K. 1986. Advanced ceramics. *Scientific American* 255(4):169-176.
- Cohen, Y., and E. L. Thomas. 1985. Structure formation during spinning of poly (p-phenylenebenzobisthiazole) fiber. *Polym. Eng. Sci.* 25(17):1093-1096.
- DeMuese, M. T., E. C. Chenevy, Z. H. Ophir, J. J. Rafalko, and M. I. Haider. 1988. Structure-property relationships of a high-temperature polybenzimidazole-polyetherimide blend. Presented at the American Chemical Society Annual Meeting, Polymer Materials Science and Engineering Division, Los Angeles, California.
- D'Aniello, M. J., Jr. 1981. *J. Catal.* 69:9.
- Endo, M., and I. Koyama. 1976. Japan Patent No. 57/17622.
- Fujimoto, T., K. Ohkoshi, Y. Miyacki, and M. Nagasawa. 1984. Artificial membranes from multiblock copolymers: I. Fabrication of a charge-mosaic membrane and preliminary tests of dialysis and piezodialysis. *J. Memb. Sci.* 20(3):313-324.
- Goldman, L. M., B. Blanpain, and F. Spaepen. 1986. *J. Appl. Phys.* 60:1374.
- Guerra, G., S. Choe, D. J. Williams, F. E. Karzsz, and W. J. MacKnight. 1988. Fourier transform infrared spectroscopy of some miscible polybenzimidazole/polyimide blends. *Macromolecules* 21:231.

- Helminiak, T. E., C. L. Benner, F. E. Arnold, and G. E. Husman. 1978. U.S. Patent Appl. No. 902525.
- Hirai, T. 1982. CVD of  $\text{Si}_3\text{N}_4$  and Its Composites. The Nineteenth University Conf. on Ceramic Science. R. F. Davies, H. Palmores, and R. L. Porter, eds.
- Husman, G. E., T. Helminiak, W. Adams, D. Wiff, and C. L. Benner. 1980. ACS Symposium Series 132, p. 203. Washington, D.C.: American Chemical Society.
- Kaldor, A., D. M. Cox, D. J. Trevor, and M. R. Zakin. 1986. Z. Phys. D--Atoms Molecules and Clusters 3:195.
- Karasz, F. E. 1986. Glass transitions and compatibility: Phase behavior in copolymer-containing blends. Pp. 225-236 in Polymer Blends and Mixtures, D. J. Walsh, J. S. Higgins, and A. Maconnachie, eds. Dordrecht (Netherlands): Martinus Nijhoff Publishers.
- Kesting, R. E. 1985. Synthetic Polymeric Membranes. New York: Wiley Interscience.
- Klier, K., P. J. Hutta, and R. Kellerman. 1977. ACS Symposium Series 40, p. 108. Washington, D.C.: American Chemical Society.
- Komiyama, M. 1985. Design and preparation of impregnated catalysts. Catal. Rev.--Sci. Eng. 27(2):341-372.
- Krause, S. J., T. Haddock, G. E. Price, P. G. Lehnert, J. F. O'Brien, T. E. Helminiak, and W. W. Adams. 1986. Morphology of a phase-separated and a molecular composite PBT/ABPBI polymer blend. J. Polym. Sci. Part B 24:1991-2016.
- Lackey, W. J., A. W. Smith, D. M. Dillard, and D. J. Twait. 1987. P. 1008 in Proc. 10th Int. Conf. on CVD. Pennington, New Jersey: The Electrochemical Society.
- Lloyd, D. R., ed. 1984. Materials Science of Synthetic Membranes. ACS Symposium Series No. 269. Washington, D.C.: American Chemical Society.
- Newnham, R. E., D. P. Skinner, and L. E. Cross. 1978. Mat. Res. Bull. 13:525.
- Nickl, J. J., K. K. Schweitzer, and P. Luxemberg. 1972. Chemical Vapor Deposition of the Systems Ti-Si-C and Ti-Ge-C. Proc. Third Internat. Conf. on CVD. F. A. Glaski, ed. Hinsdale, Ill: American Nuclear Society.

- Pinnavaia, T. J. 1983. Science 220:365.
- Roy, R. 1985. Exploitation of Sol-Gel Route in Processing of Ceramics and Composites. Final Report, Air Force Grant AFOSR 83-0212.
- Roy, R. 1987. Ceramics by the solution-sol-gel route. Science 238(4834):1664-1669.
- Stinton, D. P., and W. J. Lackey. 1985. Simultaneous chemical vapor deposition of Si-C-dispersed phase composites. Ceramic Eng. Sci. Proc. p. 707.
- Takayanagi, M. 1983. Polymer composites of rigid and flexible molecules. Pure Appl. Chem. 55(5):819-832.
- Thomas, E. L., D. M. Anderson, C. S. Henkee, and D. Hoffman. 1988. Nature 334:598.
- Tibbetts, G. C., and M. G. Devour. 1986. U.S. Patent No. 4,565,684.
- Trevor, D. J., R. L. Whetten, D. M. Cox, and A. Kaldor. 1985. J. Am. Chem. Soc. 107:518.
- Tsai, T. T., F. E. Arnold, and W. F. Hwang. 1985. High-strength, high-modulus ABA block copolymers. Am. Chem. Soc. Polymer Preprints 26(1):144-145.
- Tzou, M. S., H. J. Jiang, and W. M. H. Sachtler. 1986. Appl. Catal. 20:231.

## CHARACTERIZATION METHODS

Nanometer-scale materials have certain distinguishing features that must be characterized in order to understand the relationships between their unique composition and structures and their properties. Since many materials properties, like magnetic, optical, and electrical properties, depend strongly on the atomic arrangements in the material (e.g., nearest-neighbor distances, coordination numbers), whereas others such as mechanical properties can depend also on morphological structure, knowledge of the structure of nanophase materials is important on both atomic and nanometer scales. Among the features that need to be elucidated are (1) grain and pore size distributions, morphologies, particle size, and surface area; (2) the nature and morphologies of their grain boundaries and interphase interfaces; (3) composition profiles across grains and interfaces; (4) perfection and the nature of intragrain defects; and (5) identification of residual trapped species from processing (e.g., gas or surfactant entrapment).

Because of the ultrafine scale of these nanophase materials, characterization can be a challenge in itself, and some traditional characterization tools are no longer easily applied. For the characterization of the structure and morphologies of nanoscale materials, traditional tools such as electron microscopy and x-ray and neutron scattering are both necessary and useful. However, for microchemical analysis of the materials on the requisite fine scale, further advancements in the state of the art of instrumental capabilities will be necessary in order to obtain the desired lateral spatial resolution. Useful more conventional techniques include Rutherford Back Scattering (RBS), Electron Energy Loss Spectroscopy (EXAFS), X-Ray Photoelectron Spectroscopy (XPS), Nuclear Magnetic Resonance (NMR), Raman and infrared spectroscopy, Mössbauer, and traditional adsorption techniques.

## X-RAY AND NEUTRON SCATTERING

X-ray and neutron scattering are valuable techniques for the determination of an unknown atomic structure of a material, even in cases of highly disordered systems like amorphous phases. As seen by electron microscopy, a nanocrystalline material consists of crystalline grains that are separated by grain boundaries of about 0.5 to 1 nm thickness (around two to four nearest-neighbor atomic distances). The volume fraction of such an interfacial component changes with grain size and is about 0.3 to 0.6, for example, for a mean grain diameter of 5 nm. X-ray diffraction curves for a nanocrystalline sample therefore will be composed of a part that originates from the crystalline grains, with their well-known structure, and a significant part that originates from atoms located in the boundary regions. Even if it is assumed that the local atomic structure of these grain boundaries is similar to that of more extended grain boundaries, it may be expected that the aggregate of all the different boundaries in a nanophase material (i.e., the interfacial component of the structure) will exhibit an aggregate structure that is apparently different from known solid-state structures. This expectation is based on the fact that a nanophase material consists of a high number-density of different interfaces (about  $10^{19}$  per  $\text{cm}^3$  for a grain size of 5 nm) with atomic structures strongly depending on the misorientation of the adjacent grains.

A recent x-ray study (Zhu et al., 1987) of nanocrystalline iron with 4- to 6-nm grain sizes has indicated that no preferred interatomic distances like those found in a crystalline or amorphous structure occur in the best-fit interfacial structure (i.e., all interatomic distances appear to occur with similar probabilities, except those forbidden because of interatomic penetration). Hence, according to this x-ray study, the interfacial component (i.e., the sum of all boundaries of this nanophase material) represents an aggregate solid-state structure without long-range or short-range order. Further support for this view comes from a recent EXAFS study of nanocrystalline metals (Haubold et al., 1988). The local atomic structures of individual nanocrystalline interfaces, however, are likely to manifest ordered structural units as known from grain boundaries in normal polycrystalline materials. This has recently been shown to be the case for nanophase  $\text{TiO}_2$  by Raman spectroscopy (Melendres et al., 1989). The actual local atomic nature of nanophase boundaries needs to be further elucidated in general, and atomic resolution electron microscopy on nanophase materials can be expected to facilitate such an elucidation. Beyond such studies of atomic structure, x-ray and neutron small-angle scattering can also be useful tools for the study of grain- and pore-size distributions and grain boundary characteristics, particularly as a function of sintering temperatures, as shown by recently completed small-angle scattering investigations (Epperson et al., 1989; Wallner et al., 1989).

Because of the likelihood of random orientation of crystallites in some three-dimensional nanostructures, the use of single-crystal techniques is of



dubious value. The Rietveld powder profile technique should be extended to handle these types of problems. Because of its general applicability to multiphase systems and the possibility of extension to include determinations of both grain size and inhomogeneous strain, this technique offers the potential of being a central tool in the study of atomic arrangements in three-dimensional nanostructures. With the use of high-resolution diffractometers on high-intensity synchrotron sources, even milligram sizes of samples can be measured. The technique can be easily extended to monitor the influence of time, temperature, and pressure on the atomic arrangements in the nanostructure. Because the x-ray technique averages over significant volumes of material, it offers a complementary tool to STEM and other atomic-imaging techniques.

A different approach must be employed when the study of lamellar nanostructures using x-ray scattering is being considered. Low-angle x-ray diffraction is a powerful tool for the analysis of layer structure in periodic multilayers, particularly for those that are largely or completely amorphous. A theory for the scattering of x-rays from such periodic amorphous or largely amorphous arrays has been developed. It incorporates all of the results of the full dynamical theory of x-ray scattering (which in general is needed to make the correct first approximation to the analysis of the x-ray scattering from many multilayer systems), including absorption, extinction (i.e., depletion of the incident beam intensity), and multiple scattering. In addition, this theory provides the only systematic basis for handling the case of nonperiodic finite number of layers (John Keem, 1989, private communication).

Information concerning the interfacial atomic arrangements is contained in the higher-order low-angle scattering peaks and interpeak scattering. At this time there has been no detailed analysis of this type of data and correlation of the results to real-space models for the interfacial atomic arrangements as obtained from a theoretical model or an empirical model constructed with the aid of Scanning Transmission Electron Microscopy (STEM). This is an area ripe for further study for its own value and for the value of development as a tool for others to use in the characterization of their nanostructures.

Extended x-ray absorption fine structure (EXAFS) technology is well suited for the study of highly dispersed particles 2 nm in diameter that are typically outside the detection capability of conventional x-ray diffraction (XRD) or transmission electron microscopy (Sinfelt et al., 1984). EXAFS yields information about local atomic structure, including nearest-neighbor distances and the number of atoms coordinated to the metal of interest. EXAFS has been used to determine the average particle size, to identify particle morphology (hemisphere versus raft), to identify the distribution of atoms in bimetallic and multimetallic clusters (segregation of one component to the surface), to identify the interaction of catalyst particles with the support, and to identify the oxidation states of metals or promoters. In addition,

EXAFS can be used to study the impact of pretreatment on the surface composition of bimetallic clusters and the impact of impurities, such as sulfur and carbon, on the segregation of metals at the surface of particles.

An EXAFS investigation by Meitzner and coworkers (1985) of the structure of bimetallic Re-Cu, Ir-Cu, and Pt-Cu clusters explored the effect of varying miscibility of the components on the structure of the clusters. These authors showed the interesting result that in the bimetallic clusters the atoms of Re, Ir, and Pt are all coordinated to Cu as extensively as they are to atoms of their own kind. This good coordination to Cu in the cluster configuration is in contrast to the only slight miscibility of Ir and Cu and the complete immiscibility of Re and Cu in the bulk. The miscibility of these metals is attributed to the high dispersion of the metal clusters.

## TRANSMISSION ELECTRON MICROSCOPY

### Structural Imaging

Because of the ultrafine grain size of nanophase materials, transmission electron microscopy is an important tool for the direct characterization of grain-size distribution and morphologies. In addition, atomic-resolution transmission electron microscopy holds the promise for elucidating the atomic structure of nanophase interfaces in a manner difficult to achieve with other structural probes. A high-resolution electron micrograph of nanophase  $\text{TiO}_2$  is shown in Figure 16.



FIGURE 16 High-resolution transmission electron micrograph of nanophase  $\text{TiO}_2$  (rutile) after sintering for one-half hour at  $500^\circ\text{C}$  (Siegel and Hahn, 1987).

The atomic planes of the rutile structure are clearly seen, as are crystallographic and morphological relationships among the grains. The atomic structure of grain boundaries in nanophase Pd has been very recently studied by atomic-resolution electron microscopy (Thomas et al., 1989). Comparisons between observed and calculated images of these boundaries indicate structures that are rather similar to those found in conventional polycrystalline boundaries (see frontispiece).

Figure 17 shows a rather typical grain-size distribution for such a nanophase material (in this case  $\text{TiO}_2$ ) in the as-compacted state determined from dark-field images. TEM measurements on both an oxide (Siegel et al., 1988) and a metal (Hort, 1986) indicate rather good grain-size stability (see sections on stability in Chapter 5) with increasing temperature and only modest grain growth taking place until about  $700^\circ\text{C}$  and  $400^\circ\text{C}$  in nanocrystalline  $\text{TiO}_2$  and Fe, respectively.

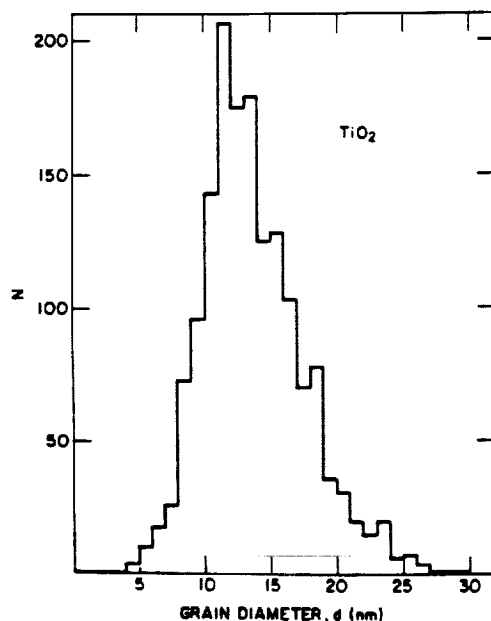


FIGURE 17 Grain-size distribution for an as-compacted  $\text{TiO}_2$  (rutile) sample determined using TEM (Siegel et al., 1988).

### Analytical Electron Microscopy

Analytical electron microscopy (AEM) is the only technique that can provide both structural and chemical information about individual catalyst particles at near-atomic-level spatial resolution. The companion technique of high-resolution electron microscopy (HREM) produces atomic-level images of metal particles and their supports (Smith et al., 1983). AEM is really a group of techniques, each of which can provide different information about

catalysts: (1) x-ray emission spectroscopy (XES) for elemental analysis and elemental distribution images (Lyman, 1986); (2) electron energy loss spectroscopy (EELS) for analysis of light elements and chemical shift effects (Lyman et al., 1984); and (3) convergent beam electron diffraction (CBED) for identification and structure determination of small particles (Cowley, 1984). Unfortunately, high- or ultrahigh-vacuum environments are generally required for these techniques.

The morphology of the particles can limit the characterization; for example, catalysts prepared using nonporous oxide particles as model supports permit more detailed characterization of the structure of the metal crystallites and the metal support interface (edge-on views) than is easily possible with porous supports (Datye and Logan, 1986).

## SPECTROSCOPIES

### Optical Spectroscopy

The literature on the application of infrared (IR) spectroscopy to the study of adsorbed molecules on supported metals is extensive. The frequency bands for adsorbed molecules such as NO and CO provides information on the state of the metal on the support (e.g., dispersion). The wide availability of Fourier transform infrared spectroscopy (FTIR) has renewed interest in this technique. For example, in situ studies of catalytic reactions are possible using cells that can be pressurized with reactants (or flow through) and heated to high temperatures.

Diffuse reflectance spectroscopy is a characterization technique particularly well suited for the study of materials that strongly scatter light (and poorly transmit light) in the 7 to 0.05 eV energy range (UV-VIS-IR). When applied in the infrared region, this technique is used to study vibrational modes of molecules adsorbed on surfaces. Thus, information is gained about how molecules interact with surfaces (Kortum, 1969; Klier, 1980).

Raman spectroscopy has recently been used to probe the grain and grain-boundary structures in nanophase  $\text{TiO}_2$  (Melendres et al., 1989). It was found that the strong Raman-active lines representative of the rutile structure dominated all of the observed spectra, independent of average grain size (10 to 100 nm) and annealing treatment. These Raman data gave no indication of grain-boundary structures in nanophase  $\text{TiO}_2$  that are significantly different from those in conventional polycrystals. This method can be usefully applied to the study of other nanoscale materials with strong Raman-active features.

### Nuclear Spectroscopy

With Mössbauer spectroscopy, the local atomic environments of probe atoms are characterized in terms of hyperfine parameters. Herr and coworkers (1987) used this method as a further test of the proposed two-component model of nanocrystalline Fe deduced from their x-ray analysis (Zhu et al., 1987). The Mössbauer spectrum of a nanocrystalline pellet of Fe with 6-nm grain size compacted to 5 GPa could be fitted with two components in accord with their two-component (crystal plus interface) structural model. It was found that one subspectrum can be described by the Mössbauer parameters of crystalline body-centered-cubic Fe. The second subspectrum is characterized by an enhanced hyperfine magnetic field, a larger line width, and an increased isomer shift in comparison to the crystalline component.

Positron annihilation spectroscopy (PAS) is very sensitive to small defects with increased free volume relative to crystal interstices (like vacancies, vacancy clusters, grain boundaries, voids, etc.) and can therefore be used to investigate the structure of nanocrystalline materials in a regime that is not easily accessible to other techniques (e.g., electron microscopy). PAS can be used to investigate the sintering behavior of nanophase materials as a function of compaction pressure or temperature by following the shrinkage and disappearance of internal voids, as a complement to small-angle x-ray or neutron scattering measurements. Positron-lifetime measurements on a number of nanocrystalline metals by Schaefer and coworkers (1987) and on nanocrystalline  $\text{TiO}_2$  (Siegel et al., 1988) have clearly indicated the presence of voids in as-consolidated samples. Furthermore, reduction of this porosity in nanophase  $\text{TiO}_2$  as a function of increasing sintering temperature could be followed by PAS (Siegel et al., 1988). Such results along with those from complementary SANS experiments (e.g., Epperson et al., 1989) should help to elucidate the sintering behavior of nanophase materials.

Improvements in the sensitivity of nuclear magnetic resonance (NMR) have made it possible to use this technique to study simple molecules, especially those containing C and H adsorbed on the surfaces of supported metal particles in 1- to 5-nm diameter clusters (Wang et al., 1986). NMR gives both structural information and kinetic parameters and is suitable for examining high-surface-area catalysts. Studies reported to date have provided information on the bonding and structure of molecules such as CO, ethylene, and acetylene adsorbed on the metal. In addition, NMR gives information on the motion of adsorbed species, adsorption parameters, and the structure and composition of adsorbed intermediates. NMR is proving to be a popular tool for studies of support materials, especially zeolites. Most of these studies have dealt with the nuclei  $^{27}\text{Al}$  and  $^{29}\text{Si}$  as well as  $^{17}\text{O}$ ,  $^{13}\text{C}$ ,  $^{31}\text{P}$ ,  $^{11}\text{B}$ , and  $^7\text{Li}$  (Stucky and Dugen, 1984; Hanson et al., 1984).

### Electron Spectroscopy

X-ray photoelectron spectroscopy (XPS) has been widely applied to the characterization of supported catalysts. This technique provides information on elemental composition and chemical environment, since XPS involves the excitation of core electrons. XPS is very surface-sensitive, sampling not more than 6 nm, and can be used for the characterization of multimetallic catalysts. The area under the peaks is a measure of concentration, while peak position provides information on the oxidation state. Limitations of the technique are signal overlap and degradation of the sample in the beam.

### CALORIMETRY

Differential scanning calorimetry is a relatively simple technique that can be used very effectively in the study of the structure and stability of nanometer-scale materials. For example, the finest microstructures, with a grain size on the order of only a few nanometers, give diffraction patterns that contain broad halos and appear featureless in dark-field transmission microscopy. It is therefore often difficult to distinguish them from "truly" amorphous structures, such as liquids and glasses, which have no translational symmetry at all.

The kinetics of the transformation of both structures to one with sharp diffraction rings are fundamentally different, however. The amorphous structure transforms by nucleation and growth of new crystals, which is observed as an exothermic peak in isothermal calorimetry. The microcrystalline structure, on the other hand, does not undergo a phase transformation, but simply coarsens by a process of grain growth. This is observed in isothermal calorimetry as a continuously decreasing exothermal signal, corresponding to the elimination of interfacial enthalpy. This has recently been used, for example, to show that sputtered Al-transition metal alloys are microquasicrystalline (Chen and Spaepen, 1988).

The high interfacial density of the nanometer-scale materials makes it possible to determine the absolute average interfacial enthalpy directly by calorimetric studies of the grain growth process (either isothermal or by scanning). This could be applied to a number of materials where absolute values of the interfacial energy are not known. At the same time, such studies could also contribute to the understanding of the grain growth process itself, which has recently seen a resurgence of interest.

### OTHER PROMISING METHODS

A number of other recent developments in microstructural and microchemical analysis methods will almost certainly have a significant impact on the characterization of nanophase materials. Because of the ultrafine scale

of these materials, new or modified techniques need to be brought to bear in this area. Among the most promising characterization methods available at present are the field ion microscope (FIM), also with atom-probe capabilities, the scanning tunneling microscope (STM), also with atomic force probe capabilities, and such analytical methods as electron-energy loss spectroscopy (EELS) utilizing ultrafine probe sizes. In the area of mechanical properties, nanoindenter studies of the elastic and plastic properties of nanophase materials should prove very useful. Clearly, the ability to synthesize and examine nanophase materials in situ under carefully controlled conditions, such as ultrahigh vacuum, will be necessary to fully elucidate their unique characteristics.

The density of nanophase materials needs to be precisely measured, but even such an apparently simple measurement as this can be difficult to accomplish for these ultrafine-grained materials with their even finer-scaled porosity. Some success in using the BET method on nanocrystalline ceramics has been recently reported (Hahn et al., 1989). Absolute measurements of density via x-ray or neutron adsorption are also viable, but additional methods more easily applied are certainly needed.

#### REFERENCES

- Chen, L. C., and F. Spaepen. 1988. *Nature* 336:366.
- Cowley, S. W. 1984. *Catalytic Materials*, ACS Symposium Series 218, p. 353. Washington, D.C.: American Chemical Society.
- Datye, A. K., and A. D. Logan. 1986. *Proc. Electron Microscopy Soc.*, G. W. Bailey, ed. San Francisco: San Francisco Press.
- Epperson, J. E., R. W. Siegel, J. W. White, T. E. Klippert, A. Narayanasamy, J. A. Eastman, and F. Trouw. 1989. *Mater. Res. Soc. Symp. Proc.* 132:15.
- Hahn, H., J. Logas, H. J. Höfler, T. H. Bier, and R. S. Averbach. 1989. *Mater. Res. Soc. Symp. Proc.* 132:35.
- Hanson, B. E., G. W. Wagner, R. J. Davis, and E. Motell. 1984. *Inorg. Chem.* 23:1635.
- Haubold, T., R. Birringer, B. Lengeler, and H. Gleiter. 1988. *J. Less Common Metals*, 145:557.
- Herr, V., J. Jing, R. Birringer, U. Gonser, and H. Gleiter. 1987. *Appl. Phys. Lett.* 50:472.

- Hort, E. 1986. Diplom Thesis, Universität des Saarlandes, Saarbrücken, Germany.
- Klier, K. 1980. Vibrational Spectroscopy of Adsorbed Species. A. T. Bell and M. L. Hair, eds. Washington, D.C.: American Chemical Society.
- Kortum, G. 1969. Reflectance Spectroscopy: Principles, Methods, and Applications. Berlin: Springer-Verlag.
- Lyman, C. E. 1986. Ultramicroscopy 20:119.
- Lyman, C. E., A. Ferretti, and N. J. Long. 1984. Analysis of a Cu/Zn catalyst by electron energy loss spectroscopy. In Analytical Electron Microscopy, D. B. Williams and D. C. Joy, eds. San Francisco: San Francisco Press.
- Meitzner, G., G. H. Via, F. W. Lytle, and J. H. Sinfelt. 1985. J. Chem. Phys. 83:353.
- Melendres, C. A., A. Narayanasamy, V. A. Maroni, and R. W. Siegel. 1989. Mater. Res. Soc. Symp. Proc. 153, in press. J. Mat Res., Vol. 4, in press.
- Schaefer, H. E., R. Wurschum, M. Scheytt, R. Birringer, and H. Gleiter. 1987. Mater. Sci. Forum 15-18:955.
- Siegel, R. W., and H. Hahn. 1987. P. 403 in Current Trends in the Physics of Materials, M. Yussouff, ed. Singapore: World Scientific Publ.
- Siegel, R. W., S. Ramasamy, H. Hahn, Z. Li, T. Lu, and R. Gronsky. 1988. J. Mater. Res. 3:1367.
- Sinfelt, J. H., G. Via, and F. W. Lytle. 1984. Catal. Rev.-Sci. Eng. 26:81.
- Smith, J. D., et al. 1983. J. Catalysis 81:107.
- Stucky, G. D., and F. G. Dugen. 1984. P. 159 in ACS Symposium Series 218. Washington, D.C.: American Chemical Society.
- Thomas, G. J., R. W. Siegel, and J. A. Eastman. 1989. Mater. Res. Soc. Symp. Proc. 153, in press.
- Wallner, G., E. Jorra, H. Franz, J. Peisl, R. Birringer, H. Gleiter, T. Haubold, and W. Petry. 1989. Mater. Res. Soc. Symp. Proc. 132:149.



Wang, P. K., J. P. Ansermet, S. L. Rudaz, Z. Wang, S. Shore, C. P. Slichter,  
and J. H. Sinfelt. 1986. Science 234:35.

Zhu, X., R. Birringer, U. Herr, and H. Gleiter. 1987. Phys. Rev. 35:9085.



## 5

### PROPERTIES

#### NANOPHASE COMPACTS

The structure-related properties of nanophase materials are expected to be different from those of normally available single-crystal, polycrystal, or amorphous materials because of their ultrafine grain size and large interfacial volume fraction. Initial investigations indicate that such an expectation is indeed justified. Birringer and coworkers (1986) have tabulated a number of properties measured on nanocrystalline metals and compared them with values for their coarse-grained (or single-crystal) counterparts and similar glassy materials. Some of these comparisons are shown in Table 1 (Chapter 1), in which it can be seen that the change in a variety of materials properties appears to be significantly greater in going from conventional crystalline material to nanocrystalline material than in going from crystalline to glassy solid, changes that are generally less than 10 percent. Very few property measurements have been made on nanophase materials to date, and the full impact of their ultrafine microstructures on their properties will only be elucidated by further research in this new area of materials synthesis. Some examples can be given here, however, of such research on nanophase metals and ceramics, dealing with their magnetic and mechanical properties and with diffusion and solid-state reactions in them, that depend on their ultrafine microstructure.

#### Magnetic Properties

A recent study (Cowen et al., 1987) of the magnetic properties of nanocrystalline Er has been carried out, and the results were compared with measurements on the coarse-grained polycrystalline Er starting material. The

results are shown in Figure 18, where the reciprocal magnetic susceptibility is plotted against temperature for three samples with different grain sizes. The three normally observed magnetic phase transitions, associated with competing exchange and anisotropic interactions, can be seen for the coarse-grained polycrystalline Er starting material at 19, 52, and 85 K in Figure 18(a). However, for the slowly evaporated nanocrystalline Er, with grain diameters in the lower end of the range 10 to 70 nm, these magnetic phase transitions are no longer observed, and a new low-temperature transition to superparamagnetic or spin glasslike behavior arises. On the other hand, for rapidly evaporated nanocrystalline Er, with grain diameters larger than in Figure 18(b) and in the upper end of the range 10 to 70 nm, the normal magnetic phase transitions reappear, but at different temperatures, while the low-temperature superparamagnetic behavior is retained. The detailed magnetic properties of these nanophase Er samples are thus strongly affected by the nanometer scale of their grains and consequently the large volume fraction of grain boundaries. How these properties depend on the grain size, the fraction and location of atoms in grain boundary sites, and the possible formation of Er-oxygen compounds at these interfaces during synthesis, however, remains to be elucidated.

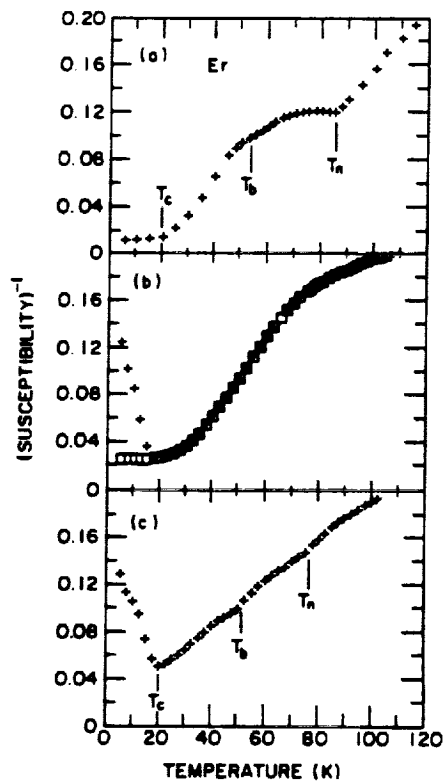


FIGURE 18 Reciprocal magnetic susceptibility versus temperature for three Er samples from the same starting material but with different grain sizes: (a) coarse-grained polycrystal, (b) slowly evaporated nanocrystal, and (c) rapidly evaporated nanocrystal (Cowen et al., 1987).

### Densification and Sintering

The synthesis of nanophase  $\text{TiO}_2$  (rutile) has recently been carried out using the gas-condensation method, and the material was subsequently studied by a variety of techniques as a function of sintering temperature (Siegel et al., 1988). Nanophase ceramics, with their high grain-boundary purity and small particle size, leading to higher reactivity among grains and shorter and more effective diffusion paths, are expected to sinter at lower temperatures than normally available ceramics. They are also expected to exhibit considerably improved sinterability and mechanical properties, owing to a lack of brittle second phases in their interfaces and more effective crack-energy dissipation via their ultrafine grain-boundary networks. Small Ti particles were first produced in a He-gas atmosphere and then oxidized on the cold-finger of the production chamber prior to in situ compaction at about 1.4 GPa at room temperature. The resulting  $\text{TiO}_2$  nanophase compact had a mean grain diameter of 12 nm. Grain-size distributions were determined by TEM, and Vickers microhardness was measured at room temperature on the as-compacted sample and as a function of sintering temperature up to 1400°C. The results of these microhardness measurements are shown in Figure 19; they are compared

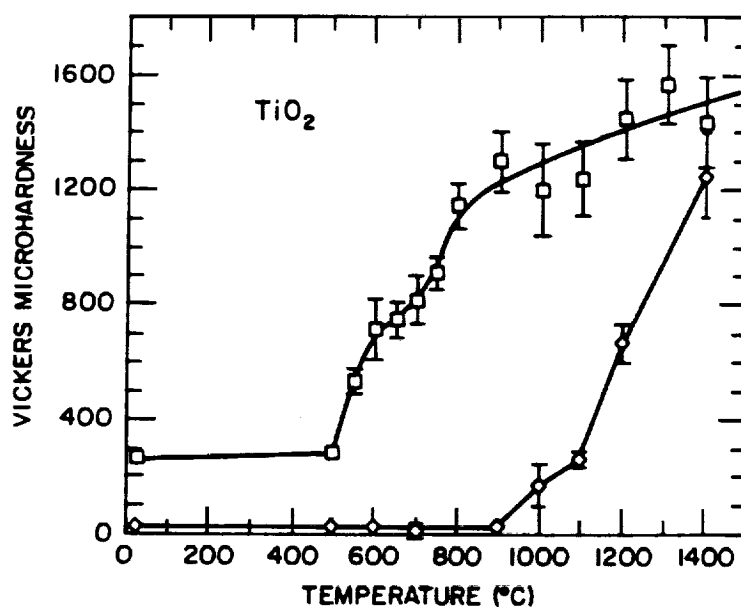


FIGURE 19 Vickers microhardness (in units of  $\text{kgf/mm}^2$ ) of  $\text{TiO}_2$  (rutile) measured at room temperature as a function of one-half hour sintering at successively increased temperatures. Results for a nanophase sample with a 12-nm initial mean grain size (squares) are compared with those for a coarser-grained compact with a  $1.3\text{-}\mu\text{m}$  initial mean grain size (diamonds) (Siegel and Hahn, 1987).

with similar measurements on a  $\text{TiO}_2$  (rutile) sample compacted at 0.32 GPa with a polyvinyl-alcohol sintering aid from commercial powders ball-milled to a mean grain diameter of  $1.3 \mu\text{m}$ . The results of these investigations on  $\text{TiO}_2$  indicate that the nanophase compacts, which are rather well bonded on compaction even at room temperature, densify rapidly upon sintering above  $500^\circ\text{C}$  with only small increases in grain size. This gives hardness values greater than those of sintered coarser-grained commercial  $\text{TiO}_2$ , but at some  $600^\circ\text{C}$  lower temperatures and without the need for compacting and sintering additives. Fracture toughness was found to be improved as well. Fracture measurements (Li et al., 1988) by SEM on similar samples also indicate improved mechanical properties for the nanophase  $\text{TiO}_2$  relative to coarser-grained conventionally prepared material, with a reduction in the temperature for transgranular fracture of  $200^\circ\text{C}$  in the nanophase samples. It is expected that more efficient mechanisms for crack-energy dissipation should be generally available in such ultrafine-grained materials through their grain-boundary networks, which represent a significant fraction of their volume.

The intent of the use of properly treated ultrafine starting materials in processing is to fabricate uniform and reproducible submicron-sized microstructures in the unfired pieces, which would be retained in the fired microstructures. However, grain growth generally occurs during sintering, especially on sintering to theoretical density. This occurrence is not necessarily a failure. Using this processing approach results in uniform and reproducible microstructures with more favorable properties, obtained at lower temperatures (Joseph Pask, personal communication).

### Diffusion and Solid-State Reactions

The study of diffusion processes in nanophase materials is of interest for a variety of reasons. First, the knowledge of such diffusion processes can contribute to the understanding of the nanocrystalline structure, particularly with respect to the nature of the interfaces. Second, because of the expected high diffusivities in a material with a large volume fraction of interfaces, doping of the interfacial regions or even alloying with a second element by diffusion along the nanophase grain-boundary network is a feasible process that would allow the tailoring or engineering of properties. Furthermore, the high diffusivities combined with the short reaction distances, resulting from the small particle sizes and high density of nucleation sites in the interfaces of nanophase materials, might permit the formation of interfacial metastable or stable phases in the solid state at fairly low temperatures. In addition, nanophase processing of ultrafine powders opens up a variety of possibilities for producing new metastable phases in bulk form by reacting binary mixtures of nanocrystals of different elements at low temperatures. The production of binary mixtures of nanocrystals in large quantities, compaction into the desired shape, and formation of the phase by solid-state reaction would be a straightforward process. The studies of diffusion and solid-state reactions occurring in

nanophase materials described in the next paragraphs form a basis for the understanding and control of such processes.

Since nanophase materials are rather new as a research topic, only a small number of diffusion experiments have been performed until now. Horváth and coworkers (1987) have reported results on self-diffusion in nanocrystalline Cu using a radioactive-tracer technique combined with sputter sectioning. The grain-boundary diffusion coefficient at 353 K in nanocrystalline Cu is 3 orders of magnitude larger than that in a coarse-grained polycrystalline Cu sample (with an assumed grain boundary width of 1 nm) and 16 orders of magnitude larger than that (extrapolated from higher temperatures) in single-crystal Cu. A rather rough estimate, due to the limited temperature range of the measurements, yields 0.64 eV for the activation enthalpy for self-diffusion, which is even smaller than that for normal grain-boundary diffusion (1.06 eV), but very close to that for surface diffusion. Yet, one must be very careful with the interpretation of this value until a detailed characterization of the samples for internal surfaces and possible relaxation processes in the grain boundaries at low temperatures is performed. Recent investigations by H. J. Höfler, H. Hahn, and R. S. Averback (unpublished results, 1988) have confirmed these high diffusivities by measurements of Ag and Bi diffusion in Cu nanocrystals and of Cu and Ag diffusion in Pd nanocrystals obtained by a variety of techniques, including electron microprobe analysis, (Rutherford) He-backscattering (RBS), secondary-ion-mass spectroscopy, and sputtered-neutral-mass spectrometry. Similarly high diffusivities appear to pertain to nanophase ceramics as well, according to recent RBS measurements of Pt diffusion into nanophase  $\text{TiO}_2$  (Siegel and Eastman, 1989).

To help provide a basis for the understanding of reaction kinetics in binary nanophase mixtures involving systems with large negative heats of mixing, and thus the tendency for phase formation, the reaction of a thin Bi film on a Pd nanocrystal was measured using He-backscattering and electron microscopy (H. J. Höfler, H. Hahn, and R. S. Averback, unpublished results, 1988). As shown in Figure 20, the formation of the equilibrium intermetallic compound  $\text{Pd}_3\text{Bi}$  was observed by He-backscattering at rather low temperatures, and electron microscopy confirmed this phase formation. It was also found that significant grain growth occurred in the reacted zone but not on the opposite face of the sample, where no Bi was available. This is indicative of a grain-growth process that is caused by chemical driving forces similar to diffusion-induced grain-boundary migration (DIGM), which results in the alloying of a zone over which a grain boundary has moved. Under the same conditions, however, no  $\text{Pd}_3\text{Bi}$  phase formation could be observed in evaporated thin-film samples, indicating again the increased diffusivities and reactivities in the nanocrystalline structure. The potential for nanophase materials processing shown by the low-temperature formation of  $\text{Pd}_3\text{Bi}$  also offers a new method for the production of bulk metastable or stable compounds at low temperatures by interdiffusion starting from a binary mixture of

nanocrystals; an example of this method is described in the following for the case of Cu-Er alloys.

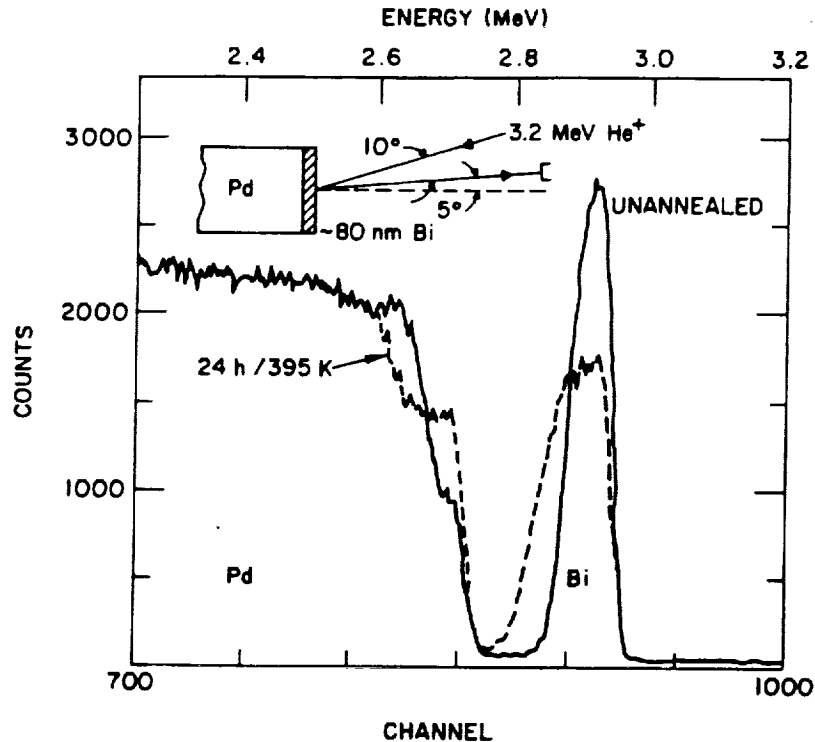


FIGURE 20 He-backscattering spectra for a nanocrystalline Pd sample with an 80-nm thick Bi film deposited onto its surface after sputter cleaning: Before annealing (solid curve) and after 24 hours at 395 K (dashed curve). The experimental setup is shown in the inset. The  $\text{Pd}_3\text{Bi}$  phase formation with a fixed composition can be seen clearly at the front edge (H. J. Höfler, H. Hahn, and R. S. Averback, 1988, unpublished results).

Cu and Er metal particles were produced simultaneously with the gas-condensation method and deposited onto the surface of a rotating cold finger in order to achieve a better mixture of the two components. The scraped powder was then compacted to about 2 GPa without exposing to air. Both chemical analysis and He-backscattering yielded a composition close to 50 atomic percent Cu. Debye-Scherrer x-ray analysis showed that, besides a small amount of unreacted Cu and Er particles, most of the sample was reacted to the equilibrium compound CuEr with a CsCl-structure. No additional phases could be identified. This experiment shows that the nanophase production method is clean enough to subsequently react particles with one another, even when highly reactive metals like Er are being used. Furthermore, it demonstrates that the intermixing of the particles of two metals in the convective He-gas



flow and on the rotating cold finger is sufficient to almost totally react the powder by compaction alone.

In the Cu-Er system, the formation of a partially amorphous phase by a combination of mechanical cold-rolling of elemental foils and their subsequent thermal annealing was reported by Atzmon et al. (1985). Yet, no formation of an amorphous phase was observed in the compacted nanophase pellet, although the composition was in the right range. The most probable reason is that heating of the sample during the compaction process caused by the mechanical energy and the release of the chemical energy of the reacting particles (owing to a large negative heat of mixing), allowed the sample to exceed the fairly low crystallization temperature of about 470 K for this composition. A solution to this problem would be to use a more appropriate system like Ni-Zr with a much higher crystallization temperature or to optimize the compaction process for minimal heating.

## MECHANICAL PROPERTIES

Some of the most significant changes in physical properties of nanometer-scale structures are found in their mechanical properties, elastic as well as plastic.

One of the most striking reports in the study of the physical properties of artificial multilayers and in situ composites has been that of the "supermodulus" in metallic artificial multilayers. It was found that, for composition modulations around 2 nm, some of the elastic moduli increased by as much as a factor of 4. A similar finding was made in ultrafine in situ composites, as illustrated in Figure 21. The lowering of the modulus with reduction in the unannealed specimens is due to the increase in dislocation density. The increase in the modulus in the annealed specimens is attributed to the "supermodulus" effect.

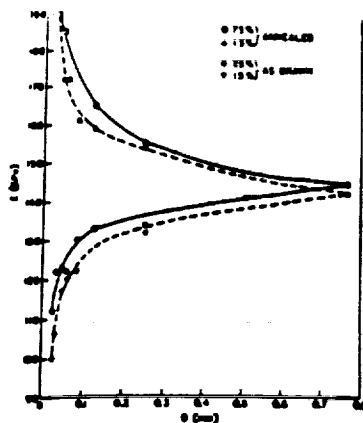


FIGURE 21 Young's modulus of in situ-formed Cu-Nb filamentary composites as a function of wire diameter, thermal history, and composition (Bevk, 1983).

The experimental situation still needs some clarification, however. A complete and consistent set of moduli for one film needs to be measured. Some investigators, using different measuring techniques or differently prepared samples, have failed to find the effect.

The theoretical understanding is in particularly great need of attention. Two categories of theories can be distinguished. Those in the first category consider the interaction between the Fermi surface of the metal and the artificial Brillouin zone boundary created by the composition modulation. The second set of theories is based on the nonlinear elastic effects resulting from the large coherency strains across the phase boundary. The reduction of the modulus of the annealed specimens of Figure 21 as a result of a small amount of plastic formation, for example, points in this direction. Both types of theories, however, are still rather unsatisfactory.

Concerning the effects of a nanometer-scale microstructure on the plastic properties, several aspects should be considered. It is well known, for example, that refining the scale of the microstructure leads to an increase in the yield strength of a material. The effect of grain boundaries as obstacles to dislocation motion is reflected in the Hall-Petch relation between grain size and yield strength. It is of great interest to explore to what extent this relation can be extended down to the 1-nm grain-size range. In addition, it would be worthwhile to know if the physical modeling of the hardening, which for "conventional" grain sizes consists of the activation of a dislocation source in a new grain by a dislocation pile-up against the boundary in an adjacent grain, should be modified to account for the observation.

The effect of second-phase particles on dislocation motion is also well known. A particularly dramatic example of the strengthening effects is found with ultrafine in situ composites. The strength of these composites is considerably above that predicted by the "rule of mixtures" from the strength of the individual components, which works well for filaments with diameters greater than a micrometer. The role of the filaments in inhibiting the dynamic recovery of the work-hardened matrix seems to be significant, resulting in higher matrix dislocation densities than could be achieved in bulk. The filaments themselves are often found to be almost dislocation-free and whisker-like.

Similarly, the plastic properties (especially hardness) of artificial multilayers have also been seen to be very different at small layer thicknesses. For example, the hardness of TiN-VN multilayers is much higher for layer repeat lengths around 2 nm than at higher repeat lengths or in thin films of the individual compounds (Helmersson et al., 1987). The "super-modulus" effect may be contributing to this through the line tension of dislocations. At the same time, the interaction of the dislocations with a high density of interfaces, which can include unusual interlayer image stress effects, can lead to strengthening effects.

Conventionally brittle materials can be made ductile by exploiting enhanced diffusional creep at low temperatures if the grain size is very small. At low temperatures, where atomic diffusion along grain boundaries dominates, the deformation rate,  $\dot{\epsilon}$ , is given by

$$\dot{\epsilon} = \frac{B\sigma\Omega\delta D_b}{d^3 kT}$$

where  $\sigma$  is the tensile stress,  $\Omega$  is the atomic volume,  $d$  is the average crystal size,  $B$  is a numerical constant,  $D_b$  is the boundary diffusivity,  $kT$  has the usual meaning, and  $\delta$  is the thickness of the boundaries. The diffusional creep rate of a polycrystal, therefore, may be enhanced by reducing the crystal size,  $d$ , and by increasing the boundary diffusivity,  $D_b$ .

Recent studies on the boundary diffusivity in nanocrystalline metals with grain sizes around 5 nm (Horváth et al., 1987; Birringer et al., 1988) indicate a thousand-fold enhancement of grain-boundary diffusion over conventional polycrystals. This enhancement ( $10^3$ ), coupled with a reduction in crystal grain size (from 10  $\mu\text{m}$  to 10 nm), could increase creep rates by approximately  $10^{12}$ .

The enhanced plasticity at low temperature may be utilized for processing by conventional extrusion or rolling methods. If desired, the material may be subsequently converted back to conventional-scale structures. For example, the surface may be laser-annealed to develop a much coarser surface grain structure with properties different from the unrecrystallized interior.

Finally, it is also useful to think of some of these artificial multilayers as custom-made composites that allow extension of the well-known advantages of composites to a much smaller length scale. The combination of a ductile but weak metallic phase with a strong but brittle compound is a classic example (e.g., pearlite). It is now possible to create metal-oxide or metal-nitride films artificially in which the spacing of the phases is much smaller than was possible by conventional methods.

## CATALYTIC PROPERTIES

The nature of the surface sites that are responsible for the catalytic reaction (active sites) has been the subject of catalysis research studies for many years, and several models have been proposed for describing the catalytically active sites. These models have been based on different characteristics of the sites, such as (1) the geometry of the sites (i.e., the distance between atoms around the site), (2) the coordination number of the catalytic sites that are associated with individual atoms, (3) sites associated with a critical ensemble of atoms, and (4) electronic structure

models that assume that a critical electronic configuration imparts activity. Research aimed at characterizing catalytically active sites has included studies of the nature of the adsorption and coordination of reactants with surface atoms, the arrangement of the reactants and intermediates on the surface, the size and configuration of the surface site, and the acid or base nature of the site.

Detailed understanding of the relationships between catalyst structure and properties has in the past been hampered by limited structural information on catalysts. New and improved characterization techniques combined with the potential for synthesizing catalysts with controlled microstructures hold potential for making connections between structure and properties in model catalyst systems that closely mimic real catalysts. Such studies also hold potential for synthesizing materials with improved catalytic properties.

A great deal of attention has been given to catalyst particle size, and many catalytic reactions have been classified as structure-sensitive or structure-insensitive, depending on the active site requirement of various catalytic reactions. Variation of the particle size of supported metal catalysts in the range of 1 to 10 nm can have dramatic effects on the activity and selectivity. Reactions that have been reported to exhibit structure sensitivity include these broad classes: oxidation (generally rates decrease with decreasing particle size), alkane transformation such as hydrogenolysis and skeletal isomerization (usually, but not always, rates increase with decreasing particle size), and some isotopic exchange and hydrogenation reactions (rates usually decrease with decreasing particle size) (Bond, 1985). An example from the recent literature is the effect of iron particle size for iron supported on MgO as the determining factor in the activity and selectivity of the iron for hydrocarbon synthesis from CO-H<sub>2</sub> (McDonald et al., 1986).

A topic of major interest is the determination of how the catalyst surface is affected by pretreatments. Some supported metal catalysts have been found to exhibit widely different activity following specific pretreatments. For example, Ru supported on alumina readily catalyzes the water gas shift reaction and ammonia decomposition following a brief oxidation of the catalyst, but this activity is lost following reduction (Taylor et al., 1974).

Progress has been made in understanding pretreatment effects through the combined use of activity and microscopy measurements. The surfaces of Ni/SiO<sub>2</sub> (Lee et al., 1986) and Rh/SiO<sub>2</sub> (Lee and Schmidt, 1986) have been examined in detail. Oxidation and reduction pretreatments were used to change the catalyst microstructure, and activity changes in the catalyst were shown to be associated with morphological changes in the active site.

The effect of oxidation-reduction pretreatments on the activity of a series of Pt/SiO<sub>2</sub> and Pt/Al<sub>2</sub>O<sub>3</sub> catalysts has been examined in detail for

several reactions, including isotopic exchange between cyclopentane and deuterium and between methylcyclopropane hydrogenation and hydrogenolysis (Inoue et al., 1978; Otero-Schipper et al., 1978; Wong et al., 1980; Pitchai et al., 1985; Burch and Garla, 1982). Factors discussed as potentially responsible for the various pretreatment effects include oxide formation and incomplete reduction, morphological changes depending on the temperature of exposure to hydrogen, the degree of dehydroxylation of the support, and the presence of some inhibitive form of adsorbed hydrogen.

The effect of the treatment of supported metal catalysts with hydrogen on surface morphology, catalyst activity, and adsorption properties is in a state of confusion at the present time (Paal and Menon, 1983).

Bimetallic catalysts that exhibit activity or selectivity for a particular reaction or sequence of reactions that cannot be explained by the activity of the individual metals are said to exhibit synergistic effects. An example is the reduction of nitric oxide by carbon monoxide over Pt-Ni/Al<sub>2</sub>O<sub>3</sub> and Pd-Ni/Al<sub>2</sub>O<sub>3</sub>; the bimetallic catalysts are significantly more effective for reducing nitric oxide than Pt, Pd, or Ni alone (Klimisch and Taylor, 1973). Likewise, the activity of a bimetallic Pt-Rh/Al<sub>2</sub>O<sub>3</sub> catalyst was shown to be substantially higher than that of a physical mixture of the two noble-metal catalysts for promoting the oxidation of carbon monoxide in a CO-NO-O<sub>2</sub> feed at low temperature (Oh and Carpenter, 1986).

The term "bifunctional catalysts" refers to catalysts that perform more than one type of reaction. Generally, separate components of the catalyst are responsible for the separate functions, and product formation is the result of sequential reactions on the catalyst.

Catalytic reactions carried out on single-crystal surfaces using various surface science techniques have advanced understanding of the mechanisms of elementary surface reactions and have provided understanding of the relationship of the structure and composition of the surface to catalytic properties.

Comparisons of the properties of supported catalysts with single-crystal catalysts with known structure can provide understanding of structural features that are important for the catalysis. A significant body of such research is only just emerging; future progress will make use of the ability to prepare and characterize model catalysts. The importance of this research for understanding the catalytic properties of supported metal catalysts is demonstrated by comparisons of the adsorption properties and catalytic activity of single-crystal and supported noble-metal catalysts. In the past, most research with single crystals was carried out under ultrahigh-vacuum conditions. Recent studies comparing nitric oxide reduction over single-crystal Rh(111) catalysts and over alumina-supported Rh catalysts at realistic pressures have revealed that the two types of Rh catalyst exhibit substantially different kinetics, and analysis of the rate data suggests that

dissociation of molecularly adsorbed NO occurs more slowly on supported Rh than on Rh(111) (Oh et al., 1986).

Studies of the crystal faces exposed on supported metal catalysts have made use of comparisons with adsorption information determined on single-crystal surfaces. For example, the infrared frequencies for CO adsorbed on supported Pd have been used to determine which low index plane CO is adsorbed onto and how the adsorbate structure is changed with pretreatment (Palazov et al., 1982). In another study in which the infrared spectra for very small amounts of CO adsorbed onto Pd/Al<sub>2</sub>O<sub>3</sub> were compared with CO IR spectra for Pd(111), it was shown that CO was adsorbed initially onto (111) facets on alumina-supported palladium crystallites (average diameter 8.4 nm) and that this adsorption could be blocked by preadsorption of CH<sub>3</sub>C (Beebe and Yates, 1986). The crystallite morphology of supported palladium particles has been shown to influence the catalytic activity of Pd/La<sub>2</sub>O<sub>3</sub> for methanol synthesis: Pd(100) was nearly 3 times more active than Pd(111) (Hicks and Bell, 1984). Masel (1986) has successfully applied orbital symmetry models to predict the preferred crystal face orientation for NO decomposition on Pt.

Strong metal support interaction (SMSI) refers to an interaction between the metal particles and the catalyst support causing suppressed H<sub>2</sub> and CO chemisorption (Tauster et al., 1978). The recent literature on SMSI has heightened awareness of the role of the support in determining catalyst activity and selectivity. Studies of the causes of SMSI have been complicated by the difficulty of looking at powders by modern surface techniques. As a result, some researchers have turned to model catalysts to discover the causes of these observations. For example, Belton and coworkers (1984), making use of Rh films on oxidized Ti, showed that both encapsulation of the metal overlayers and electronic effects contribute simultaneously to SMSI. This encapsulation was shown by both AES and temperature-programmed static secondary ion mass spectroscopy.

## STABILITY

The evolution of a microstructure with a characteristic dimension on the order of 1 to 100 nm is different from that of coarser microstructures in two important ways: (1) Since the interface-to-volume ratio in these materials is exceptionally high, the driving force for coarsening and grain growth is much greater than in conventional microstructures; (2) in multiphase or multicomponent systems, the thermodynamics of homogeneous systems must be adapted to take into account contributions from gradients in density or composition.

The driving force for grain growth is the increased chemical potential  $\Delta\mu = K\gamma\Omega/r$ , where  $\gamma$  is the interfacial tension,  $\Omega$  is the atomic volume,  $r$  is the average grain size, and  $K$  is a constant on the order of unity. For the smallest grains (1 nm), this could be as high as 50 meV per atom. The grain

growth rate in the early stages can therefore be many orders of magnitude greater than is observed for conventional microstructures.

Only limited information on the grain growth in nanophase materials is presently available, and this indicates a relatively deep metastability of the initial grain-size distribution. Grain-growth measurements by TEM in Fe with an initial average grain size of about 7 nm (Hort, 1986) and  $\text{TiO}_2$  (rutile) with an initial average grain size of about 12 nm (Siegel et al., 1988) have demonstrated a rather wide temperature range over which grain growth is quite small. An example of these data is shown in Figure 22.

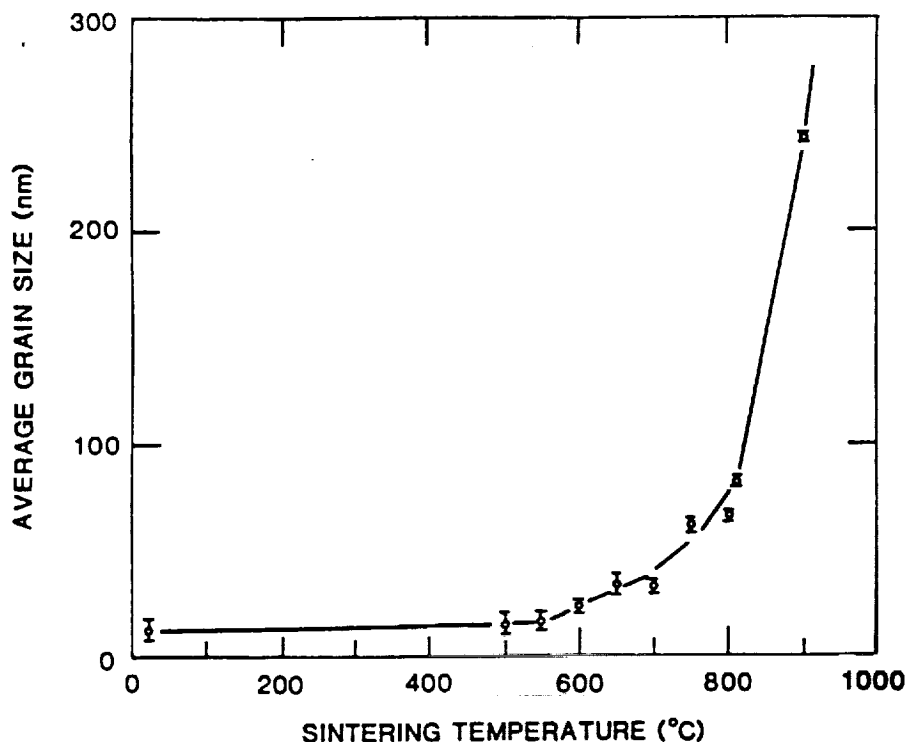


FIGURE 22 Average grain size (diameter) of nanophase  $\text{TiO}_2$  (rutile) determined by TEM as a function of sintering temperature. The sintering anneals were 0.5 hour in duration at each successive temperature (Siegel et al., 1988).

Some of the kinetic factors that determine the boundary mobility could also be affected for very small grain sizes. For example, if impurity segregation were to affect the grain boundary mobility, a large interface-to-volume ratio may lead to a decrease in the interfacial concentration of impurity, and hence to faster grain growth.

The decrease in the chemical potential resulting from the interfacial tension is also the driving force for coarsening of two-phase systems. This is well known from the study of eutectics. Figure 23 illustrates an important

mechanism identified in the coarsening of eutectic lamellae. The highest driving force is found at the tip of a receding fault line. Diffusion from this tip to the adjacent lamellae leads to thickening.

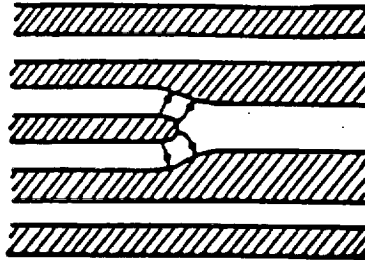


FIGURE 23 Schematic diagram of the coarsening mechanism in a lamellar structure (Spaepen, 1985).

In this mechanism, the coarsening rate,  $dr/dt$ , is independent of the scale,  $r$ , of the microstructure. A fine microstructure, however, is still relatively more affected by coarsening--for example, as measured by the time required to double  $r$ --than a coarse one. Since the coarsening rate is also proportional to the density of fault lines, the stability of artificial multilayers is greatly enhanced by the greater perfection of the individual layers. A coarsening mechanism for perfect layers, illustrated in Figure 23, is much less efficient than that of Figure 24.

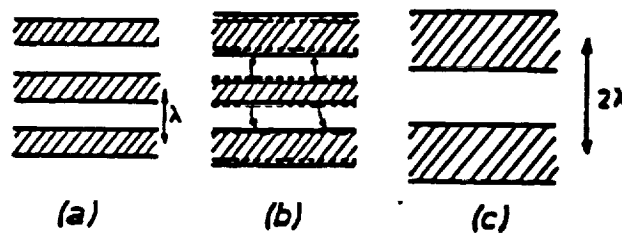


FIGURE 24 Schematic diagram of the coarsening of perfect layers by diffusion-induced doubling (Spaepen, 1985).

The thermodynamics and stability of systems that are inhomogeneous, either in density or composition, on a very fine scale was first fully formulated by Cahn and Hilliard (1958). They pointed out that the free



energy,  $F$ , of such a system must include terms due to the gradients in concentration or density:

$$F = \int [f(c) + k(\nabla c)^2] dV$$

In this expression,  $c$  is the composition (or density),  $f(c)$  is the free energy per unit volume of a homogeneous system of composition (density)  $c$ , and  $k$  is the gradient energy coefficient. This results in a modified interdiffusivity,

$$D_\lambda = D(1 + 2k\beta^2/f'')$$

where  $\lambda = 2\pi/\beta$  is the wavelength of one Fourier component of the concentration profile.

To predict the evolution of a very-fine-scale compositional inhomogeneity, it is therefore necessary to know both the bulk thermodynamics ( $f''$ ) and the gradient energy coefficient of the system. Figure 25 illustrates some of the possibilities for a continuum approximation.

The amplitude of the fine-scale composition modulation either vanishes by homogenization ( $D_\lambda > 0$ ) or grows to its two-phase equilibrium value ( $D_\lambda < 0$ ), after which coarsening sets in.

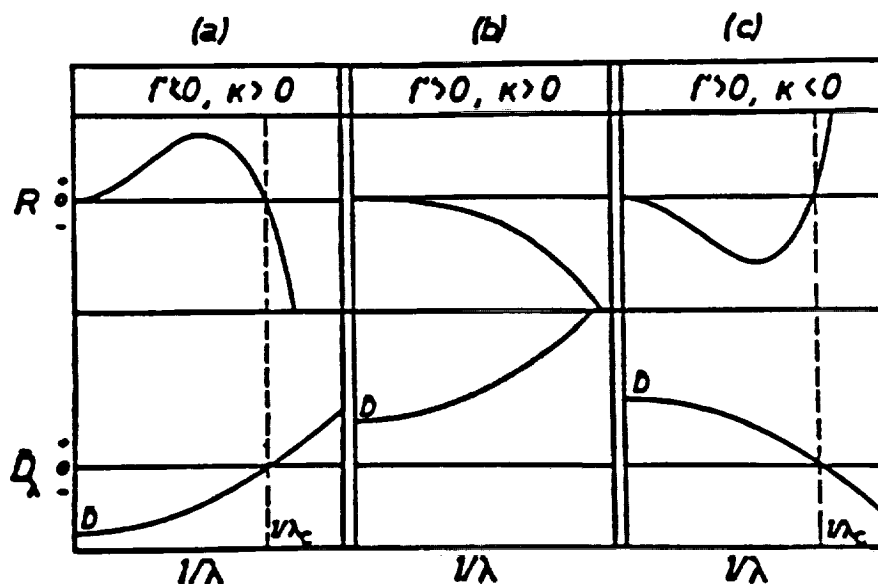


FIGURE 25 Dependence of the interdiffusivity and amplification factor  $R = D\beta^2$  on the wavelength of a composition modulation: (a) phase separating system inside the spinodal; (b) phase separating system outside the spinodal; (c) ordering system (Spaepen, 1985).

The stability of composition modulations has been very thoroughly studied. Greer and Spaepen (1985) describe the first direct determination of the gradient energy coefficients. Artificial multilayers remain unique tools for studying interdiffusion under unusual conditions (low temperature, steep gradients, unstable materials such as amorphous metals or semiconductors). The early work also demonstrated that significant effects of the gradient energy begin to occur at length scales of 10 nm or less. The thermodynamics of inhomogeneous systems should therefore be kept very much in mind in the study of the finest nanostructure.

#### REFERENCES

- Atzmon, M., K. M. Unruh, and W. L. Johnson. 1985. J. Appl. Phys. 58:3865.
- Beebe, P., and J. T. Yates, Jr. 1986. Surface Sci. Letters 173:L606.
- Belton, D. N., Y. M. Sun, and J. M. White. 1984. J. Phys. Chem. 88:5172.
- Bevk, J. 1983. Ann. Rev. Mat. Sci. 13:319.
- Birringer, R., H. Hahn, H. Höfler, J. Karch, and H. Gleiter. 1988. Defect and Diffusion Forum 59:17.
- Birringer, R., U. Herr, and H. Gleiter. 1986. Suppl. Trans. Jpn. Inst. Met. 27:43.
- Bond, G. C. 1985. Surface Sci. 156:966.
- Burch, R., and L. C. Garla. 1982. J. Catal. 73:20.
- Cahn, J. W., and J. E. Hilliard. 1958. J. Chem. Phys. 28:258.
- Cowen, J. A., B. Stolzman, R. S. Averback, and H. Hahn. 1987. J. Appl. Phys. 61:3317.
- Greer, A. L., and F. Spaepen. 1985. P. 419 in Synthetic Modulated Structure Materials, L. L. Chang and B. C. Giessen, eds. New York: Academic Press.
- Helmersson, U., et al. 1987. J. Appl. Phys. 62:481.
- Hicks, R. F., and A. T. Bell. 1984. J. Catal. 90:205.
- Hort, E. 1986. Diplom Thesis. Universität des Saarlandes, Saarbrücken.
- Horváth, J., R. Birringer, and H. Gleiter. 1987. Sol. State Commun. 62:319.

- Inoue, Y., J. M. Herrmann, H. Schmidt, R. L. Burwell, Jr., J. B. Butt, and J. B. Cohen. 1978. *J. Catal.* 53:401.
- Klimisch, R. L., and K. C. Taylor. 1973. *Environ. Sci. Technol.* 7:127.
- Lee, C., L. Schmidt, J. F. Moulder, and T. W. Rusch. 1986. *J. Catal.* 99:472.
- Lee, C., and L. Schmidt. 1986. *J. Catal.* 101:123.
- Li, Z., S. Ramasamy, H. Hahn, and R. W. Siegel. 1988. *Mater. Letters* 6:195.
- Masel, R. I. 1986. *Catal. Rev.-Sci. Eng.* 28:335.
- McDonald, M. A., D. A. Storm, and M. Boudart. 1986. *J. Catal.* 102:386.
- Oh, S. H., and J. E. Carpenter. 1986. *J. Catal.* 98:178.
- Oh, S. H., G. B. Fisher, J. E. Carpenter, and D. W. Goodman. 1986. *J. Catal.* 100:360.
- Otero-Schipper, P. H., W. A. Wachter, J. B. Butt, R. L. Burwell, Jr., and J. B. Cohen. 1978. *J. Catal.* 53:414.
- Paal, Z., and P. G. Menon. 1983. *Catal. Rev.-Sci. Eng.* 25:229.
- Palazov, A., G. Kadinov, C. Bonev, and D. Shopov. 1982. Infrared spectroscopic study of the interaction between carbon-monoxide and hydrogen on supported palladium. *Bulgarian Acad. Sci. Inst. Organ. Chem/Bü-1113, Sofia*; *J. Catal.* 74(NI):44-54.
- Pitchai, R., S. S. Wong, N. Takahashi, J. B. Butt, R. L. Burwell, Jr., and J. B. Cohen. 1985. *J. Catal.* 94:478.
- Siegel, R. W., S. Ramasamy, H. Hahn, Z. Li, T. Lu, and R. Gronsky. 1988. Synthesis characteristics and properties of nanophase  $\text{TiO}_2$ . *J. Mater. Res.* 3:1267.
- Siegel, R. W., and J. A. Eastman. 1989. *Mater. Res. Soc. Symp. Proc.* 132:3.
- Siegel, R. W., and H. Hahn. 1987. P. 403 in *Current Trends in the Physics of Materials*, M. Yssouff, ed. Singapore: World Scientific Publ.
- Spaepen, F. 1985. *Mater. Res. Soc. Symp. Proc.* 37:295.
- Tauster, S. J., S. C. Fung, and R. C. Garten. 1978. *J. Am. Chem. Soc.* 100:170.

Taylor, K. C., R. M. Sinkevitch, and R. L. Klimisch. 1974. J. Catal. 35:34.

Wong, S. S., P. H. Otero-Schipper, W. A. Wachter, Y. Inoue, M. Kobayashi,  
M. Butt, J. B. Burwell, Jr., and J. B. Cohen. 1980. J. Catal. 64:84.

## 6

### SELECTED APPLICATION AREAS

#### ELECTROCERAMICS

In considering the properties of electroceramic composites, relevant areas of interest are phase morphology, symmetry, and microstructural scale. Some of the morphological aspects have been discussed and need no further elaboration. Symmetry considerations have been extensively discussed in papers by Newnham and coworkers (1978). In what follows, the influence of scale and periodicity are examined, with emphasis on the need to develop appropriate nanoscale composite structures.

A good deal has been written about the importance of scale in magnetic, optical, and semiconductor materials. Many of the same effects occur in ferroelectrics (critical domain sizes, resonance phenomena, electron tunneling, and nonlinear effects). In ferromagnetic materials, there are three kinds of magnetic structures for small particles. Multidomain structures are common for particles larger than a critical size; magnetization in large particles takes place through domain wall motion. Below this critical size, single domain particles are observed, and switching takes place by rotation rather than wall movement, thereby raising the coercive field. Very small particles exhibit a supermagnetic effect in which the spins rotate in unison under thermal excitation. Only modest magnetic fields are required to align the spins of adjacent particles. Analogous behavior in ferroelectric particles has yet to be fully established, but a variety of interesting experimental results are accumulating. In  $\text{BaTiO}_3$  ceramics, single domain behavior is observed in grains less than approximately  $1\text{ }\mu\text{m}$ , while dielectric phenomena resembling those found in superparamagnetism are found in relaxor ferroelectrics. The fluctuating microdomains in this superparaelectric state are about 20 nm across. Composite materials made up of single domain and superparaelectric particles have yet to be investigated in a systematic way with proper control of the connectivity and surrounding environment. The

controlled synthesis of submicrometer ferroelectric grains will do much to stimulate research in this area.

Surface treatment of the ferroelectric phase allows control of the mechanical boundary conditions. Titanlyl coupling agents are effective in bonding PZT to epoxy. Mechanical pull tests have been used to demonstrate the strength of the ceramic-polymer bond. Improved stress transfer and large piezoelectric coefficients in piezoelectric composites are obtained as a result of better bonding. Polymers are about a hundred times more compliant than ceramics. If a ceramic grain is surrounded by polymer, the mechanical constraints are relatively small. This means that more complete poling is possible, as demonstrated in ferroelectric composites. Electrical boundary conditions can also be controlled by adjusting the dielectric constant and conductivity of the surrounding phase.

Periodicity and scale are important factors when composites are to be used at high frequencies where resonance and interference effects occur. When the wavelengths are on the same scale as the component dimensions, the composite no longer behaves like a uniform solid. An interesting example of unusual wave behavior occurs in composite transducers made from poled ferroelectric fibers embedded in an epoxy matrix. When driven in thickness resonance, the regularly spaced fibers excite resonance modes in the polymer matrix, causing the matrix to vibrate with much larger amplitude than the piezoelectric fibers. The difference in compliance coefficients causes the nonpiezoelectric phase to respond far more than the stiff ceramic piezoelectric. Composite materials are therefore capable of mechanical amplification from prepoled PZT fibers mounted in a polymer matrix. Domain-divided transducers operate on a similar principle. Multidomain crystals and ceramics have been used as acoustic phase plates and high-frequency transducers.

The extension of this thinking to phenomena associated with optical excitations automatically focuses attention on equivalent nanoscale structures. Specifically for wavelengths of 400 to 800 nm (optical spectra), to avoid serious scattering the internal structures must be below the 10- to 20-nm scale. In ferroelectrics, the superparaelectric internal polar structures of the relaxor materials offer the possibility of tailoring optically isotropic or anisotropic behavior under external electric field control. The recent demonstrations of ferroelectricity in some species down to 20 nm indicate that these anisotropies can be exploited in suitable assembled nanostructures.

A wide range of potential property modifications, including shape-induced optical birefringence, shape-controlled optical nonlinearity, and potential modes for inducing optical bistability, remain to be explored. It is clear that there will be corresponding magnetic nanocomposites and that for these materials additional versatility can be expected because of the nanoscale interaction with the transport phenomena and the associated optical

absorption. Highly transparent ferromagnets, new types of indirectly coupled magnetoelectrics, and piezomagnets of enhanced properties are to be expected.

At these very fine nanoscales, new work to explore the possibility of super paraelasticity could give rise to families of highly nonlinear elastic materials with potential for tailoring the nonlinearity.

Clearly on all other electro-, magneto-, and elasto-optical systems, regular periodicities in the nanoscale internal structures will give rise to interesting new pass or stop bands in their interaction with electromagnetic or acoustic waves, analogous to the Brillouin zone structures in crystalline systems. Again, much work remains to be done to develop the technologies necessary to assemble composites on the regular scaling necessary for these realizations.

### ULTRASTRUCTURED CERAMICS

In conventional ceramic processing the powders employed are often characterized by uncontrolled geometry and chemistry. This results in microstructures (irregularly shaped particles or spheres) and ultrastructures (interphases, secondary phases, and pores between spheres) that produce levels of performance far below the theoretical limit (Figure 26).

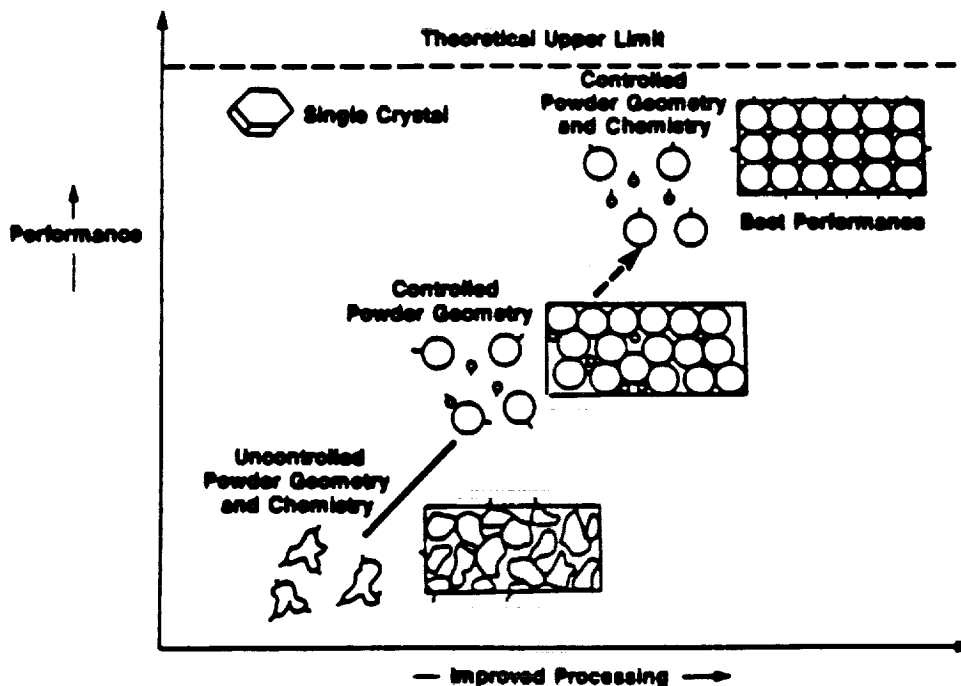


FIGURE 26 The impact of ultrastructure processing on ceramic performance.

The attainment of properties that approach theoretical values in high-temperature structural ceramics by the ultrastructure processing approach is schematically shown in Figure 27. The complete control of raw materials includes the design of molecules and chemistry for powders that, upon densification, provide the compositional stoichiometry necessary for glass-free grain boundaries. The viability of the ultrastructure concept in the chemical processing of mullite ( $3\text{Al}_2\text{O}_3 \cdot 2\text{SiO}_2$ ) has been demonstrated.

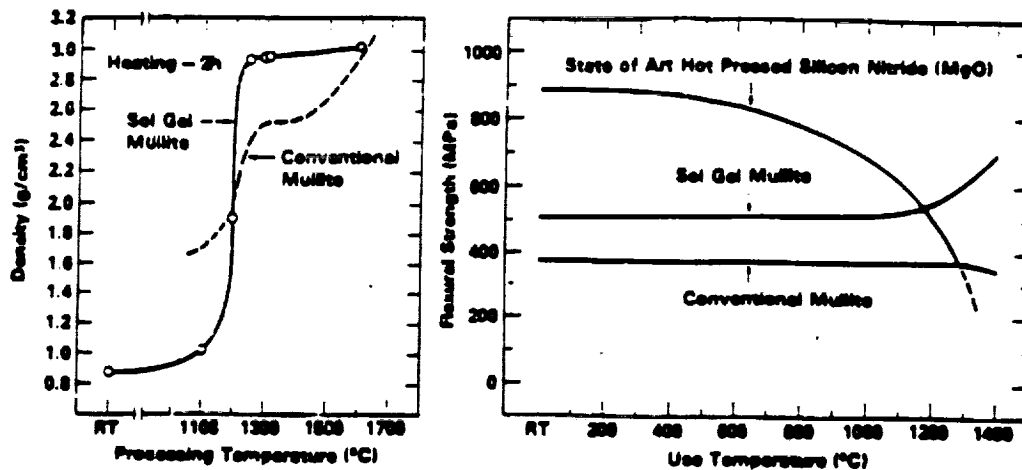


FIGURE 27 Comparison of conventional and sol-gel mullite.

In comparison to other high-performance materials such as silicon nitride,  $\text{Si}_3\text{N}_4$ , mullite is not considered to be a useful high-strength material at low temperatures. Its potential becomes apparent only at elevated temperatures, where  $\text{Si}_3\text{N}_4$  matrix ceramics start losing their strength (Figure 27).

Mullite-forming gels were made from colloidal boehmite ( $\text{AlOOH}$ , aluminum monohydroxide) and tetraethoxy-silane (TEOS). Upon sintering at  $1200^\circ\text{C}$ , these gels form dense (greater than 99 percent of theoretical density) and translucent mullite. Conventional mullite prepared from mixed powders requires  $1600^\circ\text{C}$ . This ability to sinter mullite at temperatures significantly lower than the usual  $1600^\circ\text{C}$  sintering temperature represents a very important processing accomplishment. Sintering of the same sol-gel-derived mullite at  $1250^\circ\text{C}$  results in infrared-transparent mullite, forming the basis for sol-gel passive infrared optics for the 3 to 5 micron region (Figure 28).



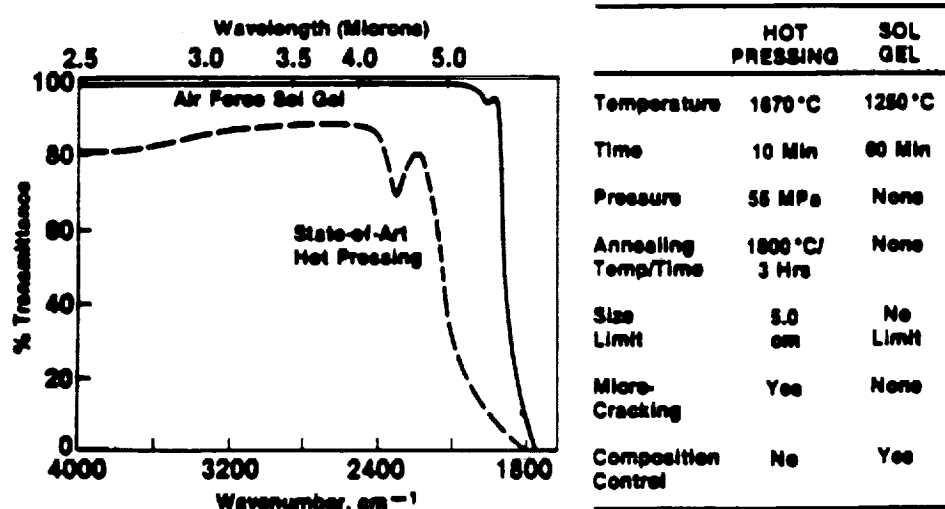


FIGURE 28 Infrared-transparent mullite from sol-gel.

## PERMANENT MAGNETS

Rapid solidification (i.e., melt spinning) of  $\text{Re}_2\text{Fe}_{14}\text{B}$ -type materials has permitted the development of permanent magnets whose performance depends in a very important way on submicron-scale microstructures. Two different types of microstructures have been identified in these materials, which lead to significantly different permanent magnet behavior. The mean grain size of the two microstructures is submicron and very similar, approximately 20 nm to 30 nm. However, another submicron structural feature controls the magnetic performance differences. It is a 1-nm to 2-nm-thick uniform intergranular phase. The presence of the submicron intergranular phase shuts off the short-range intergrain ferromagnetic exchange interactions by effectively isolating the grains from magnetic interactions with each other. When the intergranular phase is absent, ferromagnetic exchange couples the magnetizations of the two grains at their surfaces, leading to significant enhancement of the remanent magnetization of all the grains. Thus the submicron microstructure acts as a switch for enhancement of the magnetic properties in these materials.

Specifically, it was shown by Croat et al. (1984a,b) that material with compositions in the vicinity of  $\text{Re}_2\text{Fe}_{14}\text{B}$  stoichiometry could be melt-spun at specific quench rates (i.e., specific wheel speeds) producing material with coercivities in excess of 10 kOe and energy products up to 14 MGOe. [Similar performances were produced by Koon (1980) with heat treatment of amorphous melt spun material of similar composition.] The values by Croat et al. were in good agreement with the predictions for remanence and energy product of

crystallographically isotropic permanent magnets predicted by Stoner and Wohlfarth (1948), wherein the limits to the magnitude of the remanent magnetization ( $4\pi M_r$ ) are less than one-half the saturation magnetization ( $4\pi M_s$ ), and the energy product is less than  $(4\pi M_r/M_s)^2$ . Bright- and dark-field transmission electron micrographs of optimum as-quenched material (Croat et al., 1984a,b) are shown in Figure 29. It is clear that the sample consists of a two-phase microstructure with small (approximately 30-nm diameter) grains of the principal phase,  $\text{Re}_2\text{Fe}_{14}\text{B}$  (Herbst et al., 1984) surrounded by a very thin film of an amorphous phase some 1 to 2 nm in thickness. In permanent magnets with this type of microstructure, it is believed that magnetic domain walls are pinned in the amorphous grain boundary regions, thus generating coercivity.

The submicron microstructure shown in Figure 29 has no amorphous intergranular phase. The mean grain size for this type of material has been determined to be between 14 and 23 nm (Keem et al., 1988). In contrast to the

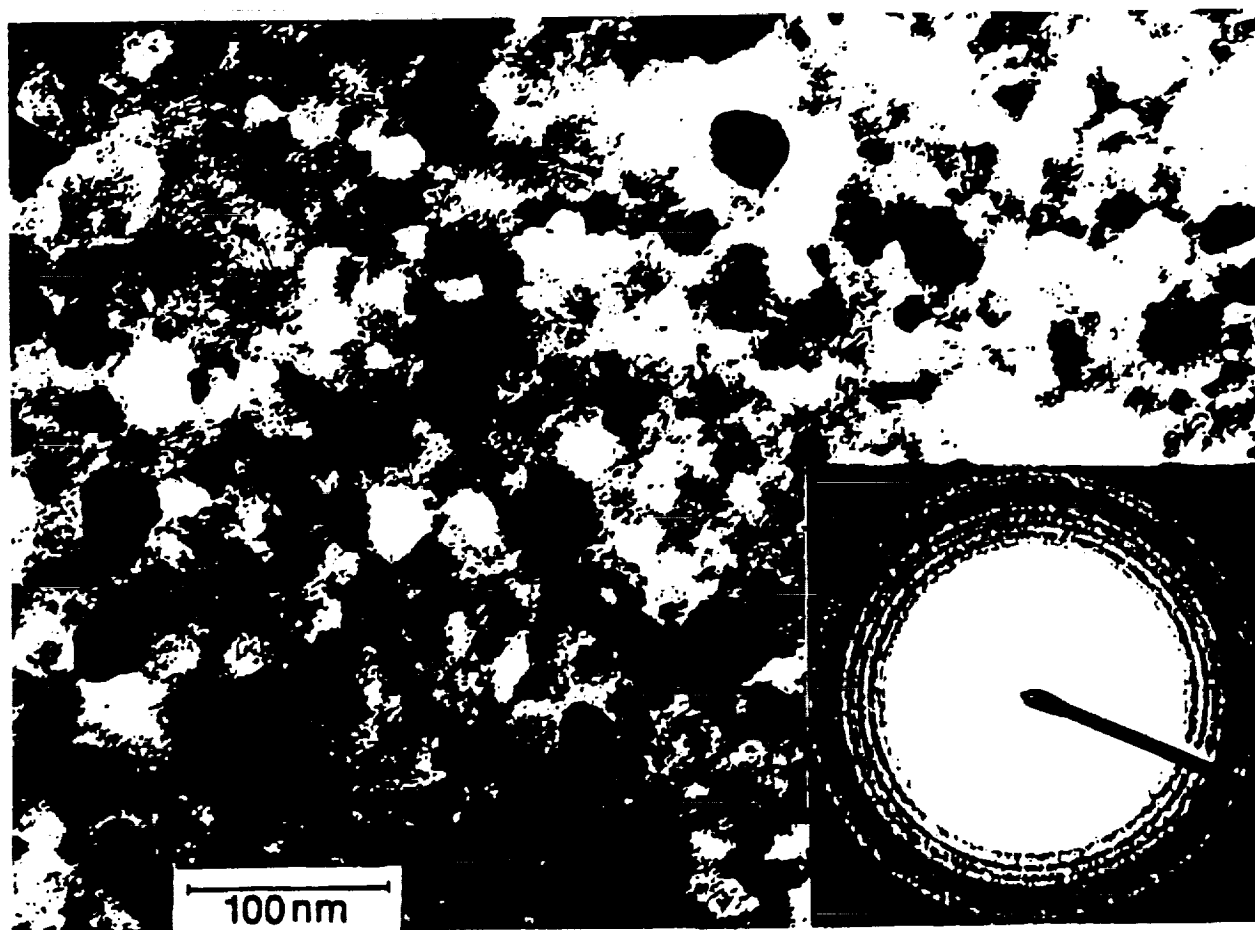


FIGURE 29 Bright-field image and selected area diffraction of enhanced remanence material. No evidence of intergranular phases is found in either the image or the selected areas diffraction patterns (Keem et al., 1988).

material with the intergranular phase,  $\text{Re}_2\text{Fe}_{14}\text{B}$  material with a slightly smaller grain size and no intergranular phase has magnetic performance that significantly exceeds the Stoner-Wolfarth limits, with remanences up to 10 kG and energy products in excess of 19 MGOe. The enhancement behavior has been attributed to the intergrain ferromagnetic exchange interaction (Keem et al., 1988). Remanence enhancement is limited to less than full polarization of the adjacent grains because of an accommodation between the intergrain exchange and intergrain anisotropy of the single-domain grains. It has been shown (Keem et al., 1988) that the presence of any intergranular phase damps this intergrain interaction and essentially eliminates the remanence enhancement.

#### POLYMER-SILICA MICROCOMPOSITES

Liquid crystalline solutions of rigid-rod macromolecules such as poly-p-phenylenebenzobisthiazole (PBZT) can be solution-processed into high-performance fibers and films. After coagulation into water, the microstructure consists of a highly oriented three-dimensional interconnected network of 20-nm-diameter microfibrils (Cohen and Thomas, 1988) (Figure 30).

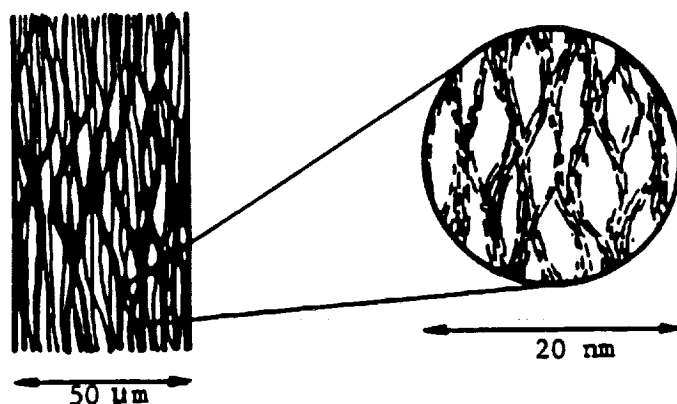


FIGURE 30 PBZT-sol-gel glass interpenetrating networks (Cohen and Thomas, 1988).

This high-strength and high-stiffness polymer framework has recently been exploited for novel polymer-glass composites. The process involves exchange of the water phase in the wet coagulated PBZT film for an alkoxide solution, which is then hydrolyzed to form a PBZT-sol-gel composite that can then be further densified to yield a PBZT-silica composite in which both phases are continuous. The liquid-crystal solution can be processed to yield a spectrum of variously oriented PBZT networks that can then be infiltrated with a variety of materials for specific applications. A particular target is the improvement of compressive strength of neat PBZT fibers. The low overall

material density and near-zero coefficient of thermal expansion plus the ability to form laminates by interdiffusion of the glass phase provides strong motivation for employment of PBZT-silica microcomposites for aerospace structural applications.

## CATALYSTS

The application of new catalysts that replace current catalysts will be based primarily on performance criteria. Preparation techniques might be transferred from model catalyst systems, if favorable properties are identified and the preparation can be scaled up conveniently. New applications will be based on the potential for new product schemes and the economics for the entire process, of which the catalyst is just one part. The cost of the catalyst can be a factor if the preparation scheme is particularly complex, the raw materials are expensive, and the catalyst is used in very high volume, as for exhaust emission control catalysts.

Broad classes of catalytic reactions that make use of submicron-sized catalytic particles include emission control catalysis, catalytic reforming, synthesis gas catalysis, Ziegler process for polyethylene, and oxidation catalysis. Other processes that similarly incorporate a catalytic component are photocatalysis and oxygen sensors. Possible future catalytic processes include catalytic activation of fuel for energy conversion.

The performance of a catalyst is determined by measuring product yield. Catalysts are evaluated by monitoring their activity, selectivity, and durability under realistic conditions. Testing the activity of a catalyst for a particular reaction is the best way to choose a catalyst. Moreover, important discoveries are made in doing kinetic measurements, where serendipity can play a role. Catalyst characterization that is not related to performance is ancillary if the concern is economics.

## CERMETS

Metal-ceramic (cermet) composites are routinely produced by conventional powder-metallurgy methods. A limitation to the approach has been the inability to obtain a microstructure in which the hard ceramic phase is less than 1 to 5 mm in cross section. Both the chemical-synthetic approach and the gas-condensation method provide the means for generating novel cermet materials with submicron-scale structures. Such ultrafine structures present the opportunity to synthesize a new class of cutting-tool materials, which will have the ability to form and maintain a very fine cutting edge that is resistant to chipping. For this reason, it is believed that nanophase composite cermets, such as Co-WC, will find great utility for such high-value-added applications as microtome blades and surgeon's scalpels. A number of

the other synthesis methods also discussed in Chapters 2 and 3 have the potential for generating similar ultrafine composite structures.

## MULTILAYER COATINGS

An important structural application of multilayer thin films is as protective coatings for Co-WC cutting tools. A typical composite film comprises three vapor-deposited layers of TiC, TiN, and  $\text{Al}_2\text{O}_3$ , each of which performs a specific function that contributes to the overall performance and durability of the cutting tool. The first example of an application of a nanophase-composite coating has inspired much recent activity in the coatings industry to devise and exploit multilayer films for a variety of applications, including protective coatings for mirrors, wear-resistant surfaces on polymers, and low-friction bearings. In this context, particularly intriguing is the low-temperature synthesis of superhard materials such as diamond and cubic BN. An interesting feature of such materials is the inherently nanoscale structure of the deposited films, which themselves are an integral part of a nanoscale architecture.

For certain multilayered systems with compatible structures, the possibility exists of generating a strained-layer superlattice that exhibits the supermodulus effect. Exceptionally stiff coatings on stiff substrates have been made for experimental purposes. Potential applications are being considered for producing superstiff coated filaments for reinforcement purposes in composite structures.

## REFERENCES

- Cohen, Y., and E. L. Thomas. 1988. Microfibrillator network of a rigid rod polymer: I--Visualization by electron microscopy. *Macromolecules* 21:433.
- Croat, J. J., J. F. Herbst, R. W. Lee, and F. E. Pinkerton. 1984a. High-energy product Nd-Fe-B permanent magnets. *Appl. Phys. Lett.* 44(1):148-149.
- Croat, J. J., J. F. Herbst, R. W. Lee, and F. E. Pinkerton. 1984b. Pr-Fe and Nd-Fe-based materials: A new class of high-performance permanent magnets. *J. Appl. Phys.* 55:2078.
- Herbst, J. F., J. J. Croat, F. E. Pinkerton, and W. B. Yelon. 1984. *Phys. Rev. B.* 29:4176.
- Keem, J. E., G. B. Clements, A. M. Kadin, and R. W. McCallum. 1988. P. 27 in *Hard and Soft Magnetic Materials With Applications. Proceedings of a Conference Held in ASM's Materials Week 1987. Metals Park, Ohio: ASM International.*

Koon, N. C., C. M. Williams, and B. N. Das. 1980. 26th Annual Conference on Magnetism and Magnetic Materials, Dallas, Texas, November 11-14.

Newnham, R. E., D. P. Skinner, and L. E. Cross. 1978. Mat. Res. Bull. 13:525.

Stoner, E. C., and E. P. Wohlfarth. 1948. Philos. Trans. R. Soc. Lond. Ser. A 240:599.

## SUMMARY AND RECOMMENDATIONS

Although the study of nanophase materials is still in its infancy, it is already quite clear that an exciting new area of research has opened up and that new materials with novel and useful properties will emerge. Just which avenues of endeavor will be most profitable are not clear at this writing. However, the demonstrated success in synthesizing nanophase metals, single-phase and multiphase alloys, and ceramics with different and sometimes improved properties over those previously available indicates that these avenues will be widespread. Furthermore, the possibilities for synthesizing nanophase composites appear highly encouraging.

The report reflects the many different avenues of arriving at nanophase structures. Since the field is new the committee is recommending a broad approach to the making of such structures without waiting to prioritize the research. Priorities will vary depending on specific materials and applications.

Much work needs to be done to realize the full potential of nanophase materials. Some examples are these:

- Macromolecular synthesis of polymers continues to be one of the most exciting and innovative areas of materials research. Recent advances include group transfer polymerization, aluminum catalyzed ring-opening polymerization, and cationic polymerization of vinyl ethers. These techniques provide efficient routes to a rich variety of molecular architectures, exhibiting a wide range of self-assembled structures and interesting properties. Further research in these and related areas will almost certainly yield additional payoffs, but this pales in comparison to what could be achieved by a concerted effort to replicate what is routinely accomplished in nature (i.e., through biotechnological approaches).

- Reductive pyrolysis is a promising new initiative for the synthesis of nanophase cermets. It represents a radical departure from traditional powder metallurgy methods of making such materials and offers the potential for obtaining improved properties at lower manufacturing cost. Scale-up of the process needs to be addressed, along with its applicability to other cermet systems.
- Gel synthesis methods present opportunities for fabricating novel bicontinuous composites. Although sol-gel methods have been devised for making porous ceramic preforms with controlled interconnected porosity and pore size, scant attention has been given to the difficult problem of infiltrating the very fine pores with matrix materials. The properties of such bicontinuous nanophase composites also need to be investigated.
- The versatility of the laser pyrolysis, colloidal synthesis, and cryochemical synthesis methods for producing nanophase materials has been demonstrated. It remains to address the challenge of scale-up of these processes and to demonstrate that lowered sintering temperatures offer some real payoffs in terms of cost and performance.
- The new technique of cryomilling is a significant advance on the state of the art for producing dispersion strengthened materials. A new generation of oxide-dispersion strengthened (ODS) alloys can be expected from this process, which will have a major impact on advanced aerospace systems. Techniques have already been worked out for making bulk parts with improved high-temperature properties in aluminum- and iron-based alloys. It remains now to extend the technology to the new generation of intermetallic matrix materials, particularly the nickel and titanium aluminides.
- Surface modification by ion implantation is a proven technology that has gained much prominence in the thin-film-device industry. It remains now to exploit this technology for structural applications (e.g., to enhance wear and corrosion resistance).
- The gas-condensation method will require a number of modifications to make it suitable for the production of nanophase materials of practical sizes and dimensions. An important innovation would be to develop the capability for synthesizing and consolidating powders on a large scale in an ultrahigh-vacuum system, to avoid contaminating the final product. It appears that there are no impediments, at least in principle, to achieving this goal. Particle sizes and resulting nanophase grain sizes (less than 5 nm in scale) also need to be investigated for their effects on materials properties.
- Nanophase materials have been produced by novel rapid solidification methods, such as electrohydrodynamic atomization. Further work along these lines is needed, as well as the synthesis of powders and thin films by laser ablation methods.



- Much progress has been made in the synthesis of ultrafine carbon and SiC filaments by catalytic methods. It remains now to fabricate filamentary reinforced composites from these high-specific-strength filaments, making use of polymeric, ceramic, or metallic-matrix materials. Another opportunity area is to devise new methods for the catalytic growth of other useful filamentary materials (e.g., TiC and AlN).

- Multilayer structures produced by MBE, electrodeposition, and cluster beam deposition are becoming important in structural materials. Opportunities exist to exploit these technologies to fabricate thin-film coatings that exhibit the supermodulus effect. Applications of such coatings to tool bits and high-performance fibers are potential payoff areas.

- Many different dispersed phase composites have been synthesized by CVD methods. Useful applications have been found for pyrolytic carbon that is reinforced with submicrometer-sized SiC particles. Promising new ceramic systems for high-temperature structural applications have been identified. Further research is needed to optimize their mechanical and physical properties.

- Although major advances have been made in the synthesis of polymer blends, self-reinforcing polymers, and block copolymers, further work is needed to optimize their materials properties. Efforts should also be made to capitalize on the recent breakthrough in understanding of the three-dimensional morphologies of bicontinuous block copolymers.

- Many different methods have been devised for making high-surface-area catalysts, including impregnation, ion exchange, thermal decomposition, vapor deposition, and intercalation methods. Further research is needed to enhance catalytic activity and selectivity for specific chemical processes. Complex multicomponent, multiphase ceramic materials offer the potential for multifunctional capabilities.

- Membrane research continues to be driven by diverse industrial needs (e.g., desalinization, pollutant removal, and chemical separations). Important areas of research include sintered particle membranes, solution-cast polymer filters, and molecular sieves. Microphase separation of block copolymers appears to be a particularly promising area of current research, with potential for control of pore size, morphology, and interconnectivity down to nanoscale dimensions.

- Traditional tools, such as transmission electron microscopy and x-ray and neutron scattering have been used successfully to characterize nanoscale materials. However, little work has been done on chemical mapping at the requisite fine scale. There is an urgent need to perform such studies, utilizing FIM atom-probe and scanning tunneling microscopy techniques. Analytical electron spectroscopy methods utilizing finer electron probe sizes should also be investigated. Other useful techniques include RBS, EXAFS, XPS,

NMR, Raman, infrared, Mössbauer, and positron annihilation spectroscopies, calorimetry, and chemisorption.

- The properties of nanophase materials are significantly different from those found in their conventional polycrystalline counterparts. Major changes are observed in sinterability, saturation magnetization, magnetic susceptibility, yield strength, fracture strength, density, thermal expansion, hardness, elastic modulus, and diffusivity. So far all measurements have been performed on relatively small quantities of material. There is a need to demonstrate that such remarkable property changes can be realized in bulk materials produced by scaled-up commercially viable processes.

The enhanced elastic and plastic properties of nanophase materials are particularly intriguing. The supermodulus effect in particular is already beginning to find useful application in hard coatings. Again, making brittle ceramics ductile by exploiting enhanced diffusional creep at low temperatures in nanophase materials is clearly of crucial importance to the structural ceramics field and should be given high priority for future research.

- Nano-dispersed phases have been exploited in catalysis for decades. In fact, it is in this area that the nanostructure field has reached its highest level of maturity, both from the scientific and technological perspectives. Nevertheless, much work remains to be done to optimize catalyst systems to achieve the desired conversion efficiency, activity, and selectivity. In addition to addressing problems associated with control of particle size, stability, morphology, interactions, and pretreatments, there is a need to develop bifunctional and multifunctional catalyst systems for advanced processes.

- Ceramics frequently contain voids and inhomogeneities. While grain growth would likely result from consolidation of nanoscale ceramics, the probable benefits of relatively fine grain and uniform composition resulting from nanoscale starting material should be explored.

- Many applications for nanophase materials have been identified, but progress has been hampered by lack of sufficient quantities of material for performance evaluation studies and field testing. Thus, in addition to significantly augmenting the current level of support for basic research in the field, there is also a critical need to support work dedicated to the scale-up and manufacture of nanophase materials.

The processing of catalytic materials on a very large scale is routine industrial practice. Rapid progress is also being made in the commercialization of Fe-Nd-B alloys by rapid solidification technology. These successes leave one optimistic that ways will be found to scale up many of the synthesis and processing methods described in this report, which today are only laboratory-scale techniques. A case in point is the synthesis of Co/WC by reductive pyrolysis. A potential solution to this problem is to conduct

the whole operation in a fluid-bed reactor, where the reactive gas species are added to the fluidizing medium. Another example is the gas-condensation method, where scalability seems possible by utilizing high-vacuum electron-beam technology to produce the powders. The continuous collection of these powders for in situ consolidation and subsequent processing by means of gas-flow techniques can replace the static collection methods currently used in the laboratory.



## BIBLIOGRAPHY

- Andres, R. P., R. S. Averback, W. L. Brown, L. E. Brus, W. A. Goodard III, A. Kaldor, S. G. Louie, M. Moskovits, P. S. Peercy, S. J. Riley, R. W. Siegel, F. Spaepen, and Y. Wang. 1989. Research opportunities on clusters and cluster-assembled materials: A Department of Energy-Council on Materials Science panel report. *J. Mater. Res.* 4:704.
- Baker, R. T. K., and P. S. Harris. 1978. The formation of filamentous carbon. *Chem. and Phys. of Carbon* 14:83-165.
- Bowen, H. K. 1986. Advanced ceramics. *Scientific American* 255(4):169-176.
- Donovan, T. M., J. O. Porteus, S. C. Seitel, and P. Kratz. 1981. Multithreshold HF/DF pulsed laser damage measurements on evaporated and sputtered silicon films. Pp. 305-312 in *Laser-Induced Damage in Optical Materials: 1980*, H. E. Bennett, A. J. Glass, A. H. Guenther, and B. E. Newnam eds. National Bureau of Standards Special Publication 620.
- Johnson, D. W. 1985. Sol-gel processing of ceramics and glass. *Am. Cer. Soc. Bull.* 64:1597-1602.
- Kimoto, K., Y. Kamiya, M. Nonoyama, and R. Uyeda. 1963. An electron microscope study on fine metal particles prepared by evaporation in argon gas at low pressure. *Jpn. J. Appl. Phys.* 2:702.
- Klein, L. C., and G. J. Garvey. 1984. Drying and firing monolithic silica shapes from sol-gel. Pp. 88-99 in *Ultrastructure Processing of Ceramics, Glasses, and Composites*, L. L. Hench and D. R. Ulrich, eds. New York: Wiley-Interscience.
- Klein, L. C. 1985. Sol-gel processing of silicates. *Annual Rev. Mater. Sci.* 15:227-248.

- Martin, P. M., and W. T. Pawlewicz. 1981. Influence of sputtering conditions on H content and Si-H bonding in a-Si:H alloys. *J. Noncrystall. Solids* 45(1):15-27.
- McCandlish, L. E., D. E. Polk, R. W. Siegel, and B. H. Kear, eds. 1989. Multicomponent Ultrafine Microstructures. *Mater. Res. Soc. Symp. Proc.* 132:1-243.
- Pawlewicz, W. T., D. D. Hays, and P. M. Martin. 1980. High-band gap oxide optical coatings for 0.25 and 1.06 mm fusion lasers. *Thin Solid Films* 73(1):169-175.
- Pawlewicz, W. T., I. B. Mann, W. H. Lowdermilk, and D. Milam. 1979. Laser damage resistant transparent conductive indium tin oxide coatings. *Appl. Phys. Lett.* 34:196.
- Pawlewicz, W. T., and P. M. Martin. 1981. Bonding and composition diagrams for sputter deposited a-Si:H. *Solid State Comm.* 39(2):337-339.
- Pawlewicz, W. T., R. Busch, D. D. Hays, P. M. Martin, and N. Laegreid. 1980. Reactively sputtered optical coatings for use at 1064 nm. Pp. 359-374 in *Laser-Induced Damage in Optical Materials: 1979*, H. E. Bennett, A. J. Glass, A. H. Guenther, and B. E. Newnam, eds. National Bureau of Standards Special Publication 508.
- Pawlewicz, W. T., and R. Busch. 1979. Reactively sputtered oxide optical coatings for inertial confinement fusion laser components. *Thin Solid Films* 63(2):251-256.
- Siegel, R. W., and H. Hahn. 1987. Nanophase materials. P. 403 in *Current Trends in the Physics of Materials*, M. Yussouff, ed. Singapore: World Scientific Publ.
- Smith, R. D., and H. R. Udseth. 1983. Mass spectrometry with direct supercritical fluid injections. *Anal. Chem.* 55(14):2266-2272.
- Thölén, A. R. 1979. On the formation and interaction of small metal particles. *Acta Metall.* 27:1765.
- Ulrich, D. R. 1985. Chemical science's impact on future glass research. *Am. Cer. Soc. Bull.* 64:1444-1448.
- Witzke, H., and B. H. Kear. 1986. Gas phase synthesis of filamentary structures. In *Homogeneous and Heterogeneous Nucleation From Fluid Media*, W. Bartok, G. D. Cody, and B. H. Kear, eds. Exxon Research and Engineering.

## Appendix A

### Definitions of Acronyms

ABPBI	Polybenzimidazole
AEM	Analytical electron microscopy
CBED	Convergent beam electron diffraction
CVD	Chemical vapor deposition
DCCA	Drying control chemical agents
DIGM	Diffusion-induced grain-boundary migration
EDS	Energy dispersive spectroscopy
EELS	Electron energy loss spectroscopy
EXAFS	Extended x-ray absorption fine structure
FIM	Field ion microscope
FTIR	Fourier transform infrared
HREM	High resolution electron microscopy
MBE	Molecular beam epitaxy
NLO	Nonlinear optical
NMR	Nuclear magnetic resonance
PAS	Positron annihilation spectroscopy
PBZT	Poly-p-phenylenebenzobisthiazole
PMMA	Poly(methyl methacrylate)
PPTA	Poly(p-phenylene terephthalamide)
RBS	Rutherford back-scattering spectroscopy
SANS	Small angle neutron scattering
SEM	Scanning electron microscopy
SMSI	Strong metal support interaction
STEM	Scanning transmission electron microscopy
STM	Scanning tunneling microscope
TEM	Transmission electron microscopy
UHV	Ultrahigh vacuum
XES	X-ray emission spectroscopy
XPS	X-ray photoelectron spectroscopy
XRD	X-ray diffraction





## Appendix B

### BIOGRAPHICAL SKETCHES OF COMMITTEE MEMBERS

BERNARD H. KEAR received his B.Sc., Ph.D., and D.Sc. degrees in materials science and engineering from the University of Birmingham, England. From 1958 to 1963 he was with the Franklin Institute in Philadelphia, where he researched the effects of long-range ordering on the plastic properties of crystals. From 1963 to 1981 he was with the Pratt & Whitney Division of United Technologies Corporation, where he investigated the interrelationships between structure, properties, and processing in superalloys, participated in the development of single-crystal turbine blade technology, and spearheaded the development of laser surface modification treatments. From 1981 to 1986 he was scientific advisor at Exxon's Corporate Research Center, where he conducted research in chemical vapor deposition and its applicability to large-scale in situ surface modification of reactor vessels and the upgrading of the surface properties of steel structures. In 1986 he assumed his present position as State of New Jersey Professor of Materials Science and Technology at Rutgers University. He is also Director of the Center for Materials Synthesis and chairman of the Department of Mechanics and Materials Science. His current research activities are focused on chemical vapor deposition and chemical synthesis of composite materials.

L. ERIC CROSS is the Director of the Materials Research Laboratory at Pennsylvania State University. He has also been Professor of Electrical Engineering since 1968 and was an Associate Professor of Physics before that. A native of Leeds, England, he received his degrees from the University of Leeds. He was employed by the British Admiralty, ICI, the British Electric Research Association, and the University of Leeds before coming to this country. His technical interests have varied widely, currently emphasizing sensors for control or for nondestructive testing.

JOHN E. KEEM received his education at Syracuse University (B.S.) and Purdue University (Ph.D. in physics, 1976). After a year as a fellow in the Physics Department at Purdue, he moved to the General Motors Research Laboratories. He is currently with the Ovonic Synthetic Materials Company. He has worked in conduction mechanisms in oxides and in magnetic and magnetoelastic phenomena.

RICHARD W. SIEGEL received an A.B. in physics from Williams College in 1958 and an M.S. in physics in 1960 and a Ph.D. in metallurgy in 1965 from the University of Illinois in Urbana. Following two years of postdoctoral research at Cornell University, he served on the faculty of the State University of New York at Stony Brook in the Department of Materials Science. From 1974 to the present, he has been a research scientist in the Materials Science Division at Argonne National Laboratory, serving for most of this time as group leader in the areas of metal physics and defects in metals. His research has concentrated most recently on the synthesis, characterization, and properties of ultrafine-grained nanophase materials, particularly ceramics.

FRANS SPAEPEN is Gordon McKay Professor of Applied Physics at Harvard University. He received his undergraduate degree in metallurgy from the University of Leuven in Belgium and his Ph.D. in applied physics from Harvard University in 1975. He has been a faculty member of the Division of Applied Sciences at Harvard since 1977. His research interests include phase transformations, atomic transport, and mechanical properties of amorphous metals and semiconductors; the production, diffraction, stability, and mechanical properties of artificial multilayers; the structure of amorphous-crystalline interfaces and grain boundaries; and the formation and transformations of quasiperiodic crystals.

KATHLEEN C. TAYLOR is head of the Physical Chemistry Department at General Motors Research Laboratories, where she oversees research activities in catalysis, surface chemistry, corrosion science, combustion, electrochemistry, batteries, electrodeposition, and chemical processes. She received her undergraduate education at Douglass College and her Ph.D. in physical chemistry from Northwestern University in 1968. She is a member of the American Chemical Society, the Materials Research Society (President in 1987), and the Society of Automotive Engineers. In 1986 Dr. Taylor was honored as the Francois Gault lecturer in catalysis in Europe and received the Garvan Medal from the American Chemical Society in 1989.

EDWIN L. THOMAS is Morris Cohen Professor of Materials Science and Engineering at Massachusetts Institute of Technology. He received his undergraduate degree in mechanical engineering at the University of Massachusetts and his Ph.D. in materials science at Cornell University. He started his professional career at the University of Minnesota, then moved to the University of Massachusetts, where he headed the Department of Polymer Science and Engineering, before joining MIT. His research interests are in structure-property relations in polymeric materials.

KING NING TU is a Senior Manager for Thin Film Science at the IBM Watson Research Center. After obtaining his B.S. at the National Taiwan University in 1960, he received his M.S. from Brown University and a Ph.D. from Harvard University. In 1975-1976 he was a Senior Visiting Fellow at the Cavendish Laboratory, Cambridge University. His research interests have included phase transformations in alloys, kinetics in thin films, structural examination of materials by x-ray and electron diffraction, and device metallurgy.

